NANOCRYSTALS & LOADED POROUS SILICA FOR INCREASED DERMAL BIOAVAILABILITY

Inaugural-Dissertation

to obtain the academic degree

Doctor rerum naturalium (Dr. rer. nat.)

submitted to the Department of Biology, Chemistry and Pharmacy

of Freie Universität Berlin

by

Nan Jin

from Xinjiang, People's Republic of China

Berlin

June 2017

The enclosed doctoral research work was performed from September 2013 to June 2017 under the supervision of Prof. Dr. Rainer H. Müller at the Institute of Pharmacy – Pharmaceutics, Pharmaceutical Nanotechnology & NutriCosmetics, Department of Biology, Chemistry and Pharmacy, Freie Universität Berlin.

1st Reviewer: Prof. Dr. Rainer H. Müller

2nd Reviewer: Prof. Dr. Cornelia M. Keck

Date of defense: 24 July 2017

To my family

with all my love and gratitude.

CONTENTS

1. INTRODUCTION 1

1.1. Skin 2

1.1.1. Drug delivery into the skin 2

1.1.2. Skin penetration pathways and enhancement 3

1.2. Nanotechnology 5

1.2.1. Nanocrystals 5

1.2.2. Advantages and producing technologies of nanocrystals 7

1.3. Amorphization 10

1.3.1. Advantages and disadvantages of amorphous drugs 10

1.3.2. Technologies to produce commercial amorphous products 10

1.3.3. Novel smartPearls® technology 12

1.4. References 13

2. AIMS OF THE THESIS 19

3. RESULTS AND DISCUSSIONS 22

3.1. Production, characterization and storage stability of azithromycin nanocrystals for dermal prevention of infections by tick bite infections 23

3.1.1. Abstract 23

3.1.2. Introduction 23

3.1.3. Experimental Section 26

3.1.3.1. Materials 26

3.1.3.2. Optimized formulation of azithromycin nanocrystals 26

3.1.3.3. Preparation of dermal azithromycin formulation 27

3.1.3.4. Characterization 29

3.1.3.5. Dissolution test and saturation solubility 31

3.1.3.6. Ex vivo porcine ear penetration study 31

3.1.4. Results and Discussions 32

3.1.4.1. Optimized formulation of azithromycin nanocrystals 32

3.1.4.2. Characterization of the optimal formulation 38

3.1.4.3. Optimal storage temperature of nanocrystals stabilized with TPGS *43*

3.1.4.4. Physical long-term stability of the optimal formulation *43*

3.1.4.5. Dissolution test and saturation solubility *45*

3.1.4.6. Characterization of nanocrystals incorporated with gels *47*

3.1.4.7. Ex vivo porcine ear penetration study *50*

3.1.5. Conclusions 51

3.1.6. References 52

3.2. Maximum loaded amorphous azithromycin produced by dermal smartPearls® technology for prophylaxis against Lyme disease 58

3.2.1. Abstract 58

3.2.2. Introduction 58

3.2.3. Experimental Section 61

3.2.3.1. Materials *61*

3.2.3.2. Production of smartPearls® – maximum loading of azithromycin *61*

3.2.3.3. Preparation of azithromycin gels *62*

3.2.3.4. Determination of solid state *62*

3.2.3.5. Determination of the kinetic saturation solubility *63*

3.2.3.6. Stability of Syloid® porous materials in dermal gel formulations *63*

3.2.3.7. Penetration study with porcine ear skin *63*

3.2.3.8. High performance liquid chromatography (HPLC) analysis. *63*

3.2.4. Results and Discussions 64

3.2.4.1. Theory of loading drugs onto Syloid® porous materials *64*

3.2.4.2. Maximum loading detected by XRD *66*

3.2.4.3. Amorphous stability *67*

3.2.4.4. Saturation solubility studies *68*

3.2.4.5. Stability of Syloid® in gel formulations *69*

3.2.4.6. Penetration study with porcine ear skin 71

3.2.5. Conclusions 72

3.2.6. References 73

3.3. smartPearls® of flavonoids for topical anti-aging application 77

3.3.1. Abstract 77

3.3.2. Introduction 77

3.3.3. Experimental Section 81

3.3.3.1. Materials 81

3.3.3.2. Producing of anti-oxidants loaded silicas 81

3.3.3.3. Preparation of nanocrystals and gels 82

3.3.3.4. Stability of amorphous state of smartPearls® before and after incoporation into gels 83

3.3.3.5. Skin penetration study on porcine ear 83

3.3.4. Results and Discussions 84

3.3.4.1. Production of anti-oxidants loaded silicas 84

3.3.4.2. Particle size of nanocrystals 85

3.3.4.3. Distribution of anti-oxidants loaded smartPealrs® in gel 86

3.3.4.4. Stability of amorphous state of smartPearls® before and after incoporation into gels 89

3.3.4.5. Ex vivo skin penetration 92

3.3.5. Conclusions 95

3.3.6. References 95

3.4. A stable amorphization technology based on smartPearls® for dermal delivery of poorly soluble cyclosporin A 99

3.4.1. Abstract 99

3.4.2. Introduction 99

3.4.3. Experimental Section 102

3.4.3.1. Materials 102

3.4.3.2. Production of cyclosporin A loaded smartPearls®..... 102

3.4.3.3. Production of nanoparticles and gels..... 103

3.4.3.4. X-ray diffraction (XRD)..... 103

3.4.3.5. Light microscope (LM) and transmission electron microscope (TEM)..... 104

3.4.3.6. Ex vivo skin penetration study..... 104

3.4.3.7. High performance liquid chromatography (HPLC) analysis104

3.4.4. Results and Discussions 105

3.4.4.1. Amorphous state of loaded smartPearls® and nanoparticles105

3.4.4.2. Amorphous state of loaded smartPearls® in the gel..... 106

3.4.4.3. Transmission electron microscope (TEM)..... 107

3.4.4.4. Stability of Syloid® in gel formulations..... 108

3.4.4.5. Ex vivo skin penetration study..... 109

3.4.5. Conclusions 111

3.4.6. References 111

3.5. Screening silica-based carriers for amorphized hydrophobic drugs and the effect of loading concentration.....115

3.5.1. Abstract..... 115

3.5.2. Introduction 115

3.5.3. Experimental Section 118

3.5.3.1. Materials 118

3.5.3.2. Skin feeling test.....118

3.5.3.3. Loading drug into silicas.....119

3.5.3.4. Physical stability of amorphous state..... 122

3.5.3.5. Surface morphology..... 122

3.5.3.6. Drug dissolution experiment 123

3.5.4. Results and Discussions 123

3.5.4.1. Skin feeling test..... 123

3.5.4.2. Loading drug onto silicas..... 124

3.5.4.3. Physical stability of amorphous state *126*

3.5.4.4. Surface morphology *130*

3.5.4.5. Drug dissolution experiment *131*

3.5.5. Conclusions 134

3.5.6. References 134

4. SUMMARY **139**

5. ZUSAMMENFASSUNG **143**

ABBREVIATIONS **146**

PUBLICATIONS **148**

CURRICULUM VITAE **154**

ACKNOWLEDGEMENTS **157**

1. INTRODUCTION

1.1. Skin

1.1.1. Drug delivery into the skin

Human skin has an average surface area of 1.8 m^2 for adults (González-rodríguez, et al. 2016) to protect the body against the entrance of exogenous substances (Abla, et al. 2016). Its barrier function is ascribed to its structure. Detailed introduction of the skin structure is well figured in literatures (Bolzinger, et al. 2002; EI-Maghraby, 2016; González-rodríguez, et al. 2016; Ng and Lau, 2015). Generally speaking, the skin consists of three parts from surface to innermost: epidermis, dermis, and hypodermis (Abla, et al. 2016). Epidermis can be divided into two parts: the overlying stratum corneum and underlying viable epidermis. The stratum corneum includes 10-15 layers of corneocytes, which are interspersed with lipid matrix. This layer is usually described as a "brick and mortar" structure with a thickness of around 10-20 μm (Abla, et al. 2016; Ng and Lau, 2015). These densely packed corneocytes which filled with dead keratin (brick) within the lipid matrix (mortar) are the main reason why therapeutic agents could not penetrate the skin easily (Kuswahyuning, et al. 2015; Walters and Brain, 2009). The other part is named viable epidermis because these layers are full of various nucleated cells (e.g., keratinocytes, melanocytes) that can be considered as one part with a thickness of 50-100 μm (Ng and Lau, 2015). The middle part of the skin, dermis, is less lipophilic than the epidermis but distinctly thicker: 1-3 mm (Abla, et al. 2016). It is made up mainly from fibroblasts and structural proteins (Ng and Lau, 2015). Some immune cells, blood capillaries and nerve endings are also existing in this layer (Abla, et al. 2016). The hypodermis is composed principally of appendageal: sweat glands, hair follicles and sebaceous glands.

The commercial dermatological formulations have reached around $18 billion worldwide, occupying 22.5% of the global drug delivery market (Banga, 2011). The success of the dermatological formulations is ascribed to its advantages: zero hepatic first-pass metabolism, low plasma fluctuation, safe and easy application, can stop the treatment

during the application, low drug dose and less side effects (Abla, et al. 2016; Kuswahyuning, et al. 2015; Peppas, et al. 2000). It can be divided into two parts generally for dermatological formulations: topical and transdermal drug delivery. The former one includes local or regional treatment such as psoriasis, eczema and insect repellents (Atkinson, et al. 2015), where the latter one targets the systemic delivery (Murthy and Shivakumar, 2010) such as motion sickness (Singh and Morris, 2011). Usually the actives, e.g., antifungals, antibiotics and anti-aging agents can be delivered topically to the place of action (skin surface or inside the epidermis or dermis), while the actives such as nicotine and anesthetics (e.g., lidocaine) are designed to be delivered through the skin for reaching the systemic circulation (Surber, et al. 2001). One of the most successful dermatological formulation is LIDODERM® (lidocaine patch 5%), earning $750 million per year for Endo Pharmaceuticals Inc (USA) (Watkinson, 2012).

1.1.2. Skin penetration pathways and enhancement

For the drug molecules with favorable physicochemical properties such as small molecular weight (e.g., less than 500 Da), uncharged, moderate lipophilicity (e.g., log P between 1 and 3) (Abla, et al. 2016), three general pathways exist to permeate the skin: 1) The lipid matrix between the intercellular spaces can provide the intercellular route (Fig. 1, right), (Wertz, 2015), which is the principal pathway to go through skin (Walters and Brain, 2009); 2) Skin cells such as keratinocytes can provide the transcellular routes for drug molecules (Fig. 1, middle), (Abla, et al. 2016); 3) Hair follicles, sweat ducts and sebaceous glands can provide transappendageal route. Among the three described appendageal, the follicular penetration (Fig. 1, left) is the most important one (Wertz, 2015). However, the effective use of these pathways is limited due to the barrier stratum corneum. Most penetration through the skin of the actives depends on passive diffusion (Murthy and Shivakumar, 2010). To enhance the penetration through the skin, many approaches have been developed: increase thermodynamic activity, addition of chemical penetration enhancers or ion pairs,

pH adjustment, complex coacervation, producing eutectic mixture (Kuswahyuning, et al. 2015). Among these approaches, the universal method without changing the skin lipid structure is the increase of the thermodynamic activity. Thermodynamic activity can be enhanced by increasing the solute concentration. Consequently, the skin delivery rate can be improved, especially when the saturation condition of an active in the vehicle is achieved (Kuswahyuning, et al. 2015). Thus, two strategies, the nanonization and amorphization of actives, were applied in this thesis to enhance the kinetic saturation solubility of various actives in the dermal vehicles, resulting in higher skin penetration.

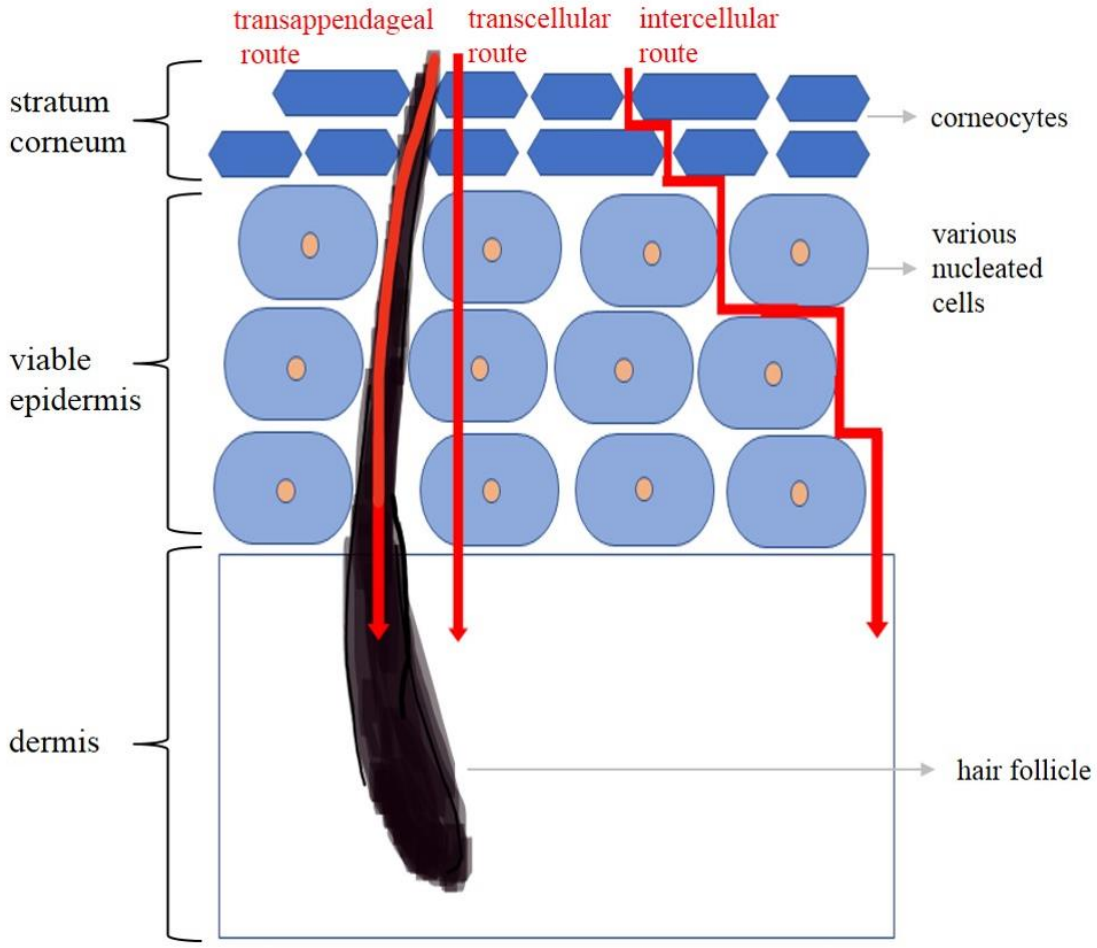

Fig. 1. Sketch of the three penetration routes through skin: transappendageal route, transcellular route and intercellular route.

1.2. Nanotechnology

1.2.1. Nanocrystals

Nanotechnology was developed by Richard Feynman in 1959 and the relative actives were called “colloids” until 1974. After then, the new name “nano” created by Norio Taniguchi was accepted by public (Müller, et al. 2014). However, 40 years later, the definition of “nano” is still in debate. According to the European Cosmetic Directive (ECD) (Pyo, 2016) as well as US Food and Drug Administration (FDA), “nano” means half amount of the particles possessing sizes below 100 nm in considering of the toxicity risk (Müller, et al. 2016). But for physical unite definition or in pharmaceutical application, “nano” usually ranges from 1 to 1,000 nm in terms of the advance of solubility (Müller, et al. 2011; Pyo, 2016). Based on the material and structure, nanocarriers for dermal delivering of chemical agents can be classified as 1) lipid-based vesicles such as liposomes; 2) surfactant-based vesicles such as micelles; 3) lipid-based particulate carriers such as solid lipid nanoparticles (SLN) and nanostructured lipid carrier (NLC); 4) polymer-based particulate carriers such as polymeric nanoparticles; 5) nanocrystals and 6) others such as microemulsions (Muzzalupo, 2016), which can be included in nanocarriers due to their internal nanostructure (Lapteva, et al. 2016).

The liposomes were first described by Alec Douglas Bangham in 1965 (Bangham, 1993). The first commercial product of liposomes was for topical administration of cosmetics and presented by Dior (France) to the world in 1986 (Müller, et al. 2014). Its name Capture, represented the function of anti-aging by the main active longoza. The success of the cosmetics application of liposomes strengthed the confidence for pharmaceutical market. A few years later, Epi-Pevaryl®, a liposome cream, for anti-mycotic therapy (drug: econazole) was developed by Johnson & Johnson GmbH (USA) (Müller, et al. 2000). There was no doubt that liposomes for topical administration bring a great success, however, it was reported that when applied onto skin, liposomes would like to stay in the

upper layers of the stratum corneum rather than go further into the epidermal layers (Abla, et al. 2016). During the period time from lab research to commercial application of liposomes, Peter Speiser published the first polymeric nanoparticles article (Couvreur, 2013) in 1976. There are currently many products in the clinical phases (Abla, et al. 2016), but only one is available on the market for the treatment of pancreatic cancer and breast cancer (Couvreur, 2013): Abraxane® injectable suspension with the drug paclitaxel, developed by Celgene Corporation (USA) and received approval from FDA in 2005. Unlike the other carriers, polymeric nanoparticles could not penetrate the stratum corneum but could go through the skin via hair follicles (Abla, et al. 2016; Couvreur, 2013). Similar to the polymeric nanoparticles the dermal microemulsions have not been launched yet, 20 years after development in the 1980s, due to high concentrations of surfactants and irritation to skin (Müller, et al. 2014). Compared to the few applications of polymeric nanoparticles on dermal, SLN and NLC showed further benefits on dermal application due to occlusive effect (Müller, et al. 2007) since their development (SLN: 1992. NLC: 1999). Dr. Rimpler GmbH (Germany) introduced the first NLC product in 2005 with the anti-aging agent coenzyme Q10, which is for dermal application: Cutanova Cream NanoRepair Q10 and Intensive Serum NanoRepair Q10 (Müller, et al. 2007). Other nanocarriers such as micellar nanoparticles got the approval from FDA in 2001, by the topical product named Estrasorb™ with the drug estradiol hemihydrate. It was developed by Novavax, Inc. (USA) as estrogen replacement therapy for symptomatic menopausal women (Abla, et al. 2016).

The first time of mentioning nanocrystals was in one patent submitted by Liversidge and his colleagues in 1991. Nanocrystals are particles of pure active agents without any matrix material, ranging from 1 to 1,000 nm (Keck, et al. 2010). Usually they are in crystalline state but in some cases amorphous state can also exist. When they are dispersed in a liquid medium with additional surfactants or polymer layers, the nanosuspension is achieved (Müller, et al. 2016). Only 10 years later, the first product based on nanocrystals,

Rapamune® (active: sirolimus), was on market for prophylaxis of immunologic risk by oral administration in 2000 developed by Wyeth Pharmaceuticals Inc., and now belongs to Pfizer Inc. (USA). The first dermal product of nanocrystals was launched on the cosmetic market in 2007, named Juvedical® Renewing Serum (Juvena, Switzerland) including the poorly soluble anti-oxidant rutin as nanocrystals (Müller, et al. 2016). Nanocrystals outweigh other nanocarriers in the following points: 1) increased kinetic saturation solubility of the active agent; 2) producible in a simple way; 3) industrially feasibility (Al-Shaal, et al. 2011); 4) less cost (Müller and Keck 2012). These benefits made nanocrystals more popular to the market (Müller, et al. 2000).

1.2.2. Advantages and producing technologies of nanocrystals

The advantages of nanocrystals for dermal delivery are ascribed to the nano size compared to the micrometer sized raw drug powders (Tab. 1): decreasing the particles radius increases both the saturation solubility and dissolution velocity of active. By this, an enhanced diffusive flux is achieved, resulting in enhanced penetration and improved dermal bioavailability. In addition, nanocrystals show increased adhesiveness to skin due to the distinctly enlarged contact area (Pyo, 2016).

Nanocrystals can be produced generally by bottom-up or top-down methods (Fig. 2): the former one includes classical precipitation method and NanoMorph technology; the latter one contains bead milling (BM), high pressure homogenization (HPH) piston-gap or jet-stream as well as the combination technology (CT) (Keck, et al. 2010). The detailed description can be found in the thesis of Dr. Jaime Salazar (Salazar, 2013) and the book chapter of Prof. Cornelia M. Keck (Keck, et al. 2010). It is hard to apply the bottom-up method on scale-up production due to difficult control and intensive cost (Pyo, 2016). Thus, no product on the market is manufactured by this method. In contrast, top-down method is favorable by industry to produce commercial pharmaceutical or cosmetic products.

Table 1: Relationship between radius and solubility/dissolution velocity/penetration.

Equation name	Equation	Equation constant	reference
Fick's first law of diffusion	$J = \frac{K_{ow} \cdot D}{L} \cdot \Delta C$	J: solute flux of the active through the stratum corneum K_{ow}: octanol/water partition coefficient D: diffusion coefficient L: length of the diffusion pathway ΔC: concentration gradient over the stratum corneum	Müller, et al. 2016; Stahl, 2015
Kelvin equation	$\log \frac{P_r}{P_\infty} = \frac{2\gamma M_r}{2.303RT\rho r}$	P_r: vapor pressure above droplet P_∞: saturated vapor pressure γ: surface tension M_r: molar volume of the active R: universal gas constant T: absolute temperature ρ: density of the particle r: radius of the droplet	Keck, et al. 2010
Noyes Whitney equation	$\frac{dc}{dt} = A \cdot D \cdot (\frac{C_s - C_0}{h})$	dc/dt: dissolution velocity A: surface area D: diffusion coefficient C_s: saturation solubility C_0: concentration of dissolved active h: diffusional distance	Müller, et al. 2013
Ostwald-Freundlich equation	$\log \frac{C_s}{C_\alpha} = \frac{2\sigma V}{2.303RT\rho r}$	C_s: saturation solubility C_α: solubility of the solid consisting of large particles σ: interfacial tension of substance V: molar volume of the particle material R: gas constant T: absolute temperature r: radius of particle	Nagarwal, et al. 2011

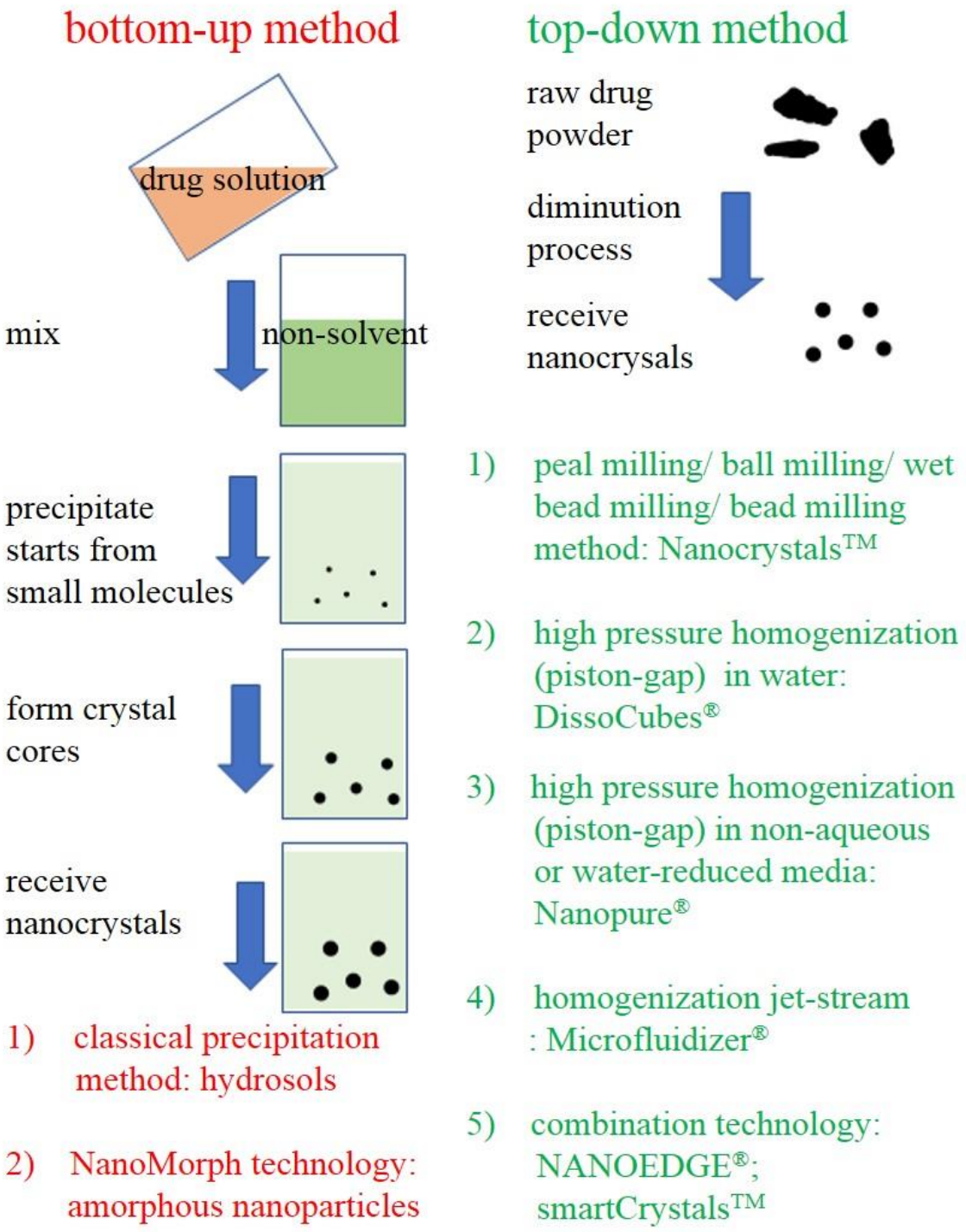

Fig. 2. Production methods of nanocrystals: bottom-up and top-down method.

Therefore, it can be employed for almost all hydrophobic actives (Gao, et al. 2013). Among the launched products containing nanocrystals (Müller, et al. 2016), most of them are produced by bead milling, such as Rapamune®, Emend® (active: aprepitant), Tricor®

(active: fenofibrate), Megace ES® (active: megestrol acetate) and Invega® (active: paliperidone). While seldom is produced by high pressure homogenization, one example is Triglide® (active: fenofibrate). Details of these commercial nanocrystals products can be found in literatures (Möschwitzer, 2013; Shegokar and Müller, 2011). The combination technology was used by Dr. Rimpler GmbH (Germany) to produce different cosmetic concentrates (Müller, et al. 2016).

1.3. Amorphization

1.3.1. Advantages and disadvantages of amorphous drugs

More than 1/3 of commercial pharmaceutical products on the market as well as 70-90% of newly developed drug candidates are hydrophobic actives (Chen, et al. 2016; Müller and Keck, 2012). For a drug candidate, its activity depends on dose, solubility and permeability (Kaushal, et al. 2004). Thus, the poor solubility of the drug candidates limits their use for promising treatments. Besides the nanocrystals, another strategy is to convert the crystalline actives to their amorphous counterparts (Chen, et al. 2016). Drug in crystalline state is characterized by long-range molecular order, repeating regularly in three-dimensional space (Kaushal, et al. 2004). Thus, it is difficult to disrupt this crystal lattice to bring the drug into a given solvent. In contrast, amorphous drug possesses short-range molecular order, arranging irregularly, which results in low energy required to break up its crystal lattice. Thus, amorphous drugs have higher solubility than in crystalline state. However, the randomness in molecular conformation of amorphous state also brings high entropy, high enthalpy, high free energy and high molecular mobility, which results in high thermodynamical instability and high tendency for re-crystallization (Löbmann, et al. 2012; Yani, et al. 2016).

1.3.2. Technologies to produce commercial amorphous products

Usually, solid dispersion can be used to generate amorphous state. Except the first

generation of solid dispersion is crystalline state, for the latter two generations, the drug molecules are dispersed in a disordered form (amorphousness) in solid matrix carriers by using polymers such as povidone (PVP), polyethyleneglycol (PEG), hydroxypropyl methylcellulose (HPMC) (second generation) or surfactants such as inulin, gelucire, poloxamer (third generation) (Wei, 2016). Preparation techniques generally include milling (Gupta, et al. 2003), thermal methods (e.g., melt quenching, hot melt extrusion), solvent evaporation (precipitation, spray drying, freeze drying) and supercritical fluid technology (LaFountaine, et al. 2016).

Spray drying is one of the most successful technologies applied among the solvent evaporation methods with many commercial products on the market: e.g., Kalydeco® (active: ivacaftor), Incivek® (active: telaprevir) and Intelence® (active: etravirine). The active, polymer/surfactant and other excipients are dissolved in a suitable solvent, followed by spraying via a nozzle into a stream of drying gas (LaFountaine, et al. 2016). The first commercial amorphous solid dispersion manufactured by spray drying is Sporanox® (active: itraconazole), an antifungal medication, by Janssen-Cilag Ltd. (UK) in 1992.

Another industrial favorable technology is hot melt extrusion of thermal methods: the solid active and the carrier are mixed/softened/melted first, followed by extrusion with a high rotation speed, and finally a downstream processing such as milling (LaFountaine, et al. 2016; Wei, 2016). Three famous products from AbbVie Inc. (USA) were produced by this method: Norvir® (active: ritonavir), FDA approved 1996; Kaletra® (active: lopinavir/ ritonavir), FDA approved 2000; Viekirax® (active: ombitasvir/paritaprevir/ritonavir) was approved 2015 in USA, EU and Japan for the treatment of chronical hepatitis C. Some other products, e.g., Onmel® (active: itraconazole), FDA approved 1992, was developed by Merz Pharmaceuticals Inc. (USA) and Noxafil® (active: posaconazole), FDA approved 2006, by Merck & Co., Inc. (USA).

Even though many products on the market are produced by solid dispersion methods like

mentioned above, there are still some problems in the producing methods (Kaushal, et al. 2004), e.g., risk of chemical degradation of temperature labile drugs for thermal methods; difficulties in finding suitable solvents for dissolving hydrophobic drugs and hydrophilic carriers for the solvent evaporation methods and difficulties in optimization of processing parameters. Moreover, the re-crystallization is a common disadvantage of these products, which hinders their application on dermal delivery.

1.3.3. Novel smartPearls® technology

The first time using mesoporous silica to load drug within its pores was in 2001 by Vallet-Regi and his colleagues (Vallet-Regi, et al. 2001). They loaded ibuprofen onto MCM-41. At the same time, Watanabe et al. (Watanabe, et al. 201) used SiO_2 to stabilize indomethacin in an amorphous solid dispersion. In 2004, Takeuchi et al. (Takeuchi, et al. 2004) developed non-porous silica (Aerosil 200, Aerosil R972) and porous silica (Sylysia 350) as carriers for tolbutamide solid dispersion, receiving meta-stable crystalline form. One year later, the same group (Takeuchi, et al. 2005) used non-porous silica (Aerosil 200) and porous silica (Sylysia 350) as drug carriers for indomethacin solid dispersion by applying spray-drying method, and got amorphous state, which was stable for at least 2 months at certain conditions. In 2009, the method of generating amorphous actives onto sponge-like matrices such as Neusilin was patented by Capsulution Nanoscience AG (Nolte, 2009) and was named as CapsMorph® by PharmaSol GmbH Berlin (Wei, 2016) for oral administration.

In 2014, PharmaSol GmbH Berlin and Grace GmbH & Co. KG (Monsuur, et al. 2014) submitted the patent publication about smartPearls®, which loads actives into the mesopores of μm-sized silicas in amorphous state for dermal application. This smartPearls® technology does not need any surfactant or polymer. The stabilization of amorphous state is realized by the small nano size of the pores as well as the interaction between the drug and the function groups of the silica. Once the active is loaded into the

mesopores of silicas via impregnation method, the small pore size (2-50 nm) will hinder the transformation from amorphous state to crystalline state. The stabilization is so effective that even in the dermal vehicle such as water-contained gel, the amorphous state can be remained for a long period of time up to 2 years by now.

1.4. References

Abla, M.J., Singh, N.D., Banga, A.K., 2016. Role of nanotechnology in skin delivery of drugs, in: Dragicevic, N., Maibach, H.I. (Eds.), Percutaneous penetration enhancers, chemical methods in penetration enhancement: Nanocarriers. Springer-Verlag GmbH, Berlin, pp. 1-10.

Al-Shaal, L., Shegokar, R., Müller, R.H., 2011. Production and characterization of antioxidant apigenin nanocrystals as a novel UV skin protective formulation. Int. J. Pharm. 420, 133-140.

Atkinson, J.P., Maibach, H.I., Dragicevic, N., 2015.Targets in dermal and transdermal delivery and classification of penetration enhancement methods, in: Dragicevic, N., Maibach, H.I. (Eds.), Percutaneous penetration enhancers, chemical methods in penetration enhancement: Drug manipulation strategies and vehicle effects. Springer-Verlag GmbH, Berlin, pp. 94-95.

Banga, A.K., 2011. Commercial development of devices and products for transdermal physical enhancement technologies, in: Banga, A.K (Eds.), Transdermal and interadermal delivery of therapeutic agents: Application of physical technologies. CRC Press Taylor & Francis Group, Bocal Raton, pp. 243.

Bangham, A.D., 1993. Liposomes: the Babraham connection. Chem. Phys. Lipids 64, 275-285.

Bolzinger, M.A., Briançon, S., Pelletier J., Chevalier, Y., 2002. Penetration of drugs through skin, a complex rate-controlling membrane. Curr. Opin. Colloid Interface Sci. 17, 156-165.

Chen, L., Okuda, T., Lu, X.Y., Chan, H.K., 2016. Amorphous powders for inhalation drug

delivery. Adv. Drug Deliv. Rev. 100, 102-115.

Couvreur, P., 2013. Nanoparticles in drug delivery: Past, present and future. Adv. Drug Deliv. Rev. 65, 21-23.

EI-Maghraby, G.M., 2016. Stratum corneum in lipid liposomes: Drug delivery systems and skin models, in: Dragicevic, N., Maibach, H.I. (Eds.), Percutaneous penetration enhancers, chemical methods in penetration enhancement: Nanocarriers. Springer-Verlag GmbH, Berlin, pp. 112-123.

Gao, L., Liu, G., Ma, J., et al., 2013. Application of drug nanocrystals technologies on oral drug delivery of poorly soluble drugs. Pharm. Res. 30, 307-324.

González-Rodríguez, M.L., Cózar-Bernal, M.J., Fini, A., Rabasco, A.M., 2016. Surface-charged vesicles for penetration enhancement, in: Dragicevic, N., Maibach, H.I. (Eds.), Percutaneous penetration enhancers, chemical methods in penetration enhancement: Nanocarriers. Springer-Verlag GmbH, Berlin, pp. 121-123.

Gupta, M.K., Vanwert, A., Bogner, R.H., 2003. Formation of physically stable amorphous drugs by milling with Neusilin. J. Pharm. Sci. 92, 536-551.

Kaushal, A.M., Gupta, P., Bansal, A.K., 2004. Amorphous drug delivery systems: Molecular aspects, design, and performance. Crit. Rev. The. Drug Carrier Syst. 21, 133-193.

Keck, C.M., Al-Shall, L., Müller, R.H., 2010. smartCrystals – review of the second generation or drug nanocrystals, in: Torchilin, V., Amiji, M.M. (Eds.), Handbook of materials for nanomedicine. Pan Stanford Publishing Pte. Ltd., Singapore, pp. 556-557.

Kuswahyuning, R, Grice, J.E., Moghimi, H.R., Roberts, M.S., 2015. Formulation effects in percutaneous absorption, in: Dragicevic, N., Maibach, H.I. (Eds.), Percutaneous penetration enhancers, chemical methods in penetration enhancement: Drug manipulation strategies and vehicle effects. Springer-Verlag GmbH, Berlin, pp. 117-126.

LaFountaine, J.S., McGinity, J.W., Williams, R.O., 2016. Challenges and strategies in thermal processing of amorphous solid dispersions: A review. AAPS Pharm. Sci, Tech. 17, 43-55.

Lapteva, M., Möller, M., Kalia, Y.N. 2016. Polymeric micelles in dermal and transdermal delivery, in: Dragicevic, N., Maibach, H.I. (Eds.), Percutaneous penetration enhancers, chemical methods in penetration enhancement: Nanocarriers. Springer-Verlag GmbH, Berlin, pp. 223-224.

Löbmann, K., Strachan, C., et al., 2012. Co-amorphous simvastatin and glipizide combinations shown improved physical stability without evidence of intermolecular interactions. Eur. J. Pharm. Biopharm. 81, 159-169.

Monsuur, F., Höfer, H., et al., 2014. Active-loaded particulate materials for topical administration. US Patent 62050587. WO 2016041992A1.

Murthy, S.N., Shivakumar, H.N., 2010. Topical and transdermal drug delivery, in: Kulkarni, V. S., (Eds.), Handbook of non-invasive drug delivery systems. Elsevier Inc., Oxford, pp. 3-6.

Muzzalupo, R., 2016. Niosomes and proniosomes for enhanced skin delivery, in: Dragicevic, N., Maibach, H.I. (Eds.), Percutaneous penetration enhancers, chemical methods in penetration enhancement: Nanocarriers. Springer-Verlag GmbH, Berlin, pp. 149-150.

Möschwitzer, J., 2013. Drug nanocrystals in the commercial pharmaceutical development process. Int. J. Pharm. 453, 142-156.

Müller, R.H., Chen, R., Keck, C.M., 2013. smartCrystals for consumer care & cosmetics: Enhanced dermal delivery of poorly soluble plant actives. Household and Personal Care Today. 8, 18-23.

Müller, R.H., Gohla, S., Keck, C.M., 2011. State of the art of nanocrystals – Special features, production, nanotoxicology aspects and intracellular delivery. Euro. J. Pharm. Biopharm. 78, 1-9.

Müller, R.H., Keck, C.M., 2012. Twenty years of drug nanocrystals: Where are we and where do we go? Euro. J. Pharm. Biopharm. 80, 1-3.

Müller, R.H., Mäder, K., Gohla, S., 2000. Solid lipid particles (SLN) for controlled drug delivery – a review of the state of the art. Euro. J. Pharm. Biopharm. 50, 161-177.

Müller, R.H., Petersen, R.D., et al., 2007. Nanostructured lipid carriers (NLC) in cosmetic

dermal products. Adv. Drug Deliv. Rev. 59, 522-530.

Müller, R.H., Staufenbiel, S., Keck, C.M., 2014. Lipid nanoparticles (SLN, NLC) for innovative consumer care & household products. Transdermal Delivery. Household and Personal Care Today. 9, 18-24.

Müller, R.H., Zhai, X., Romero, G.B., Keck, C.M., 2016. Nanocrystals for passive dermal penetration enhancement, in: Dragicevic, N., Maibach, H.I. (Eds.), Percutaneous penetration enhancers, chemical methods in penetration enhancement: Nanocarriers. Springer-Verlag GmbH, Berlin, pp. 284-285.

Nagarwal, R.C., Kumar, R., et al., 2011. Nanocrystal technology in the delivery of poorly soluble drugs: An overview. Curr. Drug Deliv. 8, 398-406.

Ng, K.W., Lau, W.M., 2015. Skin deep: the basics of human skin structure and drug penetration, in: Dragicevic, N., Maibach, H.I. (Eds.), Percutaneous penetration enhancers, chemical methods in penetration enhancement: Drug manipulation strategies and vehicle effects. Springer-Verlag GmbH, Berlin, pp. 4-7.

Nolte, M., Mayer, J., et al., 2009. Stabilization of amorphous drugs using sponge-like carrier matrices. US Patent 0196873. WO 2009153346A2.

Pyo, S.M., 2016. Nanocrystals & lipid nanoparticles for optimized delivery of actives. PhD thesis, Free University of Berlin, pp. 2-5.

Romero, G.B., Chen, R., Keck, C.M., Müller, R.H., 2015. Industrial concentrates of dermal hesperidin smartCrystals® – production, characterization & long-term stability. Int. J. Pharm. 482, 54-60.

Salazar, J., 2013. Combinative particle size reduction technologies for the formulation of poorly soluble drugs. PhD thesis, Free University of Berlin, pp. 5-23.

Shegokar, R., Müller, R.H., 2011. Nanocrystals: Industrially feasible multifunctional formulation technology for poorly soluble actives. Int. J. Pharm. 399, 129-139.

Singh, I., Morris, A.P., 2011. Performance of transdermal therapeutic systems: Effects of biological factors. Int. J. Pharm. Investig. 1, 4-9.

Stahl, J. 2015. Dermal and transdermal formulation: How they can affect the active compound, in: Dragicevic, N., Maibach, H.I. (Eds.), Percutaneous penetration

enhancers, chemical methods in penetration enhancement: Drug manipulation strategies and vehicle effects. Springer-Verlag GmbH, Berlin, pp. 209-211.

Surber, C., Schwarb, F.P. Tassopoulos, T. 2001. Percutaneous penetration as it relates to the safety evaluation of cosmetic ingredients, in: Bronaugh, R.L., Maibach, H.I. (Eds.), Topical absorption of dermatological products. Marcel Dekker Inc., New York, pp. 209-213.

Takeuchi, H., Nagira, S., Yamamoto, H., Kawashima, Y., 2004. Solid dispersion particles of tolbutamide prepared with fine silica particles by the spray-drying method. Powder Technology 114, 187-195.

Takeuchi, H., Nagira, S., Yamamoto, H., Kawashima, Y., 2005. Solid dispersion particles of amorphous indomethacin with fine porous silica particles by using spray-drying method. Int. J. Pharm. 293, 155-164.

Vallet-Regi, M., Rámila, A, del Real, R.P., Pérez-Pariente, J., 2001. A new property of MCM-41: Drug delivery system. Chem. Mater. 13, 308-311.

Walters, K.A., Brain, K.R., 2009. Topical and transdermal delivery, in: Gibson, M. (Eds.), Pharmaceutical preformulation and formulation: A practical guide from candidate drug selection to commercial dosage form. Informa Healthcare USA Inc., New York, pp. 475-479.

Watanabe, T., Wakiyama, N., et al., 2001. Stability of amorphous indomethacin compounded with silica. Int. J. Pharm. 226, 81-91.

Watkinson, A.C., 2012. Transdermal and topical drug delivery today, in: Benson, H.A.E., Watkinson, A.C. (Eds.), Transdermal and topical drug delivery: Principles and practice. John Wiley & Sons, Inc., Hoboken, pp. 362-364.

Wei, Q., 2016. Nanocrystals & loaded porous silica for increased oral bioavailability. PhD thesis, Free University of Berlin, pp. 11-18.

Wertz, P.W., 2015. Epidermal lipids and the intercellular pathway., in: Dragicevic, N., Maibach, H.I. (Eds.), Percutaneous penetration enhancers, chemical methods in penetration enhancement: Drug manipulation strategies and vehicle effects. Springer-Verlag GmbH, Berlin, pp. 16-17.

Yani, Y., Chow, P.S., et al., 2016. Pore size effect on the stabilization of amorphous drug in a mesoporous material: Insights from molecular simulation. Micropor. Mesopor. Mat. 221, 117-122.

2. AIMS OF THE THESIS

The aims of the thesis were to develop nanocrystals by top-down method and develop novel amorphous formulations by smartPearls® technology for dermal application, which possess increased skin penetration of poorly water-soluble actives.

1. Develop optimized azithromycin nanocrystals for dermal application on prophylaxis against Lyme disease (**chapter 3.1**).

None of the commercial azithromycin gels on the market is aimed to prevent or treat Lyme disease, although there are two groups working on topical azithromycin formulation for the treatment of Lyme disease. Azithromycin ethanol-solution-gel demonstrates its effectiveness in human clinical phase III trial and azithromycin Lipoderm cream in a murine model. Both of them used azithromycin not as nanocrystals, however they can increase adhesiveness of the dermal formulation to skin, enhance kinetic saturation solubility, improve dissolution rate and enhance skin penetration of the hydrophobic azithromycin. Azithromycin nanocrystals were produced by another group using HPH. However, their nanosuspension only consisted of 1% w/w drug and the diameter of the so produced nanocrystals was around 400 nm. This work aimed to find another method which cost less energy and less time to produce a stable azithromycin nanosuspension having a higher drug content and smaller particle diameter. In this study, different production methods (HPH, BM, combination technology), different production parameters (HPH cycle numbers, milling time) and different nonionic stabilizers (TPGS, poloxamer 407, poloxamer 188, Plantacare® 810 UP, Plantacare® 2000 UP and Tween® 80) were used to obtain optimized azithromycin nanocrystals suitable for dermal application. The aptitude of the optimized nanocrystals on kinetic saturation solubility, dissolution velocity, physical stability and skin penetration was compared to raw drug powder, the clinical effective dermal formulation and the dermal formulation with penetration enhancer.

2. Evaluate the feasibility of smartPearls® technology on dermal application (**chapter 3.2, 3.3, 3.4**).

CapsMorph® absorbs drug solution in mesoporous silicas to generate the amorphous state of actives for oral administration. This technology has already proven its superiority regarding kinetic saturation solubility and dissolution rate compared to raw drug powder and even nanocrystals. It also showed stability of amorphous state for at least 5 years by now. But if this amorphous active will keep the benefits and remain stable when incorporated into a water-containing medium such as gel has to be investigated (**chapter 3.2**). As well as if the advantages will remain when the loaded active in mesoporous silica is in crystalline state (**chapter 3.3**) and if this amorphous active in mesoporous silica will show superior penetration efficacy than the corresponding amorphous nanoparticles (**chapter 3.4**). This work intended to illuminate the abovementioned questions. A new technology transferred from CapsMorph®, named smartPearls®, working on dermal application was investigated herein. Initial research of this new technology was managed in this study. Various active agents (e.g., azithromycin, rutin, cyclosporin A, etc.) were loaded onto mesoporous silica Syloid® SP53D-11920 via smartPearls® technology for dermal application. Their aptitude on stabilize amorphous state, kinetic saturation solubility, dissolution rate, and skin penetration were compared to nanoparticles (crystalline or amorphous state) and raw drug powder (crystalline or amorphous state).

3. Screen silica-based carriers for amorphized hydrophobic drugs and investigate the effect of loading concentration (**chapter 3.5**).

smartPearls® products have been confirmed possessing a long physical stability and a high dermal bioavailability in **chapter 3.2, 3.3, and 3.4**. But basic mechanisms of this novel technology still have to be investigated. This work aimed to compare different silica-based carriers (Neusilin® SG2, AEROPERL® 300 Pharma, and Neusilin® US2) with Syloid® SP53D-11920 as drug vehicle for amorphized azithromycin. Their aptitude regarding skin feeling, drug loading and physical stability was compared. The influence of the loading concentration on the properties of drug loaded smartPearls® (e.g., drug loading amount, physical stability, dissolution rate and kinetic saturation solubility) was evaluated as well.

3. RESULTS AND DISCUSSIONS

3.1. Production, characterization and storage stability of azithromycin nanocrystals for dermal prevention of tick bite infections

3.1.1. Abstract

Azithromycin was optimized as nanocrystals with the drug content of 10.0% (w/w) and the surfactant D-α-tocopheryl polyethylenglycol 1000 succinate (TPGS) content of 1.0% (w/w) using bead milling in 10 minutes. The photon correlation spectroscopy (PCS) diameter of the bulk population was 189 nm, laser diffraction (LD) diameter 90% was 370 nm. Spherical morphology of the optimal nanocrystals was observed by transmission electron microscope (TEM). They were stable over 1 year of storage at 4 °C with the particle size within the nanometer range which was confirmed by PCS, LD and light microscope. An acceptable physical stability of 2 years was also obtained when stored at 4 °C. No bacterial attack to the nanocrystals was observed before 3 years storage at 4 °C. The saturation solubility of the nanocrystals was up to triple compared to the raw drug powder (RDP) in water. When incorporated into the gel base, highest penetration efficacy was achieved by the optimal nanocrystals compared to 1) the clinical effective ethanol-solution-gel, 2) the gel with propylene glycol and 3) the gel with RDP in the *ex vivo* porcine ear penetration study. Even though propylene glycol improved saturation solubility of nanocrystals, it could not bring benefit to nanocrystals in the penetration study. Based on this optiaml azithromycin nanocrystals, topical administration for enhanced dermal bioavailability of azithromycin seems to be feasible.

3.1.2. Introduction

The rate of Lyme disease has been increasing in recent years around the whole world (Huber, et al. 2010). People suffer from Lyme disease after infected-tick bite due to the bacterium *Borrelia burgdorferi* (Hinckley, et al. 2014; Zimering, et al. 2014). It could occur when you are in wild, play with your dogs or cats, or even walk in your garden as

long as there is infected tick hiding there. Serious symptoms on skin, joints and nervous system such as erythema migrans rashes, oligoarticular arthritis, and meningitis could happen if the Lyme disease was not treated promptly (Hinckley, et al. 2014). There was one vaccination (active: recombinant outer surface protein A) on the market to prevent Lyme disease between 1999 and 2002. However, its single price was more than 60 dollars and it only worked after multiple injections (Nadelman, et al. 2001) which could still not provide a 100% guarantee. What is worse, this vaccination was withdrawn due to many problems (Piesman, et al. 2014). The other existing solutions mainly focused on antibiotics. Usually oral antibiotics such as doxycycline or amoxicillin are administered in the early treatment to patients who have been bitten by ticks (Shapiro, et al. 2014). However, bacterial resistance to administered antibiotic or malaise and toxicity has to be considered when using antibiotics systematically (Knauer, et al. 2011). These side effects can be reduced when drug concentrations are kept at a minimum and the antibiotic is administrated topically.

Topical treatments of antibiotics such as amoxicillin, doxycycline, and erythromycin (Shin and Spielman, 1993) for Lyme disease were studied in a rodent model. Among those, erythromycin was the one worked worst. However, its derivative azithromycin (AZ) showed similar effectiveness in the treatment of early Lyme disease as amoxicillin but with less side effects (Massarotti, Et al. 1992). When compared to doxycycline and erythromycin, azithromycin even possessed superior efficacy (Piesman, et al. 2014). These advantages of azithromycin should be ascribed to its lower minimum inhibitory concentration and quicker onset time (Knauer, et al. 2011; Piesman, et al. 2014). Considering the difficult diagnosis in the early stage of Lyme disease and serious clinical signs in its late stage (Knauer, et al. 2011; Piesman, et al. 2014), quick initiation of a dermal azithromycin treatment after tick exposure should pave the way for preventing Lyme disease.

There are already some groups studying azithromycin topical formulation such as ethanol-solution-gel (Knauer, et al. 2011; Schwameis, et al. 2017) and azithromycin Lipoderm cream (Piesman, et al. 2014). The former one was demonstrated effective in human clinical phase III trial and the latter one was effective in a murine model. But both of them used azithromycin raw drug powder in their dermal vehicles, which would reduce the dermal bioavailability due to the hydrophobicity of azithromycin (Mishra, et al. 2009). Nanocrystals are assumed to be a good alternative herein. Their advantages on dermal application are ascribed to the nano size compared with micrometer sized raw drug powders: 1) The decreased particle radius brings enhanced saturation solubility due to Ostwald-Freundlich equation (Mauludin, et al. 2009); 2) The smaller size results in enlarged curvature of the particle surface, followed by increased dissolution pressure and dissolution velocity according to Kelvin equation (Pardeike, et al. 2010); 3) The nano size causes enlarged surface area, combined with the increased concentration gradient due to the increased saturation solubility, they facilitate enhancing dissolution velocity based on Noyes-Whitney equation (Müller, et al. 2011). Both of the increased saturation solubility and increased dissolution velocility will lead to enhanced diffusive flux of the drug through the stratum corneum because of Fick’s first law of diffusion (Zhai, et al. 2014). Thus, improved dermal bioavailability is achieved in considering of the enhanced penetration (Müller, et al. 2011). Moreover, nanocrystals can obtain increased adhesiveness to skin due to the enlarged contact area (Pyo, 2016). Thus, this study was designed to optimize azithromycin nanocrystals for topical administration as well as to investigate the effect of nanonization on its anti-Lyme disease potential compared to the clinical effective ethanol-solution-gel and the gel with penetration enhancer.

3.1.3. Experimental Section

3.1.3.1. Materials

Azithromycin (AZ) in short for azithromycin dihydrate (contains 95.4% azithromycin) was bought from Haohua Industry (Jinan, China). Capryl glucoside (Plantacare® 810 UP), decyl glucoside (Plantacare® 2000 UP), poloxamer 188 (Kolliphor® P188), poloxamer 407 (Kolliphor® P407) and D-α-tocopheryl polyethylenglycol 1000 succinate (Kolliphor® TPGS) were kindly provided from BASF SE (Ludwigshafen am Rhein, Germany). Hydroxypropyl cellulose (Klucel GF®, viscosity of 2% in water at 25 °C 300 mPa s, MW 370,000 Da), Miglyol® 812, and polysorbat 80 (Tween® 80) were purchased from Caesar & Loretz GmbH (Hilden, Germany) and 1,2-Propanediol (propylene glycol) by Alfa Aesar GmbH & Co. KG (Karlsruhe, Germany). Yttrium-stabilized zirconium oxide milling beads having a diameter of 0.1 mm were obtained from Hosokawa Alpine (Augsburg, Germany). Ethanol at 96% was used of analytical grade. The Milli-Q water was obtained by reverse osmosis from a Millipak® Express 20 Filter unit (MPGP02001, Merck, Millipore KGaA, Darmstadt, Germany).

3.1.3.2. Optimized formulation of azithromycin nanocrystals

3.1.3.2.1. Optimized production by high pressure homogenization (HPH)

The high pressure homogenizer Micron LAB 40 (HPH, APV GmbH, Mainz, Germany), equipped with a water jacket for temperature control, was first used to produce azithromycin nanocrystals. The formulations contained 10.0% (w/w) azithromycin and 1.0% (w/w) surfactant dispersed in Milli-Q water. Pre-suspension was produced by suspending the coarse azithromycin powder in the aqueous surfactant solution via high shear mixing using an Ultra-Turrax T25 (Janke & Kunke Gmbh & Co. KG, Germany) for 1 minute at 8,000 rpm. The so obtained pre-suspension was first homogenized by HPH at low and moderate pressures (250 and 500 bar, 2 cycles each) and subsequently at 1,500 bar

for 20 homogenization cycles. The whole homogenization process was performed at 5 °C. Particle size was monitored in dependence of homogenization cycles after 1, 5, 10, 15 and 20 cycles.

3.1.3.2.2. Optimized production by bead milling (BM)

Bead milling (BM) was also applied to produce azithromycin nanosuspensions to compare the results with the HPH method. Pre-suspensions with the same composition were identically produced as in section 3.1.3.2.1. Next, wet bead milling was performed with yttrium-stabilized zirconium oxide beads (0.1 mm diameter) using a discontinuous propeller mill (PML 2, Bühler AG, Uzwil, Switzerland) at a rotation speed of 2,000 rpm. The process was performed at 5 °C by controlled circulation of cooled water through an outer jacket. Particle size was analyzed in dependence of milling time after 5, 10, 15 and 30 minutes.

3.1.3.2.3. Production of nanocrystals by combination technology (CT)

Combination technology (smartCrystals-technology) (Pyo, 2016) with the combination of bead milling and HPH was performed in this study to produce nanocrystals as well. The best two receipts selected from the bead milling method were first possessed by bead milling, a relatively low energy process (Al-Shaal, et al. 2011) as described in section 3.1.3.2.2. In the second subsequent step, these nanosuspensions were passed through HPH (relatively high energy process) at low pressure of 300 bar for 1 cycle at 5 °C to further reduce the particle size for increased physical storage stability.

3.1.3.3. Preparation of dermal azithromycin formulation

3.1.3.3.1. Preparation of azithromycin ethanol-solution-gel as reference

Ethanol-solution-gel consisted of 10.0% azithromycin raw drug powder (RDP), 77.5% ethanol (94%), 0.5% polyacrylate, 5.0% HPC and 7.0% Miglyol® 812 was produced as

described (Knauer, et al. 2011). This formulation was selected as reference (gel A) due to its demonstrated effectiveness in clinical studies up to phase III (Schwameis, et al. 2017).

3.1.3.3.2. Preparation of azithromycin nanocrystals containing dermal gel

Hydroxypropyl cellulose (HPC) powder at 10.0% (w/w) was added to 75 °C hot Milli-Q water respectively in a mortar, followed by stirring using a pestle to obtain a fine suspension (10.0% HPC gel base). After 24 hours in a fridge (4 °C ± 2 °C), a transparent gel base free of lumps and air bubbles was obtained. Evaporated Milli-Q water during production and storage was added as last step to the gel base. The best azithromycin nanosuspension at 10.0% (w/w) was incorporated into the 10.0% HPC gel base with a final concentration of 5.0% azithromycin and 5.0% (w/w) HPC (gel B). To obtain gel C and gel E, propylene glycol (PG), a common penetration enhancer (Watkinson, et al. 2009), was first mixed with the gel base to get a homogeneous appearance, followed by the mixture with the best formulation (gel C) or RDP (gel E) to obtain a 5.0% (w/w) HPC gel contains 20.0% (w/w) PG and 5.0% (w/w) azithromycin. The gel with RDP but without penetration enhancer (gel D) was also prepared as comparison. Surfactant was added in the gel to exclude its influence when compared the difference between nanosuspension and RDP. The final amount of each excipient for gel B – gel D is listed in Tab. 1.

Table 1: Composition (w/w) of azithromycin HPC gels.

	azithromycin	propylene glycol (PG)	HPC	TPGS	Milli-Q water
gel B	5.0% nanocrystals	/	5.0%	0.5%	89.5%
gel C	5.0% nanocrystals	20.0%	5.0%	0.5%	69.5%
gel D	5.0% RDP	/	5.0%	0.5%	89.5%
gel E	5.0% RDP	20.0%	5.0%	0.5%	69.5%

3.1.3.4. Characterization

3.1.3.4.1. Photon correlation spectroscopy (PCS)

Photon correlation spectroscopy (PCS, Zetasizer Nano ZS, Malvern Instrument, UK) was used to measure the mean particle diameter and polydispersity index (PDI) of nanocrystals by dynamic light scattering. The PCS diameter stands for the intensity weighted mean diameter of the bulk population and the PDI represents the width of the size distribution. For the measurement 10 µl nanosuspension was diluted in 10 ml Milli-Q water. 10 single measurements were done for one sample and the mean calculation. The detectable size range of PCS is from approximately 3 nm to 3 µm (Romero, et al. 2016).

3.1.3.4.2. Laser diffractometry (LD)

Laser diffractometry (LD, Mastersizer 2000, Malvern Instrument, UK) was used to detect large particles or aggregates beyond the PCS measuring range by static light scattering. Its measuring range is from around 20 nm to 2,000 µm (Romero, et al. 2016). The results were displayed by volume weighted diameters d(v)50% and d(v)90%, meaning that 50% or 90% of the particles were below the given value of d(v)50% or d(v)90%, respectively. The real refractive index of 1.532 and imaginary refractive index of 0.01 were used for azithromycin and real refractive index of 1.330 was used for water to calculate the volume diameters following the Mie theory.

3.1.3.4.3. Zeta potential (ZP)

Zeta potential (ZP) represents the electrostatic charge on the surface of the particle (Pyo, et al. 2016) and can be converted from the electrophoretic mobility of a particle (Müller and Jacob, 2002), determined by electrophoretic light scattering in the Zetasizer Nano ZS (Malvern Instrument, UK). It can be used to predict the physical stability of colloidal suspensions, where absolute values higher than 30 mV represent a electrostatically good stabilized system. The measurements were performed in two different media: conductivity

adjusted Milli-Q water (50 µS/cm, pH 5.5), and original medium (aqueous phase of the formulation).

3.1.3.4.4. Light microscope (LM)

Light microscope (BA210LED) equipped with a digital camera (Moticam 3.0 MP, both from Motic Deutschland GmbH, Germany) was used at magnifications of 100 and 600 to detect large particles or aggregates within nanosuspensions. Another light microscope (Orthoplan, Leitz, Germany) equipped with a digital camera (CMEX-1, Euromex microscope, Netherlands) was used for the detection of any microcrystals in gel samples at a magnification of 160.

3.1.3.4.5. Transmission electron microscope (TEM)

The morphological examination of the optimal formulation was performed by a high resolution transmission electron microscope (TEM, Tecnai^{TM} G^2 20 S-TWIN, FEI Co., USA). 5 µl nanosuspension was dropped on cooper grids (400 mesh) with hydrophilized carbon films and stained with 1% (w/v) uranyl acetate. The supernatant liquid was removed by filter paper and the left grid air-dried. An acceleration voltage of 160 kV was performed in the TEM analysis.

3.1.3.4.6. X-ray diffraction (XRD)

The crystalline state of the optimal formulation and RDP was estimated by X-ray diffraction (XRD, Philips PW 1830, Netherlands). The experiments were performed in symmetrical reflection mode with a Cu-Kα line as the source of radiation. Standard runs using a 40 kV voltage, a 25 mA current and a scanning rate of 0.04°/2 seconds over a range of 0.6-40° were applied. The tested nanosuspension was mixed with a guar gum (1.5% w/w) until creamy and put into a sample holder with a volume of 0.06 ml. The RDP was directly put into the sample holder.

3.1.3.5. Dissolution test and saturation solubility

Dissolution test and saturation solubility study were performed in an Innova 4230 shaker (New Brunswick Scientific GmbH, Nürtingen, Germany) at 25 °C and 100 rpm. Besides Milli-Q water, water-propylene glycol mixture (20% propylene glycol w/w) was also selected as dispersion medium. Samples were filled in 40 ml glass vials and the dispersion medium added, resulting in an azithromycin concentration of 2% (w/w). All vials were sealed with caps to avoid evaporation during shaking. 2 ml sample was withdrawn from each vial using a syringe after 1, 2, 4, 8 and 24 h and an equivalent amount of dispersion medium was replenished. All withdrawn samples were diluted immediately 2 times by the dispersion medium to avoid re-crystallization. Un-dissolved drug was separated by Amicon® ultra centrifugal filter units with a molecular weight cut-off of 3,000 Da (Millipore Ireland Ltd, Tullagreen, Ireland) at 2,082 × g (Sigma 3K18 centrifuge, Harz, Germany) at room temperature for 15 minutes. The azithromycin concentration of particle free solution passed through the filter representing the amount of dissolved drug was analyzed by HPLC. All experiments were done in triplicate.

3.1.3.6. Ex vivo porcine ear penetration study

The stratum corneum of porcine ear skin is demonstrated to be suitable for human dermatological research due to its layer thickness and morphological similarity (Gallagher, 2005). Freshly excised porcine ears were obtained from domestic pigs in a local abattoir. The ears were washed and hairs removed by careful shaving before the performance of the penetration assay. 100 mg of each gel (gel A – gel E) was evenly applied onto the porcine ear skin having an area of 1.5 × 1.5 cm^2. After 20 minutes penetration time, adhesive tapes (tesafilm® crystal clear, No. 57315, 10 m × 15 mm, teas SE, Norderstedt, Germany) were pressed onto the treated areas using a roller for evenly distributed pressure. The skin was stripped sequentially and the removed tapes were

collected in individual glass vials. 30 tapes in total were used to remove the stratum corneum on one with sample treated area. The azithromycin in each tape was extracted in 2 ml acetonitrile/DMSO (1:1, v/v) mixture by shaking (Innova 4230 shaker, New Brunswick Scientific GmbH, Nürtingen, Germany) for 3 h at 120 rpm and 25 °C. Afterwards, the extracts were centrifuged at 15,493 × g for 15 minutes (Heraeus Megafuge Centrifuge 3.0R, Kendro Laboratory Products GmbH, Hanau, Germany) and the so obtained supernatant was analyzed by HPLC.

3.1.4. Results and Discussions

3.1.4.1. Optimized formulation of azithromycin nanocrystals

3.1.4.1.1. Screening of different surfactants and production parameters for the optimal size of azithromycin nanocrystals produced by HPH

Four nonionic surfactants TPGS, poloxamer 407, Plantacare® 810 and Plantacare® 2000 were used to produce azithromycin nanocrystals. Nonionic surfactants are selected because of their lower toxicity (Gibson, 2009) and lower irritation potential compared to ionic surfactants (Ghosh, et al. 2012). Considering the final particle size and the efficiency, 15 cycles at 1,500 bar was set as optimal parameter to produce 10.0% azithromycin nanosuspension stabilized with 1.0% TPGS, leading to a mean particle size of 427 nm with PDI of 0.403 (Fig. 1). In general, more homogenization cycles can lead to smaller particle size (Möschwitzer, 2013). However, too much energy (more cycles) can promote aggregation during storage. The aggregation happened due to the acceleration of crystals, resulted from the enhanced kinetic energy of the crystals (Kakran, 2012). In Fig. 1, TPGS stabilized nanoparticles showed a decrease in PCS diameter until 15 cycles. Further cycles even resulted in slight increase of the particle size. Similar phenomenon that size increases by more homogenization cycles also happened in the case of Plantacare® 810 UP and Plantacare® 2000 UP.

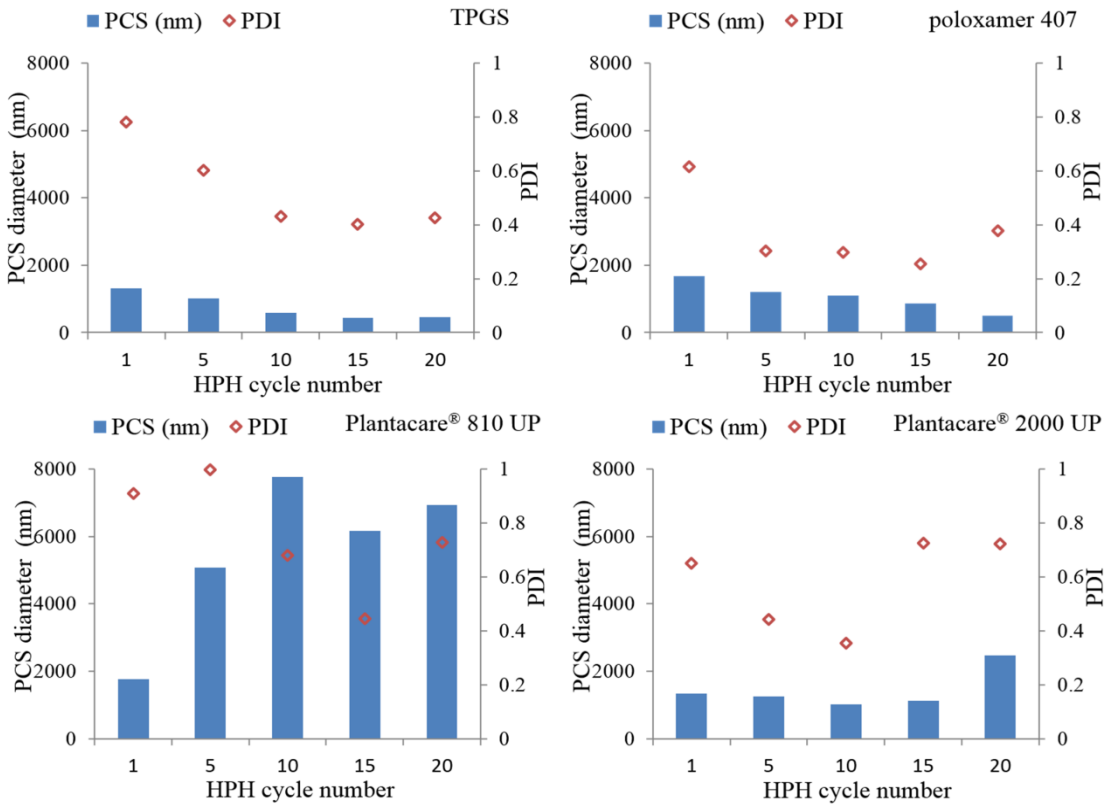

Fig. 1. PCS mean particle size and PDI of freshly produced azithromycin nanocrystals stabilized with TPGS, poloxamer 407, Plantacare® 810 UP or Plantacare® 2000 UP, in dependence of applied HPH cycle number.

3.1.4.1.2. Screening of different surfactants and production parameters for the optimal size of azithromycin nanocrystals produced by BM

By only 10 minutes, wet bead milling of TPGS stabilized formulation with PCS diameter of 189 nm and PDI of 0.194 was achieved (Fig. 2). Increasing the milling time led to gelation of the formulation. Also with poloxamer 407 azithromycin nanocrystals with PCS diameter of 185 nm and PDI of 0.234 could be achieved after slightly longer milling time of 15 minutes. The lower PDI of the TPGS stabilized formulation compared to the poloxamer 407 formulation represents a narrower size distribution and thus often a higher physical storage stability due to slower Ostwald ripening (Müller and Jacobs, 2002). The nanosuspension stabilized with Plantacare® 810 UP and Plantacare® 2000 UP gelled after 5 minutes milling due to agglomeration or crystal growth of very small particles, resulting

from the thermodynamically unstable nanosuspension (supersaturation). This phenomenon occurred with the change of the Gibbs free energy of the system during the milling process (Ghosh, et al. 2012) and the stabilizer could not provide enough coverage. Furthermore, in the cases of poloxamer 407 and Plantacare® 2000 UP, analogous enhancement of the particle size occurred with the increased milling time as what happened in HPH method. This was due to the additional input of energy enhancing the kinetic energy of the crystals, causing aggregation (Kakran, et al. 2012).

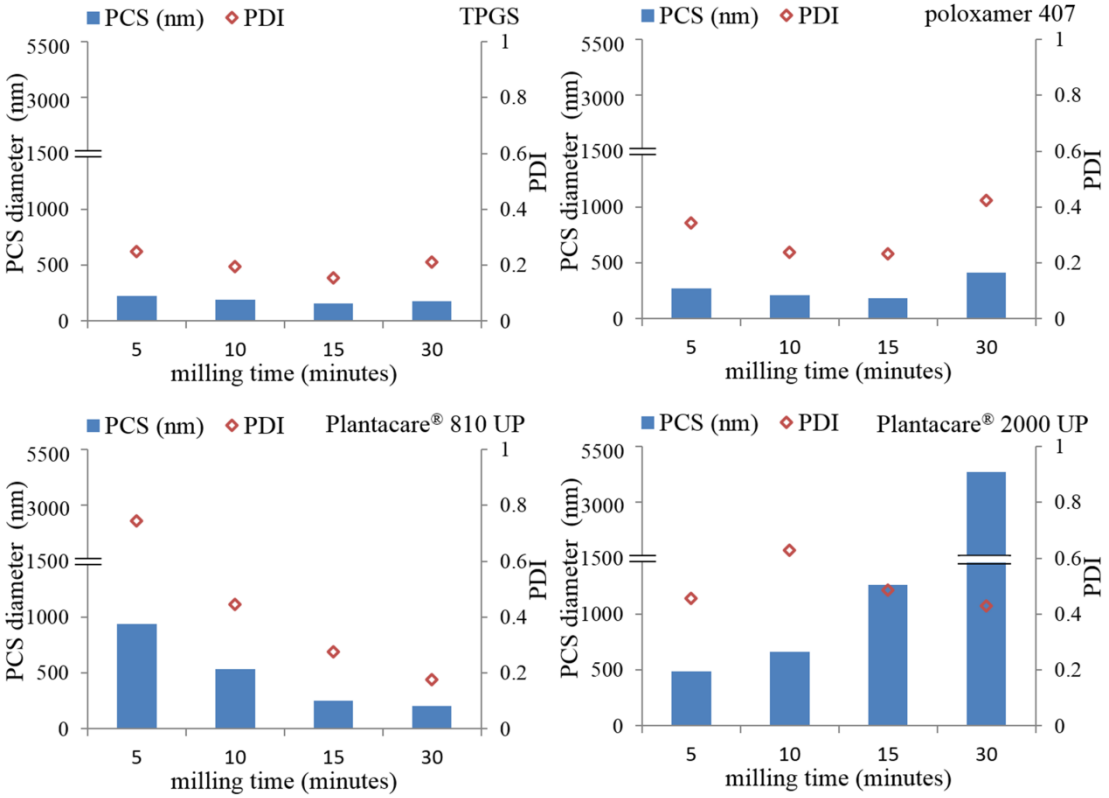

Fig. 2. PCS mean particle size and PDI of freshly produced azithromycin nanocrystals stabilized with TPGS, poloxamer 407, Plantacare® 810 UP or Plantacare® 2000 UP, in dependence of bead milling time (minutes).

3.1.4.1.3. Production of nanocrystals by combination technology (smartCrystals -technology)

The best two formulations produced by BM – one stabilized with TPGS (milling time 10

minutes) and another with poloxamer 407 (milling time 15 minutes) – were further produced by 1 HPC cycle at 300 bar and 5 °C. The particle sizes and zeta potentials of the obtained nanocrystals produced by the combination technology are shown in Fig. 3, as well as the corresponding data of BM products. In both cases of TPGS and poloxamer 407 stabilized nanosuspensions, subsequent processing by HPH in the combination technology did not lead to further size reduction but only lead to a slightly improvement in particle size distribution. In the case of TPGS, the combination technology even resulted in bigger d(v)90%. This could be explained by the possible increase in temperature during HPH process, resulting in increased solubility of drug, which followed by particle growth after cooling down. In sum, the best method to produce azithromycin nanocrystals in this study is bead milling.

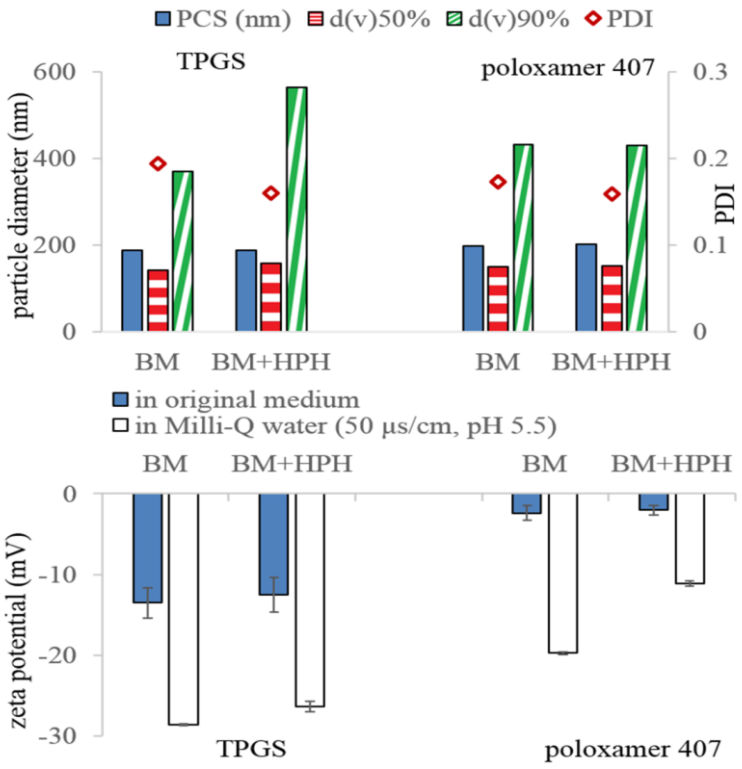

Fig. 3. Particle size (PCS diameter, LD diameter d(v)50%, d(v)90%) and PDI (upper) as well as zeta potential (lower) measured in original medium and in conductivity adjusted Milli-Q water of azithromycin nanocrystals stabilized by either TPGS or poloxamer 407 and produced by 2 methods on day 0.

The data measured in conductivity adjusted water represents the Stern potential, which is proportional to the Nernst potential, indicating the surface charge density (Mishra, et al. 2009; Pyo, et al. 2016). On contrary, the thickness of the diffuse layer (Pardeike, et al. 2011) can be predicted by the absolute value measured in original medium. Nernst potential and thickness of the diffuse layer are the two factors affecting the zeta potential. The higher the absolute value of the Nernst potential is, the higher is the absolute value of the zeta potential. The thicker the diffuse layer, the higher the zeta potential is (Mishra, et al. 2009). However, the announcement that a formulation is considered as stable when it possesses a zeta potential above |-30 mV| (Al-Shaal, 2011) is only applicable in the situation with low-molecular weight surfactants or with electrostatic contribution in dispersion medium (Mishra, et al. 2009). Steric surfactant such as TPGS or poloxamer 407 can also retain physical stability even with small absolute value in original medium. The dimension of the steric surfactant which adsorbed to the surface of the nanocrystals, shifts the shear plane further away from the particle surface, resulting in smaller measured zeta potential in original medium than that in conductivity adjusted Milli-Q water (Pardeike and Müller, 2010). That explains the fact that all the absolute value of measured zeta potential in original medium herein was smaller than their corresponding data in Milli-Q water (Fig. 3).

3.1.4.1.4. Further surfactants screening for azithromycin nanocrystals produced by BM

Two popular nonionic surfactants poloxamer 188 and Tween® 80 were further used to stabilize azithromycin nanocrystals produced by the best method – bead milling. Tween® 80 stabilized formulation had to be produced for 10 minutes by BM to obtain nanocrystals with PCS particle size of 196 nm and PDI of 0.170. While poloxamer 188 did not show a very promising particle size compared to Tween® 80. Thus, after all the screening, TPGS, poloxamer 407 and Tween® 80 were selected as stabilizers for further study.

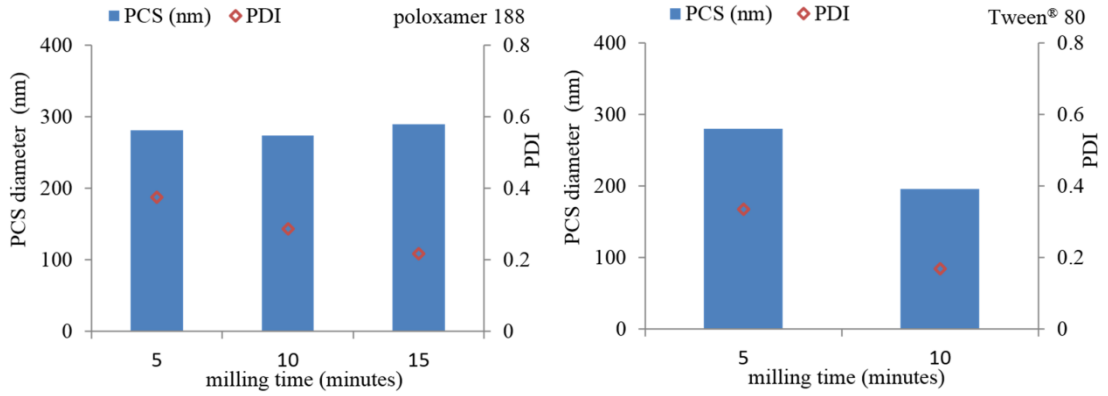

Fig. 4. PCS mean particle size and PDI of freshly produced azithromycin nanocrystals stabilized with poloxamer 188 or Tween® 80 in dependence of bead milling time (minutes).

3.1.4.1.5. Short-term stability of nanocrystals stabilized with TPGS, poloxamer 407 and Tween® 80

Azithromycin nanocrystals stabilized with TPGS, poloxamer 407 or Tween® 80 were produced by bead milling for 10, 15 and 10 minutes, respectively. Even though Tween® 80 stabilized azithromycin nanocrystals had almost similar PCS mean diameter compared with the TPGS stabilized formulation (Fig. 5), large particles or aggregates (d(v)90% > 2 µm) were already detected by LD on day 0. Why the PCS mean particle size is almost similar for both formulations even though the Tween® 80 stabilized formulation had particles larger than 2 µm can be explained by the different detecting ranges of both methods. PCS is not prone to detect the presence of large particles or aggregates as good as LD is (Romero, et al. 2016). In contrast, the formulation stabilized with TPGS had no pronounced alterations for both PCS and LD values over a period of 30 days at RT being still in nanometer dimension (PCS diameter < 240 nm with PDI < 0.2 and d(v)90% < 1 µm). Poloxamer 407 could stabilize the azithromycin nanocrystals better than Tween® 80 over 30 days, but was not as good as TPGS did. In sum, TPGS is the optimal surfactant to stabilize azithromycin nanocrystals among the test. Therefore, the physically most stable azithromycin nanocrystals at 10.0% (w/w) can be obtained by TPGS stabilization at 1.0% (w/w) and 10 minutes bead milling at 5 °C and was selected as the best formulation in this

study.

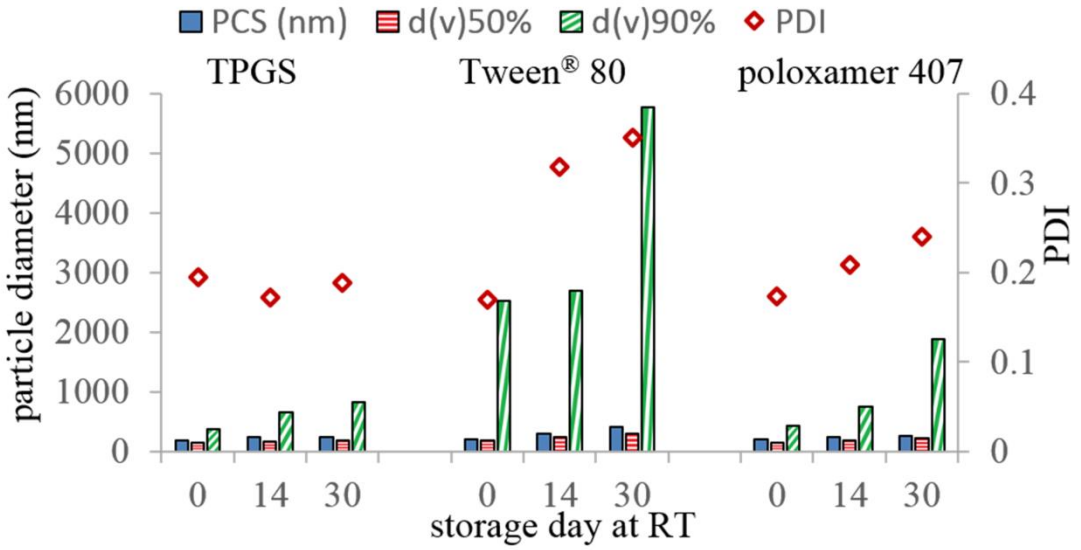

Fig. 5. Particle size (PCS diameter, LD diameter d(v)50%, d(v)90%) and PDI of azithromycin nanocrystals stabilized with TPGS, Tween® 80 or poloxamer 407 over a period of 30 days at RT.

3.1.4.2. Characterization of the optimal formulation

3.1.4.2.1. Transmission electron microscope (TEM)

The morphological characterization of the optimal formulation after 30 days storage at room temperature (RT) is shown in Fig. 6. Three different magnifications were used to analyze the particles. The best formulation (1.0% TPGS stabilized azithromycin nanocrystals at 10.0% produced by 10 minutes bead milling) had spherically shaped azithromycin particles. Most particles were smaller than 1,000 nm, consistent with the d(v)90% value shown in Fig. 5.

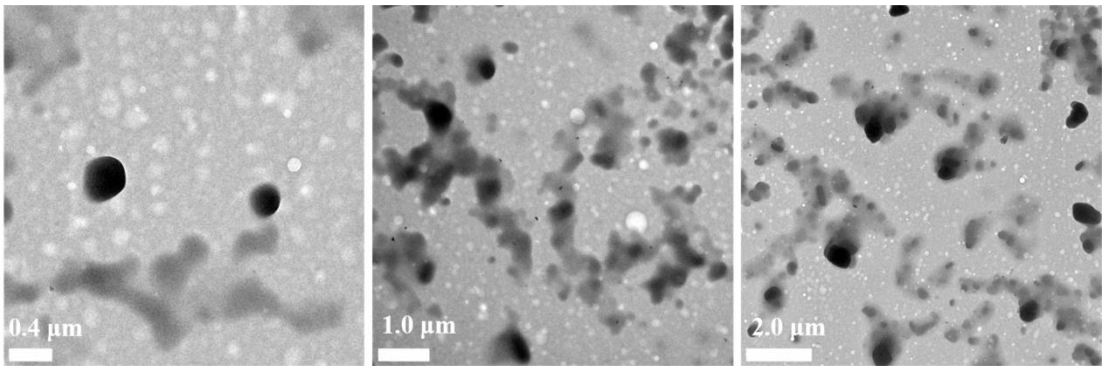

Fig. 6. TEM micrographs of the optimal azithromycin nanosuspension (black particles) after 30 days storage at RT (scale bars from left to right: 0.4 µm, 1.0 µm and 2.0 µm).

3.1.4.2.2. X-ray diffraction (XRD)

X-ray diffraction patterns of the raw drug powder (RDP) and optimal azithromycin nanocrystals (NC) can be found in Fig. 7. From RDP analysis by X-ray scattering, two main characteristic crystalline peaks of azithromycin were founded at 9.96° and 18.8° (Fig. 7, blue graph). The NC also had peaks at both positions, indicating that bead milling did not affect the crystal state of azithromycin. The increase of the baseline of nanocrystals from 20 degree (deg) to 40 degree is due to the water inside of the nanosuspension.

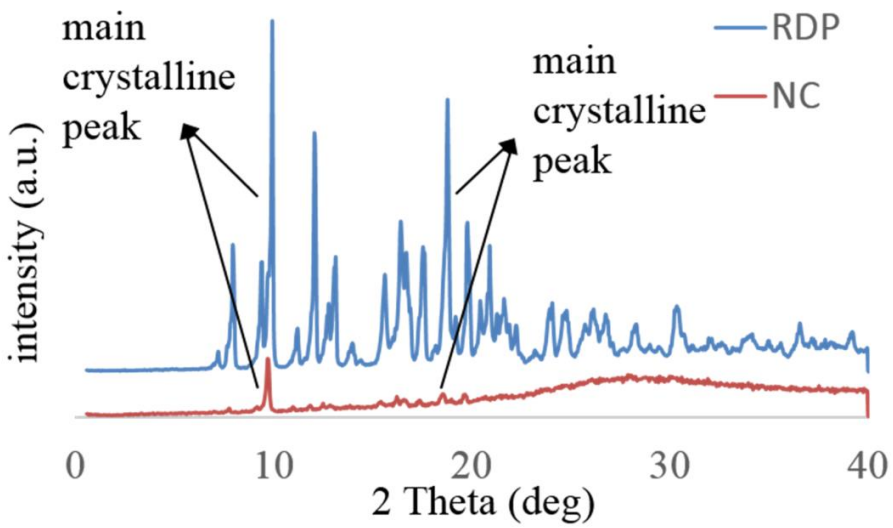

Fig. 7. X-ray diffraction patterns of azithromycin RDP (blue) and optimized azithromycin nanosuspension (NC, red).

3.1.4.3. Optimal storage temperature of nanocrystals stabilized with TPGS

Physical short-term stability data of TPGS stabilized azithromycin nanocrystals produced by 3 different methods and stored at 3 different temperatures (fridge (4 °C ± 2 °C), room temperature (RT, 20 °C ± 2 °C), oven (40 °C ± 2 °C)) are shown in Fig. 8. The samples produced by BM showed the best physical stability at all temperatures. Only by producing the azithromycin nanocrystals by BM, the particle size stayed still in nanometer range (PCS diameter < 300 nm with PDI < 0.25 and d(v)90% < 1 µm) over a storage time of 90 days independently from the storage temperature. The samples stored at 40 °C even showed the smallest PCS diameter of 215 nm and d(v)90% of 0.872 µm over a storage time of 90 days. This can be explained by the increased solubility of azithromycin by increased temperature, resulting in reduced particle size (Mishra, et al. 2009). But this does not mean that the optimal storage temperature for the nanosuspension is 40 °C. First, small particles will dissolve faster than bigger ones. If this formulation cools down to room temperature for use, re-crystallization will take place more pronounced on the surface of the bigger particles. Thus, small particles will dissolve, where the bigger particles will growth. Moreover, as shown in the upper part of Fig. 9 A, the sample stored in oven for 3 months changed its color from white to yellow. Interestingly, all other samples stored at identical conditions but stabilized by another surfactant did not change their color (Fig. 9 A middle). Thus, it can be concluded that TPGS and not the active azithromycin was ascribed to this phenomenon. The melting point of TPGS is around 37-41 °C (Shin and Kim, 2003), TPGS would become yellow liquid after melting as shown in Fig. 9 B. Usually, degradation of TPGS would not happen during melting process around 40 °C (Shin and Kim, 2003). However, the pH of the 1.0% TPGS stabilized AZ nanosuspension was around 8.5. Hydrolysis of the ester bond of TPGS might happen under this pH 8.5 situation during the storage time of 90 days at 40 °C, resulting in light yellow α-tocopherol, which would be easily oxidized under pH 8.5 and 40 °C, leading to a more yellow tocopheryl quinine (Brigelius-Flohé and Traber, 1999).

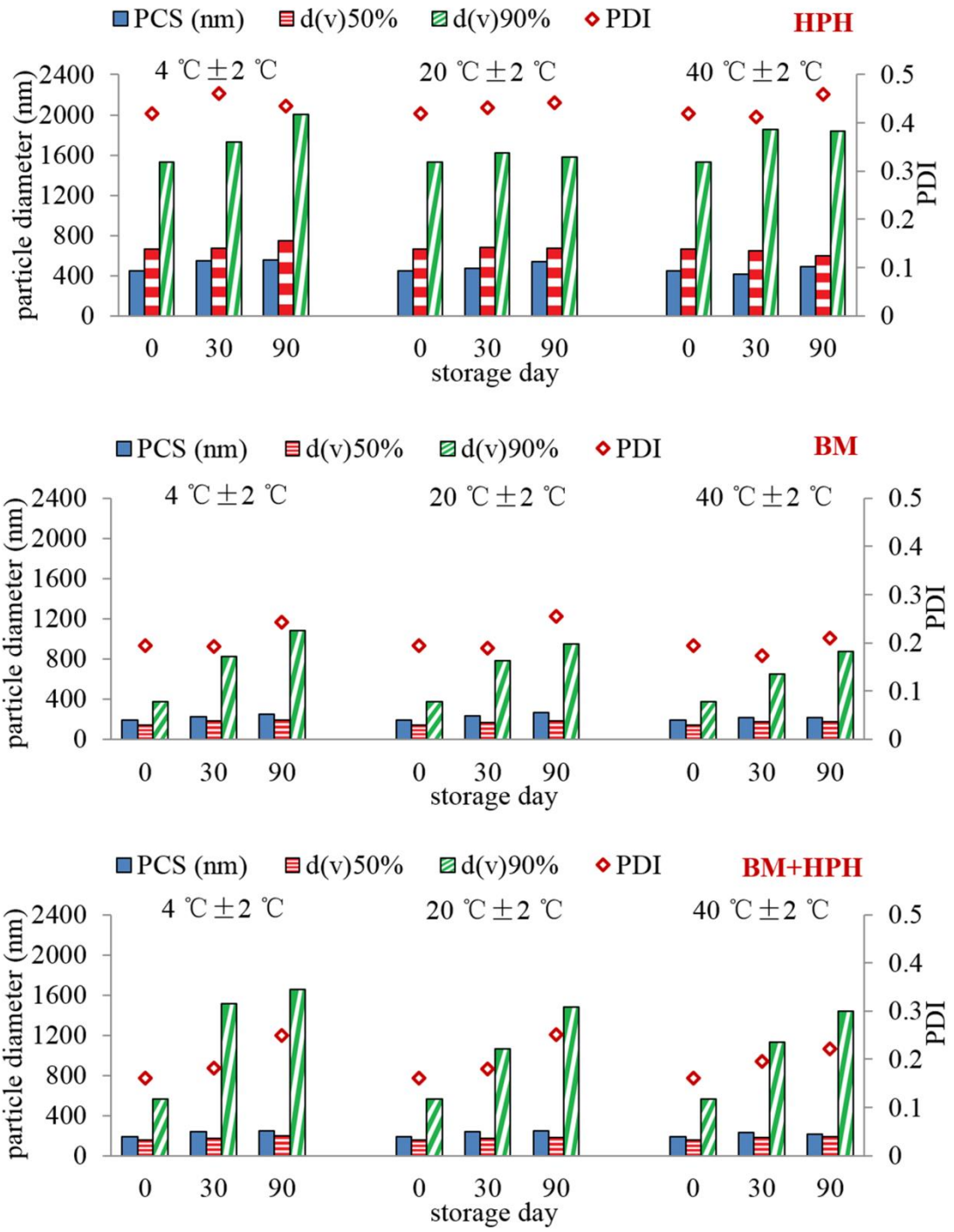

Fig. 8. Particle size (PCS diameter, LD diameter d(v)50%, d(v)90%) and PDI of TPGS stabilized azithromycin nanocrystals produced by 3 methods over a period of 90 days at 4 °C, RT and 40 °C.

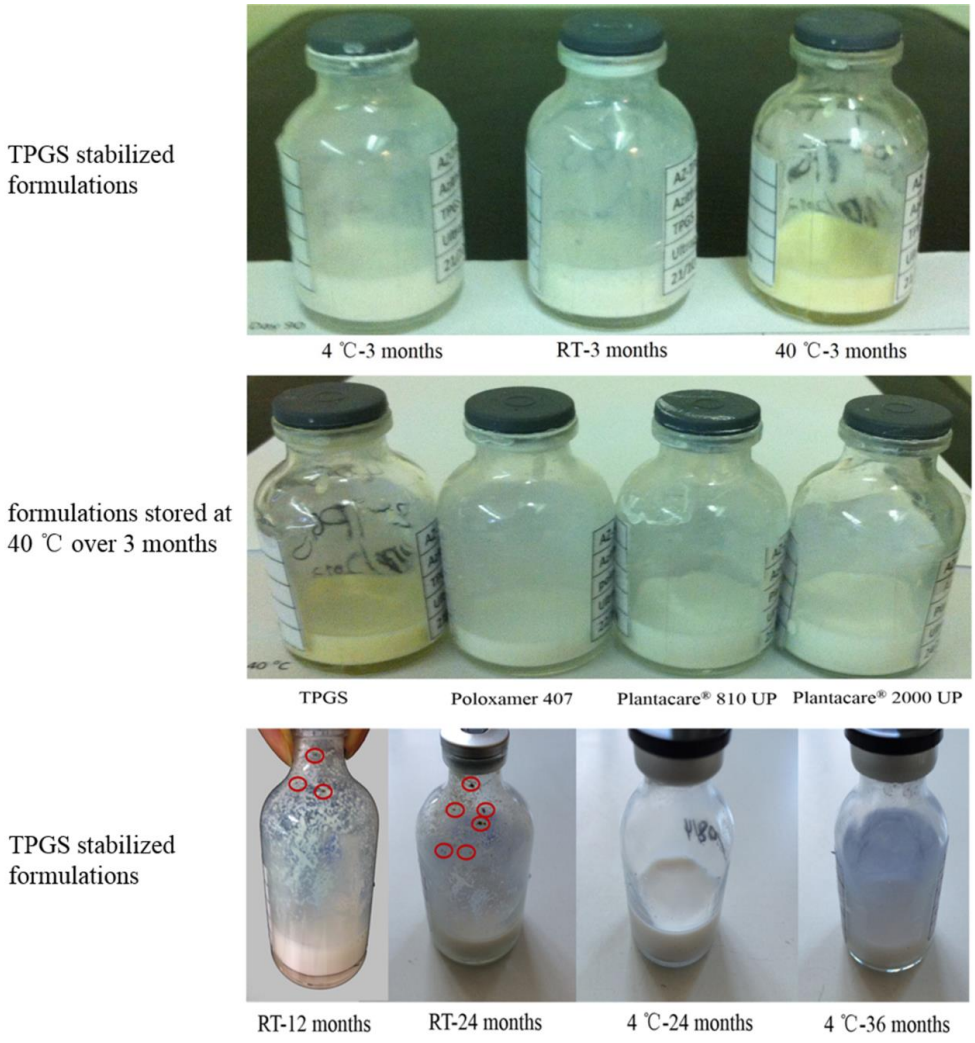

Fig. 9. (A) Macroscopic appearance of azithromycin nanosuspension stabilized with TPGS and stored for 3 months at 3 different temperatures (upper); azithromycin nanosuspension stabilized with 4 different surfactants and stored at 40 °C for 3 months (middle) and TPGS stabilized azithromycin nanosuspension stored at either 4 °C or RT over a period up to 36 months (lower) with visible bacterial growth, marked in red circles.

Fig. 9. (B) Macroscopic appearance of TPGS melted at 40 °C.

Even though the particle size of the formulation produced by BM was similar either stored at RT or 4 °C less than 3 months (Fig. 8 middle), the samples stored at RT showed d(v)90% of 2.305 µm only over a storage time of 6 months, while that stored at 4 °C only showed d(v)90% of 1.250 µm over a storage time of 24 months (Fig. 10 A). In addition, the samples had been subjected to microbial attack when stored at RT after 12 months (Fig. 9 A lower). In the opposite, the samples avoid the attack of bacterial when stored in fridge up to 36 months. Thus, 4 °C ± 2 °C is the best storage condition for TPGS stabilized azithromycin nanocrystals in considering of both particle size and antimicrobial efficacy.

3.1.4.4. Physical long-term stability of the optimal formulation

The physical long-term physical stability of the best formulation (section 3.1.4.1.5) up to 36 months at 4 °C was analyzed by PCS, LD (Fig. 10 A) and light microscope (Fig. 10 B).

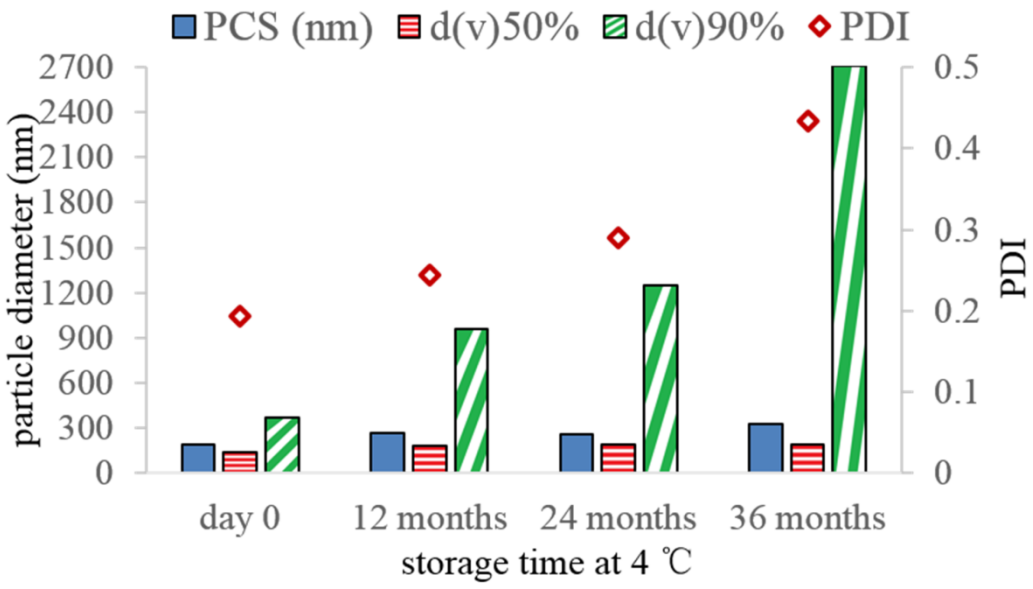

Fig. 10. (A) Particle size (PCS diameter, LD diameter d(v)50%, d(v)90%) and PDI of TPGS stabilized azithromycin nanocrystals produced by BM and stored at 4 °C over a period of 36 months.

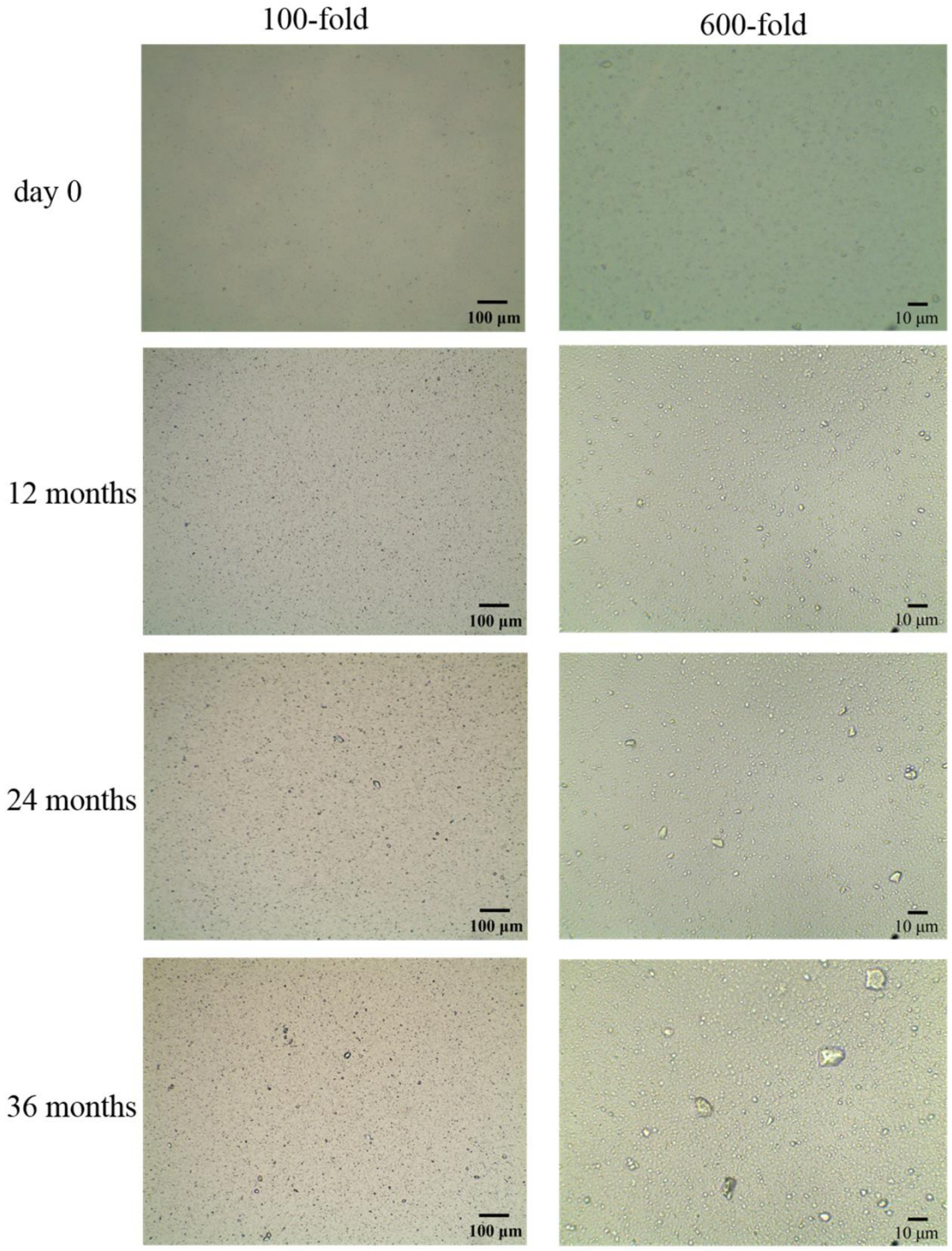

Fig. 10. (B) Light microscope pictures at 100-fold magnification (left) and at 600-fold magnification (right) of TPGS stabilized azithromycin nanocrystals produced by BM after production (day 0), 12 months, 24 months and 36 months storage at 4 °C (scale bars from left to right: 100 µm and 10 µm).

Sediment appeared after 12 months, but it was easily re-dispersible by shaking up for 10 seconds by hand. The longer the storage time, the more shaking time was necessary for re-dispersion. PCS diameter of the best formulation increased from 189 nm at day 0 to 269 nm after 12 months storage. But after 12 months storage, PCS diameter showed no pronounced alternations when compared to 24 months storage (269 nm versus 256 nm), while a slight increase in d(v)50% from 182 nm to 195 nm and d(v)90% from 957 nm to 1,250 nm was observed (Fig. 10 A). After 36 months of storage aggregation occurred, resulting in increased PCS diameter (326 nm), PDI (0.434) and d(v)90% (2,704 nm). These data are consistent with light microscope pictures shown in Fig. 10 B. Light microscope does possess the ability to monitor crystal growth reported by Gerry Steele (Steele, 2009). Homogeneous dispersed nanoparticles were observed by light microscope for the best formulation before 24 months, where aggregation and big particles were observed after 24 months at 4 °C.

3.1.4.5. Dissolution test and saturation solubility

The best nanocrystals (NC) and RDP were dispersed in Milli-Q water for the dissolution test. RDP in water with additional TPGS at identical concentration used for stabilizing the nanosuspension was also tested to exclude the influence of TPGS. According to Fig. 11 A, the addition of TPGS in water increased the dissolved azithromycin of RDP suspension but less than 2 times. On contrary, NC had around 2-3 times more dissolved azithromycin than RDP at all measuring points during the 8 h investigation period. Obviously, the dissolution velocity of NC was higher than RDP (200 µg/ml for NC and 71 µg/ml for RDP after 1 h), which can be mainly ascribed to the nanometer size following the Noyes Whitney equation (Müller, et al. 2013). It is well known that the nanometer-sized particles have an increased saturation solubility compared to its micrometer-sized counterpart due to Ostwald-Freundlich equation and Kelvin equation (Mauludin, et al. 2009; Pardeike, et al. 2010). This can be drawn from Fig. 11 A, where the amount of dissolved azithromycin is 3

times higher in the plateau area (242 µg/ml of NC versus 85 µg/ml of RDP at 4 h).

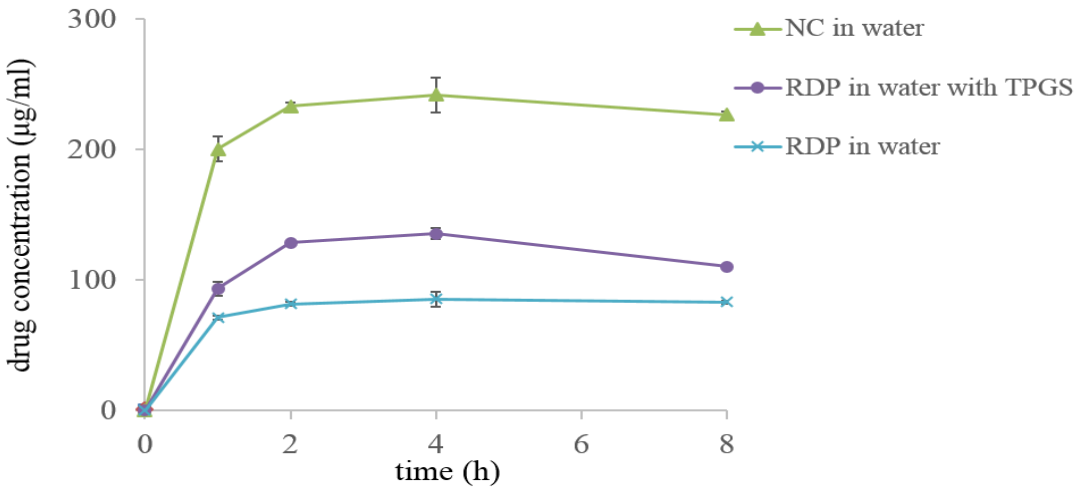

Fig. 11. (A) Dissolution profiles of the azithromycin nanocrystals (NC) in water, compared with RDP in the same dispersion medium at 25 °C after shaking of 8 h (n=3). RDP in water with TPGS was also tested herein for assessing the influence of TPGS in water.

Propylene glycol (PG) is one of the most common used penetration enhancers/cosolvent to help drugs dissolve more and penetrate more (Moser, et al. 2001). It is approved for dermal use due to its non-toxicity and well-tolerance (Ascencio, et al. 2016; Herkenne, et al. 2008). PG is also one of the humectancts, which can increase the moisturizing and occlusive effect of gels (Brown, et al. 2012). Moreover, PG is a low dielectric which can prevent the crystal growth (Zhai, 2013). 20% (w/w) PG was added into the original dispersion medium Milli-Q water to test the influence of PG on saturation solubility of azithromycin. 20% (w/w) was selected due to that the addition of 20% PG would not change the viscosity of the original gel too much (data not shown here). Thus, the influence of different viscosities of tested gels could be eliminated. In addition, 20% percentage PG could act as a preservative (Prickett, et al. 1961). More details of the influence of the percentage of the PG on drug can be read in references (Herkenne, et al. 2008; Moser, et al. 2001).

It can be concluded from the results displayed in Fig. 11 B that generally the azithromycin

dissolves much better in the dispersion medium containing PG compared to pure water. The saturation solubility of the NC in the water-PG mixture (NC in PG (20%)) was 2,648 µg/ml at 4 h, and that of the RDP in the water-PG mixture (RDP in PG (20%)) was 2,403 µg/ml at 8 h. The addition of TPGS did not make a big difference in this dispersion medium. The data was reasonable because PG is known to influence the solubility of the drug in the vehicle (Ascencio, et al. 2016; Smith, et al. 2001). The influence of PG in the dermal gel was further investigated as following.

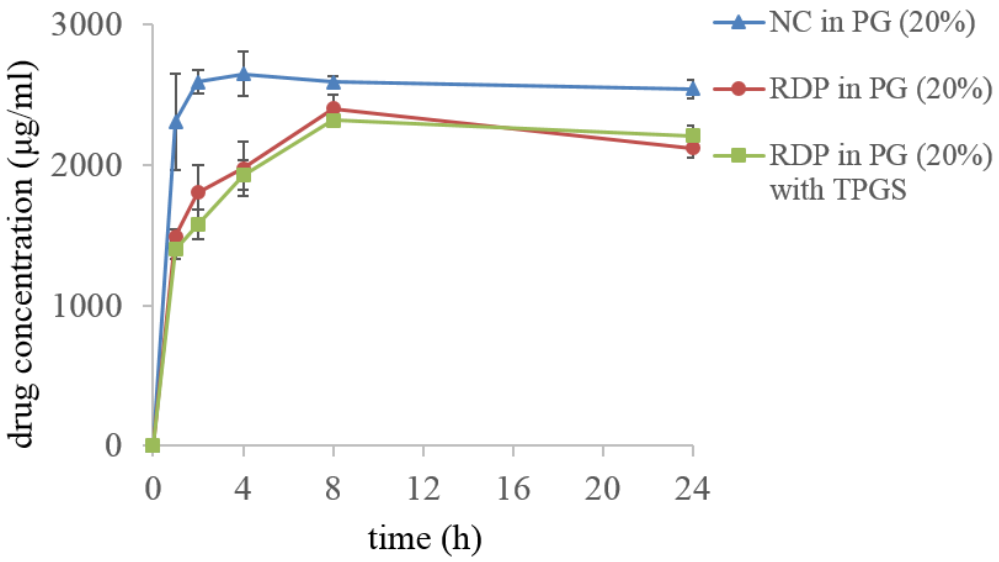

Fig. 11. (B) Dissolution profiles of the azithromycin nanocrystals (NC) in water-PG mixture (80:20, w/w) (in short: PG (20%)), compared with RDP in the same dispersion medium at 25 °C after shaking of 24 h (n=3). RDP in PG (20%) with TPGS was also tested herein for assessing the influence of TPGS in the dispersion medium.

3.1.4.6. Characterization of nanocrystals incorporated gels

The five gels were characterized by light microscope. Gel A (10.0% AZ-ethanol-solution-gel) was composed of 10.0% azithromycin RDP, 77.5% ethanol (94%), 0.5% polyacrylate, 5.0% HPC and 7.0% Miglyol® 812 (Knauer, et al. 2011). Gel B

(5.0% AZ-nano-HPC gel) was composed of 5.0% azithromycin nanocrystals with a PCS diameter of 189 nm, 0.5% TPGS, 5.0% HPC and 89.5% Milli-Q water. Gel C (5.0% AZ-nano-PG-HPC gel) was composed of 5.0% azithromycin nanocrystals with a PCS diameter of 189 nm, 0.5% TPGS, 5.0% HPC, 20.0% PG and 69.5% Milli-Q water. Gel D (5.0% AZ-RDP-HPC gel) was composed of 5.0% azithromycin RDP, 0.5% TPGS, 5.0% HPC and 89.5% Milli-Q water. Gel E (5.0% AZ-RDP-PG-HPC gel) was composed of 5.0% azithromycin RDP, 0.5% TPGS, 5.0% HPC, 20.0% PG and 69.5% Milli-Q water. The observations over a period of 14 days done by light microscope (Fig. 12) are as follows: azithromycin should be completely dissolve in gel A due to the high ethanol content of 77.5% (w/w), confirmed by the microscopic pictures at day 0. However, crystal growth could clearly be observed at day 7 and day 14. The explanation could be the supersaturation state of azithromycin in ethanol was thermodynamically unstable and resulted in re-crystallization (Moser, et al. 2001; Steele, 2009). This phenomenon was also observed by the group of R.C. McHugh (McHugh, et al. 2004), who concluded that the ethanol/water mixture with 100%, 90%, 80% and 70% (w/w) ethanol will cause crystallization or precipitation. In consideration of the high saturation solubility of azithromycin RDP/NC in PG (20%) (Fig. 11), 20% PG added into the gel was expected to keep more dissolved drug in the gel base. However, big particles were visible in this case of gel C (nanocrystal inside the gel mixed with 20% PG) at day 7 and day 14 because the supersaturated system is prone to accelerate crystal growth (Moser, et al. 2001; Steele, 2009). In addition, gel E (RDP inside the gel mixed with 20% PG) turned out possessing many big crystals in day 0. Their particle size decreased with storage time due to their solubility in PG. In contrast, no big difference was observed for gels without PG during the storage time: gel B (nanocrystal incorporated in the gel without PG) and gel D (RDP incorporated in the gel without PG). Thus, addition of the penetration enhancer PG is not a good way to keep the particle size of azithromycin nanocrystals stable in the HPC gel base.

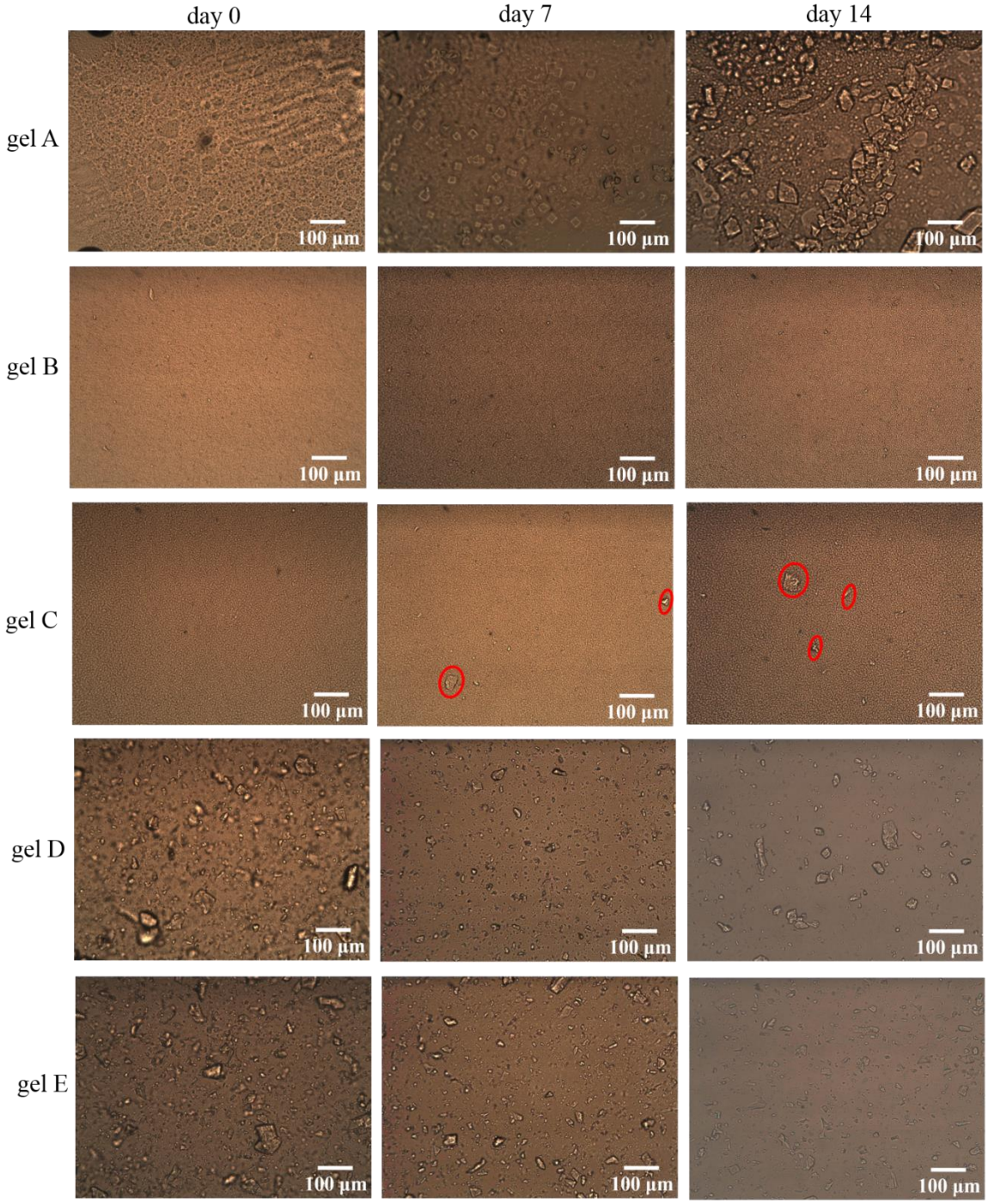

Fig. 12. Light microscope pictures at 160-fold magnification of gel A (ethanol-solution-gel), gel B (best nanocrystal in gel withtout PG), gel C (best nanocrystal in gel with PG), gel D (RDP gel without PG) and gel E (RDP gel with PG) directly after production (day 0), and after 7 and 14 days storage at room temperature (scale bar: 100 µm).

3.1.4.7. Ex vivo porcine ear penetration study

The total amount in µg of applied azithromycin with each tape is summarized in Fig. 13. The first tape was excluded from the analysis since almost the non-penetrated formulation on the skin surface was removed with it. Gel C (best nanocrystal in gel with PG) was expected to have higher penetration efficacy than gel B (best nanocrystal in gel withtout PG), regarding its higher saturation solubility of azithromycin shown in Fig. 11 and additionally due to the penetration enhancing property of PG (Smith, 2001). Surperisingly, the result was the opposite: azithromycin from gel B penetrated into deeper tapes with higher active concentrations compared to gel C according to Fig. 13. There are two possible explanations: First, the supersaturated situation of nanocrystals in gel with PG facilitated crystal growth in gel C (Steele, 2009), which was consistent with Fig. 12. Second, when applied on the skin, PG penetrated faster than the drug, which was confirmed by confocal Raman microscope (Ascencio, et al. 2016) and by stimulated Raman scattering microscope (Saar, et al. 2011). Means, PG penetrated faster and left nanocrystals behind in the upper part of the skin. With the loss of PG as solvent the azithromycin precipitated and penetration was further weakened. However, only the second explanation can additionally explain the phenomenon that gel C (best nanocrystal in gel with PG) penetrated even less than gel E (RDP in gel with PG). Because nanocrystals had higher solubility than RDP in the mixture of water and PG mentioned in Fig. 11, the absence of PG resulted in more precipitation of nanocrystals followed by less penetration.

Gel A, the one which was demonstrated effective in clinical (Knauer, et al. 2011; Schwameis, et al. 2017) only showed the higher penetration amount than gel B in tape 2 and tape 3 (Fig. 13). However, it should be kept in mind that gel A was the one with 10.0% (w/w) active while each of the other gels contained only 5.0% (w/w). In considering the penetration amount in other single deeper tape (tape 4-30) (Fig. 13), gel B (best nanocrystal in gel withtout PG) was no doubt the best one preformed in penetration study among the 5

gels. This benefited from the stable high solubility provided by the nanocrystal in the gel, increasing concentration gradient between the gel and the skin (Zhai, et al. 2014). In the end, penetration ability was increased.

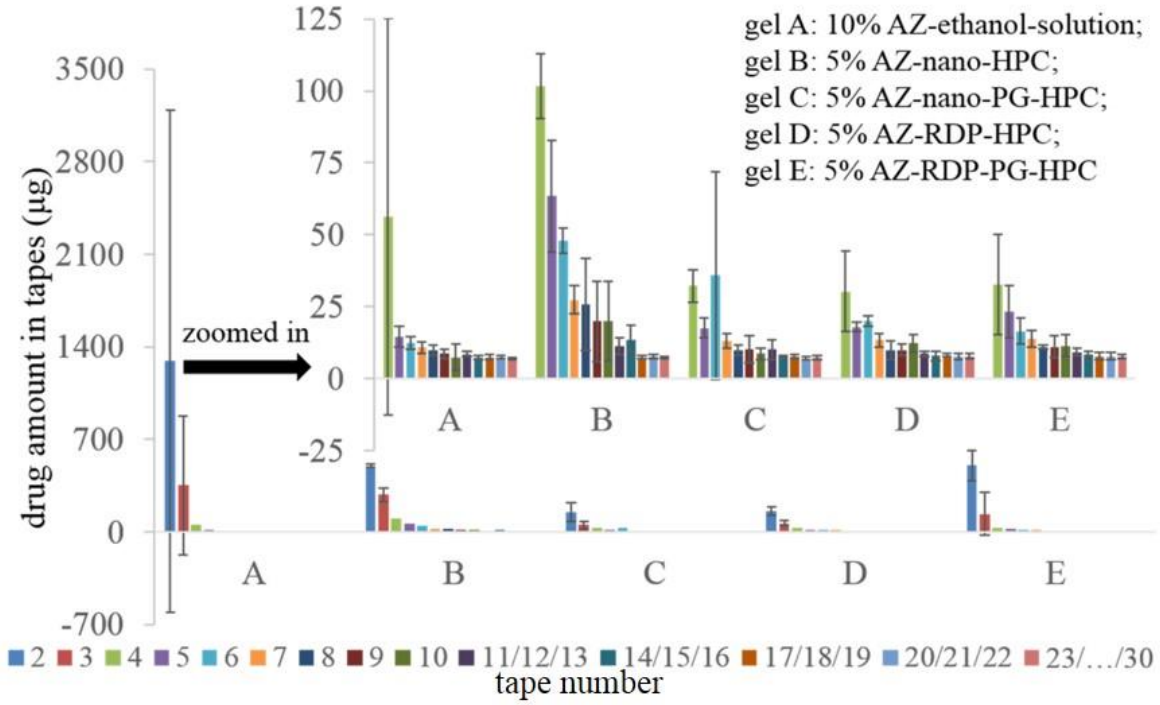

Fig. 13. Total amount of azithromycin in tapes after 20 minutes penetration (n=3). Gel A: ethanol-solution-gel; gel B: best nanocrystal in gel withtout PG; gel C: best nanocrystal in gel with PG; gel D: RDP gel without PG; gel E: RDP gel with PG.

3.1.5. Conclusions

In this study, the best azithromycin nanocrystal for dermal use is the 10.0% azithromycin nanosuspension stabilized with 1.0% (w/w) TPGS and produced by bead milling (BM) within 10 minutes. It possessed the smallest particle size, the narrowest distribution and the shortest producing time among the three tested methods (HPH, BM, combination technology/smartCrystals-technology). Six popular nonionic surfactants (TPGS, poloxamer 407, poloxamer 188, Plantacare® 810 UP, Plantacare® 2000 UP and Tween® 80) were investigated as well. After production, the PCS diameter of the best nanocrystal was

189 nm with PDI of 0.194 and d(v)50% of 143 nm and d(v)90% of 370 nm. Zeta potential was closed to -30 mV in Milli-Q water. Even after 90 days storage at 4 °C, the PCS diameter was still lower than 300 nm with PDI ≤ 0.25 and d(v)90% ≤ 1 μm. In addition to these parameters, TEM pictures of the best nanocrystal showed still homogeneous distribution after 30 days storage at RT. The long-term performance was observed too. The best nanocrystal was easily re-dispersable by hand shaking in 10 seconds after 12 months storage at 4 °C, with PCS diameter < 300 nm and d(v)90% ≤ 1 μm. Meanwhile, macroscopic observation showed the absence of bacterial growth and light microscope pictures proved homogeneous distribution. Even extend to 24 months storage at 4 °C, the result of the best formulation is still as desired. After re-dispersion by hand shaking in 1 minute, the PCS diameter was 256 nm and d(v)90% 1,250 nm. Small portion of big particles was detected by light microscope pictures. No bacterial infection was observed.

Besides, it possessed saturation solubiliy in Milli-Q water at 4 h as much as three times of the RDP. And its saturation solubility in water-PG mixture (80:20, w/w) was still higher than that of RDP. In addition, when incorporated into the 5.0% (w/w) HPC gel, the best nanocrystal formulation presented higher penetration efficacy in the tape stripping porcine ear study than the clinical effective ethanol-solution-gel, and even better than the one with penetration enhancer (PG). All those data externalize this TPGS stabilized nanocrystals can be considered as presently an optimal formulation approach for the dermal delivery of azithromycin. And it will possess a high dermal bioavailability and effective clinic application for Lyme disease.

3.1.6. References

Al-Shaal, L., Shegokar, R., Müller, R.H., 2011. Production and characterization of antioxidant apigenin nanocrystals as a novel UV skin protective formulation. Int. J. Pharm. 420, 133-140.

Arora, S.C., Sharma, P.K., et al., 2010. Development, characterization and solubility study of solid dispersions of azithromycin dihydrate by solvent evaporation method. J. Adv. Pharm. Technol. Res. 2, 221-228.

Ascencio, S.M., Choe, C., et al., 2016. Confocal Raman microscope and multivariate statistical analysis for determination of different penetration abilities of caffeine and propylene glycol applied simultaneously in a mixture on porcine skin *ex vivo*. Euro. J. Pharm. Biopharm. 104, 51-58.

Bangham, A.D., 1993. Liposomes: the Babraham connection. Chem. Phys. Lipids 64, 275-285.

Brigelius-Flohé, R. and Traber, M.G., 1999. Vitamin E: function and metabolism. FASEB J. 13, 1145-1155.

Brown, M.B., Turner, R., Lim, S.T., 2012. Topical product formulation development, in: Benson, H.A.E., Watkinson, A.C. (Eds.), Transdermal and topical drug delivery: Principles and practice. John Wiley & Sons, Inc., Hoboken, pp. 265.

Gallagher, S.J., Heard, C.M., 2005. Solvent content and macroviscosity effects on the in vitro transcutaneous delivery and skin distribution of ketoprofen from simple gel formulations. Skin Pharmacol. Physiol. 18, 186-194.

Ghosh, I., Schenck, D., et al., 2012. Optimization of formulation and process parameters for the production of nanosuspension by wet media milling technique: Effect of Vitamin E TPGS and nanocrystal particle size on oral absorption. Eur. J. Pharm. Sci. 47, 718-728.

Gibson, M., 2009. Ophthalmic dosage forms, in: Gibson, M. (Eds.), Pharmaceutical preformulation and formulation: A practical guide from candidate drug selection to commercial dosage form. Informa Healthcare USA Inc., New York, pp. 431-455.

Gonzalez-Mira, E., Nikolic, S., et al., 2012. Improved and safe transcorneal delivery of flurbiprofen by NLC and NLC-based hydrogels. J. Pharm. Sci. 101, 707-725.

Herkenne, C., Naik, A., et al., 2008. Effect of propylene glycol on ibuprofen absorption into human skin *in vivo*. J Pharma. Sci. 97, 185-197.

Hinckley, A.F., Connally, N.P., Meek, J.I., Johnson, B.J., et al., 2014. Lyme disease testing by large commercial laboratories in the United States. Clin. Infect. Dis. 459: 676-681.

Huber, G., Hüttenes, U., et al., 2010. Topical antibiotic composition for the prevention of lyme disease. US Patent 9610244. WO 2009013331A1.

Knauer, J., Krupka, I., et al., 2011. Evaluation of the preventive capacities of a topically applied azithromycin formulation against Lyme borreliosis in a murine model. J. Antimicrob. Chemother. 66, 2814-2822.

Kakran, M., Shegokar, R., et al., 2012. Fabrication of quercetion nanocrystals: Comparison of different methods. Eur. J. Pharm. Biopharm. 80(1), 113-121.

Lo, J.B., Appel, L.E., et al., 2009. Formulation design and pharmaceutical development of a novel controlled release form of azithromycin for single-dose therapy. Drug Dev. Ind. Pharm. 35, 1522-1529.

Massarotti, E.M., Luger, S.W., et al., 1992. Treatment of early Lyme disease. The American J. Medicine. 92, 396-403.

Mauludin, R., Müller, R.H., et al., 2009. Kientic solubility and dissolution velocity of rutin nanocrystals. Eur. J. Pharm. Sci. 36, 502-510.

Mishra, P.R., Al-Shaal, L., Müller, R. H., Keck, C. M. 2009. Production and characterization of hesperetin nanosuspensions for dermal delivery. Int. J. Pharm. 371, 182-189.

Moser, K., Kriwet, K.., et al., 2001. Passive skin penetration enhancement and its quantification *in vitro*. Euro. J. Pharm. Biopharm. 52, 103-112.

McHugh, R.C., Rice, A., et al., 2004. A topical azithromycin preparation for the treatment of acne vulgaris and rosacea. J. Dermatological Treatment. 15, 295-302.

Mishra, P.R., Al-Shaal, L., et al., 2009. Production and characterization of hesperetin nanosuspensions for dermal delivery. Int. J. Pharm. 371, 182-189.

Möschwitzer, J.P., Drug development in the commercial pharmaceutical development process. Int. J. Pharm. 2013, 453, 142-156.

Müller, R.H., Chen, R., Keck, C.M., 2013. smartCrystals for consumer care & cosmetics:

Enhanced dermal delivery of poorly soluble plant actives. Household and Personal Care Today. 8, 18-23.

Müller, R.H., Gohla, S., Keck, C.M., 2011. State of the art of nanocrystals – Special features, production, nanotoxicology aspects and intracellular delivery. Euro. J. Pharm. Biopharm. 78, 1-9.

Müller, R.H., Jacobs, C., 2002. Buparvaquone mucoadhesive nanosuspension: preparation, optimization and long-term stability. Int. J. Pharm. 237, 151-161.

Müller, R.H., Mäder, K., Gohla, S., 2000. Solid lipid particles (SLN) for controlled drug delivery – a review of the state of the art. Euro. J. Pharm. Biopharm. 50, 161-177.

Müller, R.H., Staufenbiel, S., Keck, C.M., 2014. Lipid nanoparticles (SLN, NLC) for innovative consumer care & household products. Transdermal Delivery. Household and Personal Care Today. 9, 18-24.

Müller, R.H., Zhai, X., Romero, G.B., Keck, C.M., 2016. Nanocrystals for passive dermal penetration enhancement, in: Dragicevic, N., Maibach, H.I. (Eds.), Percutaneous penetration enhancers, chemical methods in penetration enhancement: Nanocarriers. Springer-Verlag GmbH, Berlin, pp. 284-285.

Nadelman, R.B., Nowakowski, J., et al., 2011. Prophylaxis with single-dose doxycycline for the prevention of Lyme disease after an ixodes scapularis tick bite. N. Engl. J. Med. 345, 79-84.

Pardeike, J., Müller, R.H., 2010. Nanosuspensions: a promising formulation for the new phospholipase A2 inhibitor PX-18. Int. J. Pharm. 391, 322-329.

Pardeike, J., Strohmeier, D.M., et al., 2011. Nanosuspensions as advanced printing ink for accurate doing of poorly soluble drugs in personalized medicines. Int. J. Pharm. 420, 93-100.

Piesman, J., Hojgaard, A., et al., 2014. Efficacy of an experimental azithromycin cream for prophylaxis of tick-transmitted Lyme disease spirochete infection in a murine model. Antimicrob. Agents Chemother. 58, 348-351.

Prickett, P.S., Murray, H.L., Mercer, N.H., 1961. Potentiation of preservatives (parabens)

in pharmaceutical formulations by low concentrations of propylene glycol. J. Pharm. Sci. 50, 316-320.

Pyo, S.M., 2016. Nanocrystals & lipid nanoparticles for optimized delivery of actives. PhD thesis, Free University of Berlin, pp. 2-4.

Pyo, S.M., Meinke, M., Keck, C.M., Müller, R.H., 2016. Rutin – increased antioxidant activity and skin penetration by nanocrystal technology (smartCrystals). Cosmetics 3, 9.

Romero, G.B., Arntjen, A., Keck, C.M., Müller, R.H., 2016. Amorphous cyclosporin A nanoparticles for enhanced dermal bioavailability. Int. J. Pharm. 498, 217-224.

Saar, B.G., Contreras-Rojas, L. R., et al., 2011. Imaging drug delivery to skin with stimulated Raman scattering microscope. Mol. Pharmaceutics. 8, 969-975.

Schwameis, M., Kündig, T., et al., 2017. Topical azithromycin for the prevention of Lyme borreliosis: A randomized, placebo-controlled, phase 3 efficacy trial. Lancet Infect Dis. 17, 322-329.

Shin, C.M., and Spielman, A. 1993. Topical prophylaxis for Lyme disease after tick bite in a rodent model. J. Infect. Dis. 168: 1042-1045.

Shin, S.C., Kim, J., 2003. Physicochemical characterization of solid dispersion of furosemide with TPGS. Int. J. Pharm. 251, 79-84.

Silva, A.C., Amaral, M.H., et al., 2012. Solid lipid nanoparticles (SLN)-based hydrogels as potential carriers for oral transmucosal delivery of risperidone: preparation and characterization studies. Colloid Surf. B Biointerfaces 93, 241-248.

Smith, E.W., Surber, C., Tassopoulos, T., 2001. Topical dermatological vehicles: A Holistic Approach., in: Bronaugh, R.L., Maibach, H.I. (Eds.), Topical absorption of dermatological products. Marcel Dekker Inc., New York, pp. 461.

Steele, G., 2009. Preformulation as an Aid to product design in early drug development, in: Gibson, M. (Eds.), Pharmaceutical preformulation and formulation: A practical guide from candidate drug selection to commercial dosage form. Informa Healthcare USA Inc., New York, pp. 223-225.

Watkinson, R. M., Guy, R. H., Hadgraft, J., Lane, M. E., 2009. Optimisation of cosolvent concentration for topical drug delivery – II: Influence of propylene glycol on ibuprofen permeation. Skin Pharmacol. Physiol. 22, 225-230.

Zhai, X., 2013. Gelatin nanoparticles & nanocrystals for dermal delivery. PhD thesis, Free University of Berlin, pp. 15.

Zhai, X., Lademann, J., Keck, C.M., Müller, R.H., 2014. Dermal nanocrystals from medium soluble actives – Physical stability and stability affecting parameters. Euro. J. Pharm. Biopharm. 88, 85-91.

Zimering, J.H., Williams, M.R., et al., 2014. Acute and chronic pain associated with Lyme Borreliosis: Clinical characteristics and pathophysiologic mechanisms. Pain 155, 1435-1438.

3.2. Maximum loaded amorphous azithromycin produced by dermal smartPearls® technology for prophylaxis against Lyme disease

3.2.1. Abstract

Azithromycin was loaded onto the mesoporous silica Syloid® SP53D-11920 by smartPearls® technology and further made into a 5.0% hydroxypropyl cellulose (HPC) gel to prevent Lyme disease. Maximum loadings (32.0% w/w and 33.2% w/w) were produced by different concentrated loading solutions and were determined by X-ray diffraction (XRD). 24 months stability of amorphous state of azithromycin in the silica (33.2% loading) and 18 months stability (33.2% loading) in the gel at 4 °C were also confirmed by XRD. The addition of HPC facilitated the homogenous distribution of the loaded silica up to 24 months at 4 °C. Both the higher saturation solubility at 40 min (1,300 μg/ml versus 93 μg/ml) and the higher porcine ear penetration than the raw drug powder indicated a higher dermal bioavailability of the azithromycin loaded silica (32.0% loading), even compared to "gold standard" nanocrystals and another clinical effective azithromycin formulation with ethanol. In sum, it appears that the maximum loaded azithromycin dermal smartPearls® is a promising formulation for prophylaxis against Lyme disease.

3.2.2. Introduction

People suffer from Lyme disease for more than one century at least in North America and Europe when an infection is accidentally ignored after tick bite (Weber, 2001; Wormser, et al. 2006). Symptoms of the common vector-borne disease which due to the transfer of *Borrelia burgdorferi*, can be severe and even life-threatening (Shapiro, 2014). What is worse, exposure on woodlands and contact with dogs or cats makes tick attachment frequent. The best methods to prevent Lyme disease are vaccines and prophylactic antimicrobial therapy (Piesman, et al. 2014). But a vaccine to prevent Lyme

disease in humans is not commercial available since 2002, only 3 years after its first appearance on market (Piesman, et al. 2014). In this case, the only potential way is the administration of antimicrobial agents. The typical treatment regimens are doxycycline, amoxicillin, and cefuroxime axetil (Shapiro, 2014). But their oral long-term treatment brings patients inconvenience and side effects such as vomiting, nausea and rashes (Knauer, et al. 2011). Besides, bacterial resistance to the administered antibiotic or malaise and toxicity also has to be considered after the liberal oral administration of antibiotics (Venkatesh, et al. 2013). Thus, the demand of fewer adverse effects and better acceptance from patients necessitate dermal application of antibiotics for Lyme disease.

Azithromycin is an option in topical treatment when patients have a contraindication to other popular agents (Shapiro, 2014). In addition, compared to doxycycline – the one which is effective to the early Lyme borreliosis – it has lower minimum inhibitory concentration and superior activity against *Borrelia burgdorferi* and fewer adverse effects (Knauer, et al. 2011; Weber, et al. 1993). And with its hydrophobicity, azithromycin facilitates its penetration through the skin (Mishra, et al. 2009). What is more important, azithromycin has quicker onset time, which is a key factor in treatment of this infection (Weber, et al. 1993). Last but not the least, azithromycin was proven possessing higher potency than doxycycline when applied as dermal formulation within the first 3 days following a tick bite in a murine model system (Piesman, et al. 2014). Topical application of antibiotics has already been studied and proven effective for Lyme disease since 1993 (Shin and Spielman. 1993), but even the authors themselves not recommend their formulation for human use because DMSO was used as solvent in the carrier. Thus, a novel dermal formulation for hydrophobic azithromycin without organic solvents was in demand.

smartPearls® technology was kind of analogous to a former oral technology, CapsMorph® (Wei, et al. 2015). It combines two main approaches of increasing the

saturation solubility of the active – size reduction to the nanoscale and drug amorphization (Kawabata, et al. 2011; Monsuur, et al. 2014). Simply speaking, it encages amorphous active in the mesopores of porous µm-sized particles with nm-sized pores (e.g. Syloid®). It also avoids the basic problem of other amorphization methods – high thermodynamical instability, because of the restriction of re-crystallization resulting from the tiny space. Thus, the amorphous state with high free energy is not easy to convert to low free energy crystal state, and the amorphous state can keep even at least 4 years long (Wei, et al. 2015). The high-energy amorphous forms possess weaker interactions between molecules due to no long-range molecular order, resulting in higher affinity for a given solvent compared to low-energy crystals. Thus, higher saturation solubility is achieved (Byrn, et al. 1994; Wei, et al. 2015). Meanwhile, the nano-range size as well increases saturation solubility due to Ostwald-Freundlich equation and Kelvin equation (Mauludin, et al. 2009; Pardeike, et al. 2010). Consequently, this smartPearls® technology which integrates nanonization and amorphization will generate a high concentration gradient between dermal formulation and skin, thus increasing the diffusive flux into the skin. In the end, the penetration of the poorly soluble drug is enhanced and resulting in a high dermal bioavailability (Müller, et al. 2011).

The strongest difference between smartPearls® technology and CapsMorph® is that the first one involves water-containing dermal carriers (e.g., gel), but the latter is a dry oral formulation. Theoretically, re-crystallization is particularly favored when the amorphous materials is in contact with liquid such as water (Monsuur, et al. 2014), which makes topical amorphous formulation difficult. Thus, not only the maximum loading and stability of amorphous azithromycin in Syloid® but also the stability in the dermal carrier was investigated. To further prove the ability to penetrate skin of the novel azithromycin dermal formulation, saturation solubility and *ex vivo* penetration study with porcine ear were studied as well. For comparison, raw drug powder, "gold standard" nanocrystals with the particle diameter 189 nm (**chapter 3.1**) and an

azithromycin ethanol-solution-gel (comparable to one tested in clinical phases) (Knauer, et al. 2011; Schwameis, et al. 2017) were also tested in the penetration study.

3.2.3. Experimental Section

3.2.3.1. Materials

Azithromycin dihydrate (contains 95.4% azithromycin) was ordered from Haohua Industry (Jinan, China). Klucel GF® (Hydroxypropyl cellulose) purchased from Caesar & Loretz GmbH (Hilden, Germany) was used as gel form. Syloid® SP53D-11920 (Syloid®) was kindly provided by W. R. Grace & Co. (Worms, Germany). Ethanol (96%) was used of analytical grade. The Milli-Q water was obtained by reverse osmosis from a Millipak® Express 20 Filter unit (Merk, Germany).

3.2.3.2. Production of smartPearls® – maximum loading of azithromycin

The maximum dissolvable amount of azithromycin in 10.0 g ethanol (96%) was around 5.0 g, representing a saturation solubility C_s in ethanol (96%) of 50% (w/w). Two drug-ethanol-solutions were prepared for drug loading: one with an azithromycin concentration half of C_s (C_s50% = 5.0 g azithromycin in 20.0 g ethanol (96%)) and another with a quarter of C_s (C_s25% = 5.0 g azithromycin in 40.0 g ethanol (96%)). Then each solution was sprayed stepwise by a spraying nozzle screwed onto a glass bottle to certain amounts of dried silica. The silica was stirred using an ointment bowl and pestle after every spray to ensure that the drug solution is absorbed by the silica immediately and homogenously. Each spray is loading about 0.1 g drug-ethanol-solution. After finishing spraying a certain amount of solution, the sample was moved to one flat-bottomed glass vessel and stored in a compartment dryer at 40 °C until all ethanol was evaporated. This evaporation process was controlled via the weight loss. After cooling to room temperature, the amorphous state of the sample was monitored by X-ray

diffraction (Philips, PW 1830, Netherlands). Subsequently, these steps were repeated until reaching the maximum loading.

3.2.3.3. Preparation of azithromycin gels

For the preparation of the gel base, Milli-Q water was heated to 75 °C in an ointment bowl. Subsequently the hydroxypropyl cellulose (HPC) powder was added to the water and dispersed using a pestle until a homogenous suspension resulted. The mixture turned into a transparent gel base after storage overnight at 4 °C in the fridge. Overnight evaporated Milli-Q water was supplemented at room temperature. A weighted amount of these two maximum loaded azithromycin loaded Syloid® were incorporated into the 5.0% (w/w) HPC gel to get a final concentration of 1.0% amorphous azithromycin in the gel (AZ-Syloid-gel). 5.0% raw drug powder and azithromycin nanocrystals with the particle diameter 189 nm (**chapter 3.1**) were incorporated into the gel respectively to get a 5.0% azithromycin raw drug powder (RDP) gel (AZ-RDP-gel) and a 5.0% azithromycin nanocrystals gel (AZ-NC-gel). 10.0% ethanol-solution-gel (10.0% azithromycin RDP, 77.5% ethanol (94%), 0.5% polyacrylate, 5.0% HPC and 7.0% Miglyol® 812) was selected as a comparison which demonstrated effectiveness in clinical studies (Knauer, et al., 2011; Schwameis, et al. 2017).

3.2.3.4. Determination of solid state

A PW 1830 X-ray diffractometer (Philips, Netherlands) was used to monitor the solid state of 33.2% azithromycin loaded in Syloid® and in gels. Overloading was observed by detecting crystalline peaks (sharp peaks) in the X-ray spectrum, meaning that the drug is not more completely in the amorphous state. The samples were analyzed by placing a thin layer of the loaded silica powder or gels in the XRD. The diffraction angle range was between 0.6°-40° with a step size of 0.04° per 2 seconds. The diffraction pattern was

measured at a voltage of 40 kV and a current of 25 mA.

3.2.3.5. Determination of the kinetic saturation solubility

For kinetic solubility studies, the 32.0% (w/w) azithromycin loaded Syloid® was dispersed in Milli-Q water to get a final concentration of azithromycin of 4.8% in vials. Azithromycin and unloaded Syloid® physical mixture (35.0% azithromycin) was also dispersed in Milli-Q water to get a final concentration of azithromycin of 5.6% in vials. Furthermore, 5.6% raw drug powder was suspended in Milli-Q water for comparison. The samples were stored at 25 °C shaking with 100 rpm in an Innova 4230 shaker (New Brunswick Scientific GmbH, Nürtingen, Germany) for 60 min. To separate the dissolved drug, the samples were first centrifuged (17,968 × g) at room temperature for 10 min and subsequently the supernatant was filtered by nuclepore track-etched polycarbonate membrane filters (50 nm pore size, Whatman® 110603 filter). The drug concentration in such obtained samples was determined by high performance liquid chromatography (HPLC).

3.2.3.6. Stability of Syloid® porous materials in dermal gel formulations

To observe if the 32.0% loaded silica aggregated in the dermal carrier during storage, pictures of the gels were taken using an Orthoplan microscope (Motic, Germany) at 100-fold and 600-fold magnifications. The gel with 1% amorphous azithromycin was stored for 24 months at 4 °C. For comparison, unloaded Syloid® (5.0% w/w) was also dispersed in water without the HPC gel.

3.2.3.7. Penetration study with porcine ear skin

A penetration study via tape stripping was performed in the porcine ear skin model as

following: 100 mg AZ-Syloid-gel with 1.0% amorphous azithromycin, 100 mg AZ-RDP-gel with 5.0% azithromycin RDP, 100 mg AZ-NC-gel with 5.0% azithromycin nanocrystals and 100 mg ethanol-solution-gel with 10.0% azithromycin dissolved in ethanol were applied homogenously onto a skin area of 1.5 × 1.5 cm^2. After a penetration time of 20 min, an adhesive tape was pressed onto the skin by using a roller and then removed rapidly. One area was taped for 30 times. Afterwards, the drug was quantitatively extracted from the tape strips using 2 ml of acetonitrile/DMSO (1:1, v/v) as solvent for shaking 3 hours at 120 rpm in an Innova 4230 shaker. Subsequently, the samples were centrifuged (15,493 × g; 15 min) and the supernatant was analyzed by high performance liquid chromatography (HPLC) as described in section 3.2.3.8.

3.2.3.8. High performance liquid chromatography (HPLC) analysis

Azithromycin concentration was determined by HPLC with an auto sampler model 560, equipped with a solvent delivery pump system model 522 and a diode array detector model 540 (Kontron Instruments, Rossdorf, Germany). As column a Lichrospher-100 RP-8 reverse phase column (125 × 4 mm, 5 µm) was used. As mobile phase, a buffer/methanol mixture at a ratio of 20:80 (v/v) was used with a flow rate of 1.2 ml/min, where the buffer was composed of 4.35g/L K_2HPO_4 and H_3PO_4 of pH 7.5. The column temperature was set to 45 °C. The UV detector measured azithromycin at a wavelength of 210 nm.

3.2.4. Results and Discussions

3.2.4.1. Theory of loading drugs onto Syloid® porous materials

Simply speaking, the loading method depends on capillary force generated by the tiny pore (in this case: 6 nm pore diameter), which will draw the drug solution into the voids of pores (Wei, et al. 2015), even though inevitably a small portion will distribute on the

silica surface. With the evaporation of the solvent, the drug precipitates. The molecules in the pores could not convert to long-range molecular order from the disordered arrangement due to the confined space, thus stay amorphous state. While the other part of drug molecules on the surface may be re-crystallized during storage. Thus, theoretically the calculation is necessary to make sure the total volume of the drug solution in each spray is smaller than the total volume of the unfilled pores.

In details of the calculation: R is the weight ratio of solvent and drug, D (g/ml) is the density of this solvent, d (g/ml) is the density of the drug, P (ml/g) is the pore volume of the silica. Before loading the drug solution, the silica was dried in the compartment dryer until it reached constant weight. In 1st loading step, with the silica weight M_1 (g) and the drug need to be loaded weight m_1 (g), the volume of the drug solution is about $[(R+1)*m_1]/D$, and it should be smaller than the volume of unfilled pores, which is $P*M_1$, to make sure the drug solution can stay inside the pores as much as possible. The complete solvent evaporation is controlled via determining the weight loss. If such obtained production is in amorphous state confirmed by XRD or differential scanning calorimetry (DSC), the next step follows. If not, then dilute the drug solution and repeat this step again until the drug in this step is amorphous. The drug loading of this step is L_1, $L_1= m_1/(m_1+M_1)$. For the number nth step of loading, with the formulation weight $M_{(n)}$ (g) (n>1), and with the drug need to be loaded weight $m_{(n)}$ (g), the volume of the drug solution is about $[(R+1)*m_{(n)}]/D$, it should be smaller than the volume of unfilled pores, which is now $M_{(n)}*(1–L_{(n-1)})*P – (M_n*L_{(n-1)}/d)$. If the production in this step is amorphous, then continue with the next step. If not, compare the drug loading with the theoretical maximum loading $[M_1*P*d/(M_1*P*d+M_1)]$. If there is no big difference between these two data, then stop, this step should be the final step of the formulation. If there is big difference between these two data, then dilute the drug solution, repeat from the first step again until the drug in this final step is amorphous. The drug loading of this step is L_n, $L_n= (m_n+M_n*L_{(n-1)})/(m_n+M_n)$. In this study, D is 0.789 g/ml, d is 1.18 g/ml, and

P is 0.9 ml/g. The theoretical maximum loading of azithromycin in Syloid® SP53D-11920 is 51.5% w/w.

3.2.4.2. Maximum loading detected by XRD

Overloading was observed by detecting crystalline peaks in the X-ray spectrum, indicating that a fraction of the drug in the silica was crystalline. As shown in Fig. 1, the main crystalline peak (the highest intensity) of azithromycin was around 10 degree, the same as reported (Zhang, et al. 2010). The maximum amorphous loading of azithromycin in Syloid® was 32.0% (w/w) (no crystalline peak) produced by 3 spraying steps of higher concentrated azithromycin-ethanol-solution (C_s50%). Even though one more spraying step resulted only in 33.3% (w/w) loading, this sample showed overloading confirmed by XRD due to the sharp peak around 10 degree (Fig. 1 left). The 1st spraying step and the 2nd spraying step resulted in 16.7% and 27.4% loading, respectively. For lower concentrated azithromycin-ethanol-solution (C_s25%), each spraying step resulted in less loading silica but ended in a silica with maximum 33.2% (w/w) loading (no crystalline peak) by 7 spraying steps. Here overloading was detected as 35.0% (w/w) loading with produced by 8 spraying steps (Fig. 1 right, a sharp peak around 10 degree). More details of loading data can be found in **chapter 3.5**. The results indicate the different loading effect invented by different spraying solution concentrations. The less concentrated the spraying solution is, the more maximum loading is approachable and the more spraying steps are needed. This may be because it is easier for the drug to enter in the deep holes with the less concentrated spraying solution, resulting in more space for the next loading.

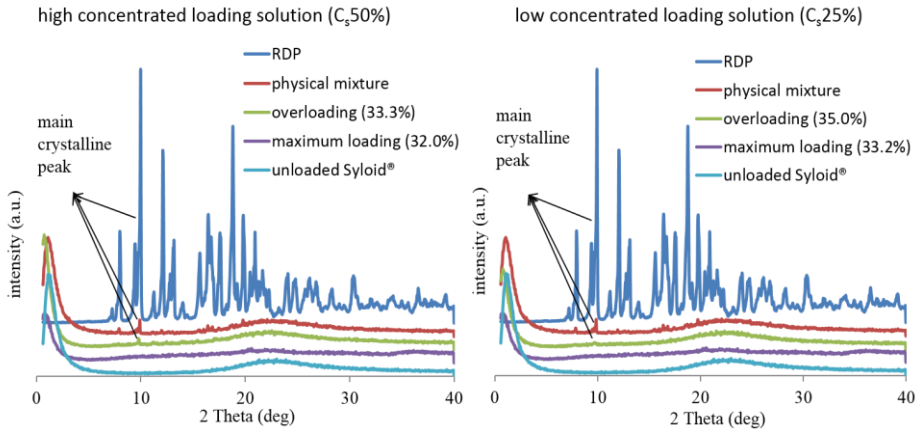

Fig. 1. X-ray spectrum (vertical axis: intensity; horizontal axis: 2 Theta) of maximum loading (left: high concentrated azithromycin-ethanol-solution (C_s50%); right: low concentrated azithromycin-ethanol-solution (C_s25%)).

3.2.4.3. Amorphous stability

The stability of amorphous state in Syloid® and in gels was also detected by XRD because it is the most suitable way for the research of the physical state of crystalline and amorphous formulations (Wei, et al. 2015). The amorphous state of the 33.2% (w/w) azithromycin-loaded Syloid® has been proven to be stable for at least 24 months by now at 4 °C (Fig. 2 left, no crystalline peak). The HPC gel base as the blank control (without drug or silica inside) showed a broad peak around 30 degree. The physical mixture of raw drug powder and HPC gel showed a crystalline peak around 10 degree, corresponding to XRD spectra of the raw drug powder. While the AZ-Syloid-gel showed no crystalline peak at day 1, 6 months and 18 months when stored at 4 °C (Fig. 2 right). It indicated that the amorphous state of the 33.2% (w/w) azithromycin-loaded Syloid® could be stable for at least 18 months even in the water-containing medium at 4 °C. Usually, amorphous solid formulation stores potential energy, which will release when it is in contact with liquid such as water (Wei, et al. 2015). In that case, the amorphous molecules will generate an unstable supersaturated state, resulting in re-crystallization once formation of crystal nuclei occurs (Brauwers, et al. 2009). The fact makes it

difficult to develop a dermal system of amorphous state (Monsuur, et al. 2014). However, the XRD result indicated the Syloid® system is not only possessing the potency of long physical stability of the amorphous state, but also makes it possible to incorporate the amorphous solid formulation into dermal gels.

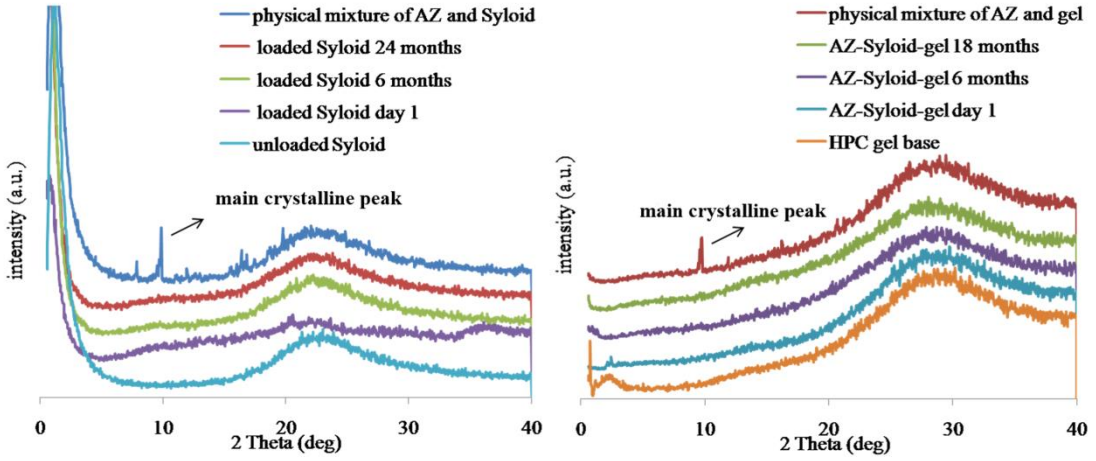

Fig. 2. X-ray spectrum (vertical axis: intensity; horizontal axis: 2 Theta) of 33.2% azithromycin-loaded Syloid® until 24 months at 4 °C (left) and AZ-Syloid-gel until 18 months at 4 °C.

3.2.4.4. Saturation solubility studies

Kinetic solubilities are shown in Fig. 3. The kinetic solubilities of raw drug powder did not change with big difference within 60 min. That of physical mixture showed lower solubilities than that of raw drug powder before 20 min, but higher solubilities than that of raw drug powder after 20 min. This may be due to the spontaneous amorphous transformation when crystalline raw drug powder physically mixed with the mesoporous materials (Qian, 2011). However, when observed the slight enhanced solubilities of physical mixture with increasing time, it was found out there was huge difference between the kinetic solubilities of the physical mixture and that of loaded silica: it showed 6 times lower solubilities (213 μg/ml) than that of loaded silica (1,300 μg/ml) in 40 min. This confirmed that the smartPearls® technology had stronger ability to make

amorphization than physical mixing. The saturation solubility of the 32.0% (w/w) loaded Syloid® after 40 min is 1,300 µg/ml, almost 14 times higher compared to that of the raw drug powder (93 µg/ml). Moreover, the loaded Syloid® showed enhanced saturation solubility by a factor 5 compared with the azithromycin nanocrystals with 189 nm diameter (242 µg/ml, **chapter 3.1**). This high solubility implied the potential high skin penetration of the azithromycin loaded Syloid®.

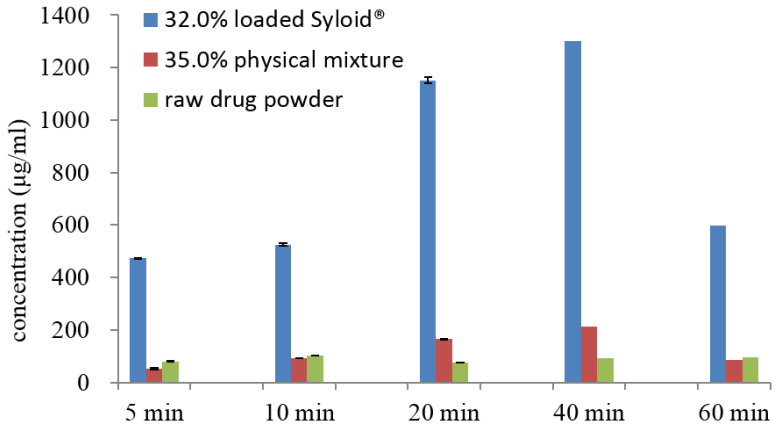

Fig. 3. Kinetic saturation solubilities of the 32.0% (w/w) azithromycin loaded Syloid®, the physical mixture (unloaded Syloid® and raw drug powder) and the raw drug powder at 25 °C in Milli-Q water as a function of time (n=3).

3.2.4.5. Stability of Syloid® in gel formulations

Some uneven distribution of the 5.0% Syloid® without loading drug in water was observed having agglomeration tendency by light microscope both in 100-fold and 600-fold (Fig. 4). By further addition of HPC, the gels with 32.0% azithromycin loaded silica (AZ-Syloid-gel) showed homogenous distribution even after 8 months, 12 months and 24 months of storage at 4 °C. This may be contributed to the high viscosity of 5.0% (w/w) HPC due to the adhesive properties of HPC in aqueous medium (EI-Kattan, et al. 2000; Fukui, et al. 2000) which avoids the casual movement of the silica particles. It is suggested that HPC ranges from 5% to 40% of the total formulation to act as the

solidifying agent (Huber, et al. 2010). From the result of microscope pictures, 5.0% (w/w) HPC in this study is suitable for carrying the Syloid®.

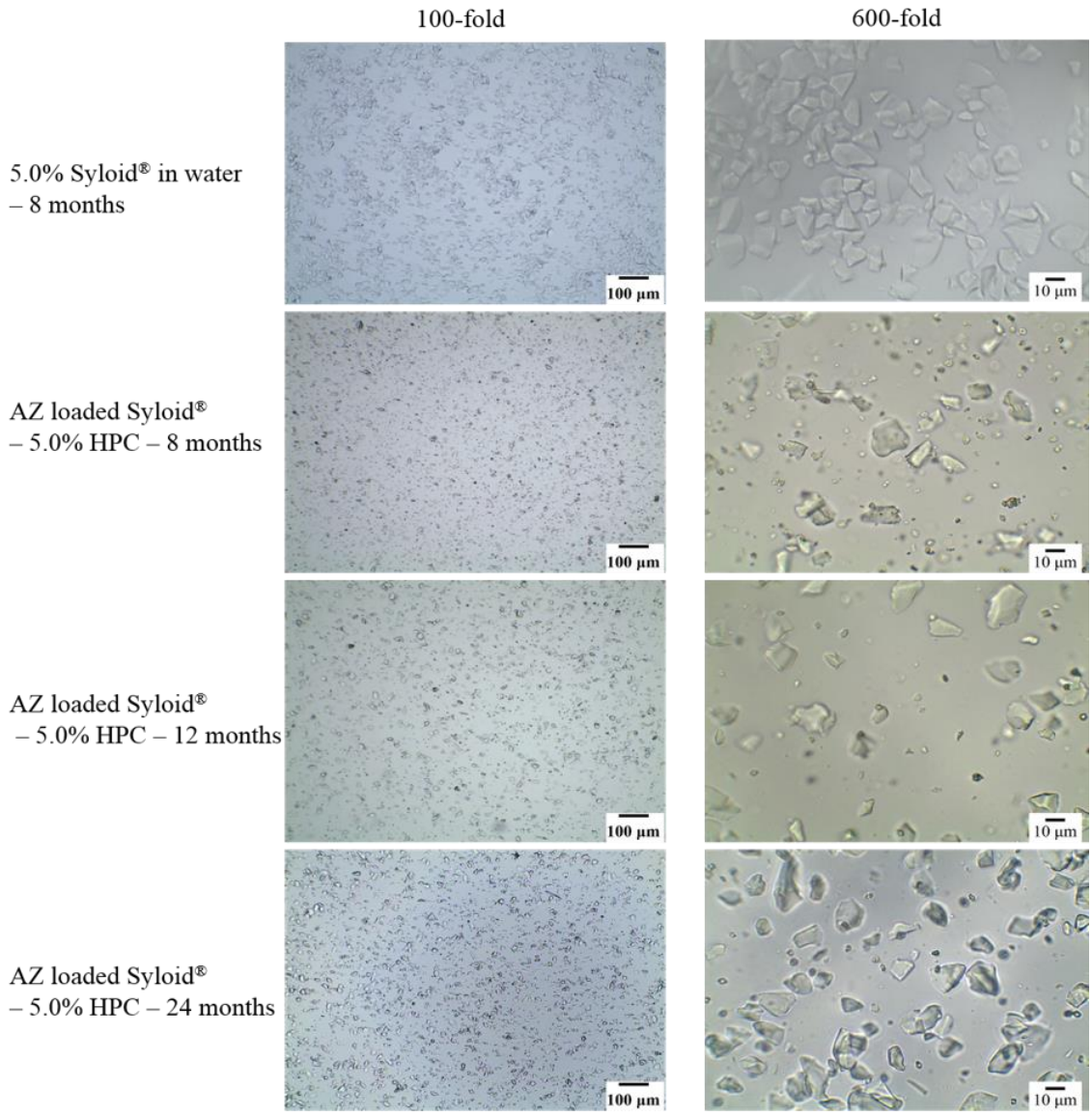

Fig. 4. Light microscope pictures at 100-fold magnification (left) and at 600-fold magnification (right) of 5.0% (w/w) unloaded Syloid® dispersed in water after 8 months storage at 4 °C, and azithromycin (AZ) loaded Syloid® in a 5.0% (w/w) HPC gel after 8 months, 12 months and 24 months storage at 4 °C (scale bars from left to right: 100 µm and 10 µm).

3.2.4.6. Penetration study with porcine ear skin

Porcine ear skin *ex vivo* is a valid model to test the penetration potency for its human counterpart (Sekkat, et al. 2002). When comparing data between different formulations in the porcine ear study, the first tape was excluded from the analysis because it was only occupied by non-penetrated drug. The data were expressed as normalized penetrated drug amount (µg/%) per cm^2 versus the tape numbers in Fig. 5. The tape number is correlated with depth of skin penetration whereas higher tape numbers stand for deeper penetration. The data indicated that the AZ-Syloid-gel demonstrated the highest penetration efficiency of the amorphous azithromycin. It had up to 30 times higher active concentration in the deep skin layers (20^{th}-30^{th} tape) compared to raw drug powder. In contrast, the ethanol-solution-gel stayed mainly close to the surface (2^{th}-7^{th} tape), showing around 3 times higher penetration than RDP there, but only half penetration efficiency compared to the AZ-Syloid-gel in the tape 2-7, even less in other deeper skin tapes. The delivery efficiency of AZ-Syloid-gel in all these tested tapes was even higher than the "gold standard" nanocrystals (particle diameter 189 nm, **chapter 3.1**). This phenomenon might be due to both the re-crystallization from the solution formulation (supersaturation sate of azithromycin in ethanol was thermodynamically unstable, **chapter 3.1**) (Moser, et al. 2001; Steele, 2009) and the increased saturation solubility of the amorphous azithromycin in Syloid® mentioned in section 3.2.4.4. According to Fick's first law of diffusion, increased saturation solubility lead to increased concentration gradient between the stratum corneum and the vehicle, and thus result in enhanced drug flux (Tam, et al. 2008; Watkinson, et al. 2009; Zhai, et al. 2014).

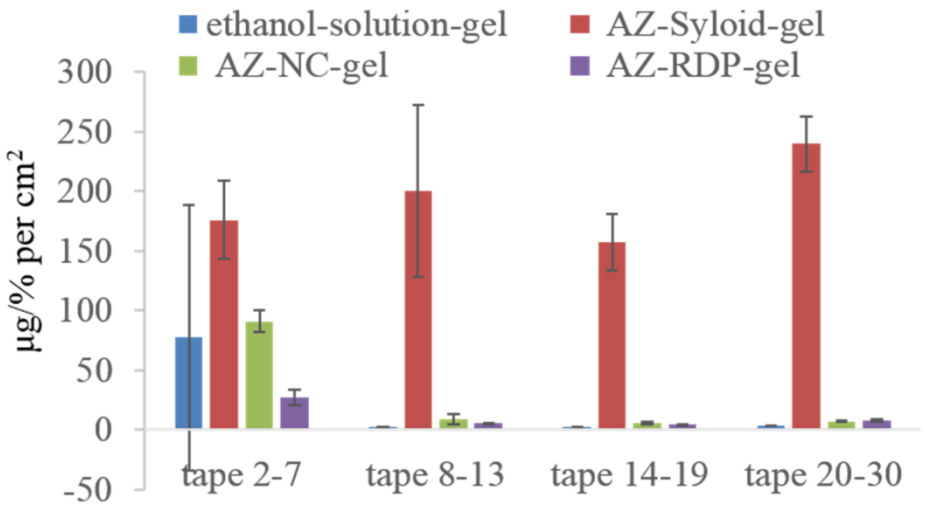

Fig. 5. Normalized amount of azithromycin in tapes after 20 minutes penetration, calculated by dividing the amount of drug (µg) by the azithromycin concentration (%) in the applied formulation per cm^2 (n=3).

3.2.5. Conclusions

When applied smartPearls® technology, one maximum azithromycin loading (33.2% loading) was achieved using azithromycin-ethanol-solution (C_s25%) after 7 loading steps. Another maximum azithromycin loading (32.0% loading) was achieved using azithromycin-ethanol-solution (C_s50%) after 3 loading steps. This 33.2% loaded amorphous azithromycin can not only be long-term stabilized loaded onto the Syloid® for 24 months at 4 °C, but also keep its amorphous state in water-containing HPC gel for at least 18 months. Besides, with the dispersion in HPC gel, azithromycin loaded Syloid® can avoid agglomeration tendency during the storage of 24 months at 4 °C, which is the problem of its dispersion in water only stored for 8 months. Moreover, the azithromycin loaded Syloid® showed much higher saturation solubility than the raw drug powder, the "gold standard" azithromycin nanocrystals with particle diameter 189 nm, the physical mixture of raw drug powder and unloaded silicas, indicating a high dermal bioavailability, which was also confirmed by the *ex vivo* penetration study. The

most exciting result was its superior efficacy of dermal penetration compared to the clinical effective ethanol-solution-gel even at lower active concentration.

Based on these results, smartPearls® is an attractive technology to generate in a simple way long-term stable amorphous azithromycin dermal formulation with increased skin penetration. It makes amorphous azithromycin exploitable in topical administration with a high dermal bioavailability for a high prophylactic effect of Lyme Borreliosis. This technology is industrially feasible because suitable porous microparticles can be purchased on the market. The 10-40 µm sized particles of the smartPearls® also avoid the controversy of nano-toxicity. In sum, applying the azithromycin loaded Syloid® gel at the site of tick exposure immediately after tick bite should decrease the risk of acquiring a Lyme disease infection.

3.2.6. References

Brouwers, J., Brewster, M.E., et al., 2009. Supersaturating drug delivery systems: the answer to solubility – limited oral bioavailability? J. Pharm. Sci. 98, 2549-2572.

Byrn, S.R., Pfeiffer, R.R., et al., 1994. Solid-state pharmaceutical chemistry. Chem. Mater. 6, 1148-1158.

EI-Kattan, A.F., Asbill, C.S., et al., 2000. Effect of formulation variables on the percutaneous permeation of ketoprofen from gel formulations. Drug Deliv. 7, 147-153.

Fukui, E., Uemura. K., et al., 2000. Studies on applicability of press-coated tablets using hydroxypropylcellulose (HPC) in the outer shell for timed-release preparations. 68, 215-223.

Huber, G., Hüttenes, U., et al., 2010. Topical antibiotic composition for the prevention of lyme disease. US Patent 9610244. WO 2009013331A1.

Kawabata, Y., Wada, K., et al., 2011. Formulation design for poorly water-soluble drugs

based on biopharmaceutics classification system: Basic approaches and practical applications. Int. J. Pharm. 420, 1-10.

Knauer, J., Krupka, I., et al., 2011. Evaluation of the preventive capacities of a topcally applied azithromycin formulation against Lyme borreliosis in a murine model. J. Antimicrob. Chemother. 66, 2814-2822.

Mauludin, R., Müller, R.H., et al., 2009. Kientic solubility and dissolution velocity of rutin nanocrystals. Eur. J. Pharm. Sci. 36, 502-510.

Mishra, P. R., Shaal, L. A., et al., 2009. Production and characterization of Hesperetin nanosuspensions for dermal delivery. Int. J. Pharm. 371, 182-189.

Monsuur, F., Höfer, H., et al., 2014. Active-loaded particulate materials for topical administration. US Patent 62050587. WO 2016041992A1.

Moser, K., Kriwet, K.., et al., 2001. Passive skin penetration enhancement and its quantification *in vitro*. Euro. J. Pharm. Biopharm. 52, 103-112.

Müller, R.H., Gohla, S., et al., 2011. State of the art of nanocrystals – Special features, production, nanotoxicology aspects and intracellular delivery. Eur. J. Pharm. Biopharm. 78, 1-9.

Pardeike, J., Müller, R.H., 2010. Nanosuspensions: a promising formulation for the new phospholipase A2 inhibitor PX-18. Int. J. Pharm. 391, 322-329.

Piesman, J., Hojgaard, A., et al., 2014. Efficacy of an experimental azithromycin cream for prophylaxis of tick-transmitted Lyme disease spirochete infection in a murine model. Antimicrob. Agents Chemother. 58, 348-351.

Qian, K., 2011. Spontaneous crystalline-to-amorphous phase transformation of organic or medicinal compounds in the presence of porous media. PhD thesis, University of Connecticut, pp. 43.

Schwameis, M., Kündig, T., et al., 2017. Topical azithromycin for the prevention of Lyme borreliosis: A randomized, placebo-controlled, phase 3 efficacy trial. Lancet Infect Dis. 17, 322-329.

Sekkat, N., Kalia, Y.N., et al., 2002. Biophysical study of porcine ear skin *in vitro* and its

comparison to human skin *in vivo*. J. Pharm. Sci. 91, 2376-2381.

Shapiro, E.D., 2014. Lyme disease. N. Negl. J. Med. 370, 1724-1731.

Shin, C.M., Spielman, A., 1993. Topical prophylaxis for Lyme disease after tick bite in a rodent model. J. Infect. Dis. 168, 1042-1045.

Steele, G., 2009. Preformulation as an Aid to product design in early drug development, in: Gibson, M. (Eds.), Pharmaceutical preformulation and formulation: A practical guide from candidate drug selection to commercial dosage form. Informa Healthcare USA Inc., New York, pp. 223-225.

Tam, J.M., McConville, J.T., et al., 2008. Amorphous cyclosporin nanodispersions for enhanced pulmonary deposition and dissolution. J. Pharm. Sci. 97, 4915-4933.

Venkatesh, M. P., Pramod Kumar, T. M., et al., 2013. Development, in vitro and in vivo evaluation of novel injectable smart gels of azithromycin for chronic periodontitis. Curr. Drug Deliv. 10, 188-197.

Watkinson, R.M., Herkenne, C. et al., 2009. Influence of ethanol on the solubility, ionization and permeation characteristics of ibuprofen in silicone and human skin. Skin Pharmacol. Physiol. 22, 15-21.

Weber, K., Wilske, B., et al., 1993. Azithromycin versus penicillin V for the treatment of early Lyme borreliosis. Infection 21, 367-372.

Weber, K., 2001. Aspects of Lyme Borreliosis in Europe. Eur. J. Clin. Microbiol. Infect. Dis. 20, 6-13.

Wei, Q., Keck, C.M., et al., 2015. CapsMorph® technology for oral delivery – theory, preparation and characterization. Int. J. Pharm. 482, 11-20.

Wormser, G.P., Dattwyler, R. J., et al., 2006. The clinical assessment, treatment, and prevention of Lyme disease, human granulocytic anaplasmosis, and babesiosis: Clinical practice guidelines by the infectious diseases society of America. Clin. Infect. Dis. 43, 1089-1134.

Zhai, X., Lademann, J., et al. 2014. Dermal nanocrystals from medium soluble actives – physical stability and stability affecting parameters. Eur. J. Pharm. Biopharm. 88,

85-91.

Zhang, Z., Zhu, Y., et al., 2010. Preparation of azithromycin microcapsules by a layer-by-layer self-assembly approach and release behaviors of azithromycin. Colloid. Surface. A. 362, 135-139.

3.3. smartPearls® of flavonoids for topical anti-aging application

3.3.1. Abstract

smartPearls® were produced by either loading 32.0% (w/w) hesperidin or 32.0% (w/w) rutin onto Syloid® SP53D-11920 in amorphous state. They did not re-crystallize for at least 1.5 years independent from storage temperature (4, 25, 40 °C) confirmed by X-ray diffraction (XRD). Even incorporating smartPearls® into 5% hydroxypropyl cellulose (HPC) gel, the loaded active still stayed amorphous for at least 1.5 years at 4 °C. In contrast, apigenin could not be successfully loaded onto Syloid® SP53D-11920 in amorphous state even with identical loading procedure as applied for hesperidin and rutin. Independent from the active state (amorphous or crystalline), smartPearls® showed homogeneous distribution in HPC gel for at least 2 years at 4 °C under light microscope. Skin penetration profiles were investigated on porcine ears, while both of the loaded silicas with amorphous active (hesperidin and rutin) expressed superior penetration and deeper location compared to the goldstandard nanocrystals. Contrarily, the apigenin loaded silica in crystalline state showed lower penetration than apigenin nanocrystals. Thus, only smartPearls® with amorphous state would be a potential dermal vehicle for anti-oxidants with increased dermal bioavailability.

3.3.2. Introduction

Skin has been studied as a promising route for the administration of therapeutic compounds due to its accessibility and large surface area since the 1950s (Tavano, 2015; Walters and Brain, 2009). Therapeutic compounds can be targeted within the skin (dermatological), regionally (local), or systemically (transdermal) (Walters and Brain, 2009). Many advantages of using skin for drug application are described, e.g., avoiding gastrointestinal absorption-related problems, having free risk of hepatic first-pass metabolism, providing zero-order drug delivery with constant plasma level, easy removal of medication in case of overdose and patient compliance (Abla, et al. 2016; Kuswahyuning, et al. 2015; Peppas, et

al. 2000). However, the numbers of commercial drug products applied on skin is limited because of the difficult percutaneous absorption. Usually, a drug molecule will have a good percutaneous absorption if it has favorable physicochemical properties, i.e., molecular weight less than 500 Da, no charge, and moderate lipophilicity with log p value between 1 and 3 (Abla, et al. 2016). However, most drug candidates have not the described physicochemical properties. Around 70-90% of the newly developed potential actives for medicine and cosmitics are hydrophobic actives (Müller and Keck, 2012). Thus, an appropriate formulation must be developed to enable the percutaneous absorption of these actives.

Human skin can be broadly divided into three parts from outer layer to inner layer in epidermis, dermis, and hypodermis. The epidermis can be further simply subdivided into overlying nonviable epidermis (stratum corneum) and underlying viable epidermis (stratum lucidum, stratum granulosum, stratum spinosum and stratum germinativum) (Abla, et al. 2016; Ng and Lau, 2015; Walters and Brain, 2009). In most cases, the stratum corneum is the main barrier for the permeation of therapeutic agents (Kuswahyuning, et al. 2015). Thus, an ideal formulation should be able to pass the active into the stratum corneum (Lauer, 2001).

There have been many ways to enable delivery through the skin such as penetration enhancers and active enhancement techniques, e.g., iontophoresis, electroporation and microporation. But chemical penetration enhancers may disrupt the skin membrane structure resulting in long-term damaged skin. Extra devices, for example electrical devices in case of iontophoresis are needed, often additionally an approval process from US Food and Drug Administration (FDA). And safety problems like sterility of microneedles and standardized application method in different clinical settings could bring difficult acceptance of patients to this technology (Abla, et al. 2016). Therefore, a novel dermal delivery system, which has both super percutaneous absorption and common acceptance of patients, is in great demand.

smartPearls® technology was developed in 2014 (Müller, et al. 2014). They are defined as silicas loaded with amorphous active for dermal application. This technology combines two principles – nanonization and amorphization – for increasing the saturation solubility of loaded actives, avoiding either the toxicity risk of the nanosize (Müller, et al. 2016) or the re-crystallization after amorphization (Monsuur, et al. 2016). With the increased saturation solubility, the concentration gradient between skin and dermal formulation is increased, leading to enhanced passive diffusion due to Fick's first law (Peppas, et al. 2000). Enhancing the passive diffusion is the most common way to improve the penetration of actives into the skin (Müller, et al. 2016). The theory of smartPearls® technology and CapsMorph® technology (Wei, et al. 2015) is the same. First, nanosize will enhance dissolution pressure, resulting in increased saturation solubility based on Ostwald-Freundlich equation and Kelvin equation (Mauludin, et al. 2009; Pardeike, et al. 2010). According to Noeys-Whitney equation, the enlarged surface area A of the nanosized particles and the increased saturation solubility will finally increase dissolution velocity (Müller, et al. 2016). Second, the amorphous state without long-range molecular order, possesses weaker interactions between molecules than the crystalline state, leading to a higher affinity for a given solvent (Byrn, et al. 1994), resulting in increased saturation solubility. The difference of smartPearls® technology and CapsMorph® technology is their administration route, being dermal for smartPearls® and oral for CapsMorph®. This leads to the special requirement that the amorphous state must stay stable in dermal vehicle, e.g., water-containing gels, for smartPearls®.

Nowadays, semisolid formulations are preferred vehicles for dermatological therapy than solutions and powders with longer retention time on the skin (Walters and Brain, 2009). Gel is selected as the vehicle in this study among the conventional semisolid topical preparations (ointment, cream, emulsion and gel) (Djekic and Primorac, 2015). Gel is a semisolid system in which a liquid phase is constrained within a three-dimensional polymeric matrix with a high degree of physical or chemical cross links. Due to its biocompatibility, good skin adhesion, low cost and low toxicity, gel plays a significant role

in pharmaceutical and cosmetical fields (Nikolic, et al. 2011; Tavano, 2015). Because of the high content of water, gel can increase the skin hydration, leading to an increased permeability of topically applied substance (Rougier, et al. 2011). The simplest gels contain water and thickeners such as natural gums (e.g., xanthan), semisynthetic materials (e.g., hydroxypropyl cellulose (HPC)), synthetic materials (e.g., carbomer-carboxyvinyl polymer) or clays (e.g. hectorite) (Walters and Brain, 2009). Due to the high hydrophilicity and the lower critical solution temperature behavior, HPC is an ideal polymer suited for gel preparation (Marsano et al., 2003). Thus, HPC gel was used in this study as vehicle to incorporate loaded silicas in it.

A successful delivery system should be able to deliver various actives owning different physicochemical properties. Besides pharmaceutical industry, much attention is paid on cosmetics industry (Müller and Keck, 2012), especially for dermal delivery (Yourick and Brouaugh, 2011). Actually, many cosmetic products with new technologies were launched to market first and smoothing the way for pharmaceutical products. For example, the first liposome cosmetic product CAPTURE (main active: longoza) was introduced to the market in 1986 by the company Dior (France) (Müller, et al. 2000). The first liposome dermal product on pharmaceutical market was Epi-Pevaryl® cream for anti-mycotic therapy (drug: econazole) by the company Johnson & Johnson GmbH (USA) at the beginning of 1990s (Müller, et al. 2000). In addition, the cosmetic market has great profit up to multi-billion dollars (Casanova and Santos, 2016). Thus, three flavonoids which has anti-aging effect (Shukla and Gupta, 2010) – apigenin (anthoxanthins), hesperidin (flavanoenes) and rutin (flavanonols) – were selected as model actives. The amorphous state of the loaded silicas, the distribution of the loaded silicas in HPC gel, the stability of the loaded silicas before and after incorporation into gels and finally penetration study the porcine ears were all analyzed. Corresponding nanoparticles as gold standard for increasing the saturation solubility were produced and used as references.

3.3.3. Experimental Section

3.3.3.1. Materials

Hesperidin and rutin were purchased from Denk Ingredients GmbH (Munich, Germany) and apigenin from Ferrer Health Tech (Barcelona, Spain). Syloid® SP53D-11920 was a kind gift from W. R. Grace & Co. KG (Worms, Germany) and Kolliphor® P188 as well as Plantacare® 2000 UP (decyl glucoside) from BASF (Ludwigshafen, Germany). euxyl® PE 9010 was purchased from Schülke & Mayr GmbH (Norderstedt, Germany). Klucel GF® (HPC) was brought from Caesar & Loretz GmbH (Hilden, Germany). Freshly produced ultra purified water was produced with a Millipak® Express 20 Filter unit (MPGP02001, Merck, Millipore KGaA, Darmstadt, Germany), possessing an electrical resistivity of 18 M-Ohm and a total organic content ≦10 ppb. All materials were used as received.

3.3.3.2. Producing of anti-oxidants loaded silicas

To achieve loaded Syloid® SP53D-11920 with apigenin, hesperidin or rutin, corresponding raw drug powders were dissolved in dimethyl sulfoxide (DMSO) in a ratio of 1:4 by weight to get drug-DMSO-solutions. Then in 3 steps 32.0% loaded Syloid® SP53D-11920 was obtained. In the first step, 10.00 g Syloid® SP53D-11920 was loaded with 2.00 g drug by adding 10.00 g drug-DMSO-solution under stirring in an ointment bowl with a pestle. To ensure that the drug solution was absorbed by the silica homogenously and immediately, the drug-DMSO-solution was sprayed manually by a spraying nozzle screwed onto a glass bottle. Subsequently, the DMSO was evaporated at 80 °C in a compartment dryer. The complete evaporation was controlled via determining the weight loss. In the second step, 9.00 g of the obtained silica was loaded with 1.60 g drug by spraying of 8.00 g drug-DMSO-solution using the same method. In the third step, 8.10 g of this silica was loaded with 0.744 g drug by spraying of 3.72 g solution.

3.3.3.3. Preparation of nanocrystals and gels

To produce these nanosuspension, wet bead milling (PML-2, Bühler AG, Switzerland) and high pressure homogenization (HPH) with an Avestin C50 (Avestin Europe GmbH, Germany) were used. The details are summarized in Tab. 1. During all bead milling productions, yttrium oxide stabilized zirconium oxide beads (Hosokawa Alpine, Germany) with 0.4-0.6 mm diameter were used as milling medium. Particle size analysis was performed by both dynamic light scattering (DLS) via photon correlation spectroscopy (Zetasizer Nano ZS, Malvern Instruments, UK) and static light scattering (SLS) via laser diffractometry (Mastersizer 2000, Malvern Instruments, UK).

Table 1: Preparation of nanosuspensions.

	apigenin	hesperidin	rutin
references	Shaal, et al. 2011	Romero, et al. 2015	Chen, 2013
coarse suspension	5% drug, 1% Plantacare® 2000 UP	18% drug, 1% Kolliphor® P 188, 1% euxyl® PE 9010	18% drug, 1% Tween® 80, 1% euxyl® PE 9010
wet bead milling	discontinuous mode	continuous mode	
	2,000 rpm, 5 °C		
	7 passages	5 passages	5 passages
after dilution	5% drug, 1% Plantacare® 2000 UP	5% drug, 1% Kolliphor® P 188, 1% euxyl® PE 9010	5% drug, 2% Tween® 80, 1% euxyl® PE 9010
high pressure homogenization	1 cycle, 300 bar	1 cycle, 500 bar	2 cycles, 300 bar

The obtained nanocrystals at respective concentrations of each drug were incorporated into 5% (w/w) HPC gel to get the final 5% (w/w) nanocrystals gel (NC gel). The corresponding raw drug powder gel (RDP gel) of 5% active with (hesperidin, rutin) or without (apigenin)

1% (w/w) euxyl® PE 9010 were produced as references. The loaded silicas were also incorporated into the 5% HPC gels to get 1% actives (Syloid gel) with (hesperidin, rutin) or without (apigenin) 1% (w/w) euxyl® PE 9010. Light microscope was performed at 100-fold and 600-fold magnifications using an Orthoplan microscope (Motic, Germany) to observe aggregation of silicas in gel during storage.

3.3.3.4. Stability of amorphous state of smartPearls® before and after incorporation into gels

The stability of amorphous state of loaded anti-oxidants in silicas were monitored by X-ray diffraction generator (XRD, Philips PW 1830, Amedo, Netherlands) before and after incorporation into gels. The experiments were performed in symmetrical reflection mode with a Cu-Kα line as the source of radiation. Standard runs using a 40 kV voltage, a 25 mA current and a scanning rate of 0.02°/second over a 2θ range of 0.6-40° were used.

3.3.3.5. Skin penetration study on porcine ear

Skin penetration study was performed by tape stripping the stratum corneum of full thickness of porcine ear skin since the porcine skin is a valid model to replace human volunteers (Sekkat, et al. 2002). The porcine ears were freshly obtained from a local slaughterhouse. The skin was remained on the isolated ear and its surface was cleaned by cutting the hairs with an electric cutter, washing with tap water and drying. 50 mg gel formulation (Syloid gel of 1% active, NC gel of 5% active and RDP gel of 5% active) of each active (apigenin, hesperidin and rutin) were applied homogenously on the external side of the porcine ear with an area of 1.5 × 1.5 cm^2. After 20 minutes penetration, an adhesive tape was pressed onto the skin using a roller and then removed rapidly. This strip process was repeated 30 times for each area. Afterwards, the active was quantitatively extracted from each tape in 2 ml acetonitrile/DMSO (1:1), shaking at 120 rpm and 25 °C for 3 hours in an Innova 4230 shaker (New Brunswick Scientific GmbH, Nürtingen, Germany). 1 ml of the obtained supernatant was centrifuged at 15,493 × g for 15 minutes

using a Heraeus Megafuge Centrifuge 3.0R (Kendro Laboratory Products GmbH, Hanau, Germany) and then analyzed by HPLC as described (Wei, et al. 2017a; Wei, et al. 2017b).

3.3.4. Results and Discussions

3.3.4.1. Production of anti-oxidants loaded silicas

Same loading procedure was applied to produce apigenin, hesperidin or rutin loaded silicas, however, amorphous loading was only achieved for rutin and hesperidin. In Fig. 1, characteristic sharp peaks appeared on the X-ray spectrum of apigenin loaded silica, missing in the X-ray spectra of the other two. According to this observation, the loading procedure succeeded in producing amorphous rutin or hesperidin loaded silica with 32.0% loading efficacy, while failing for apigenin.

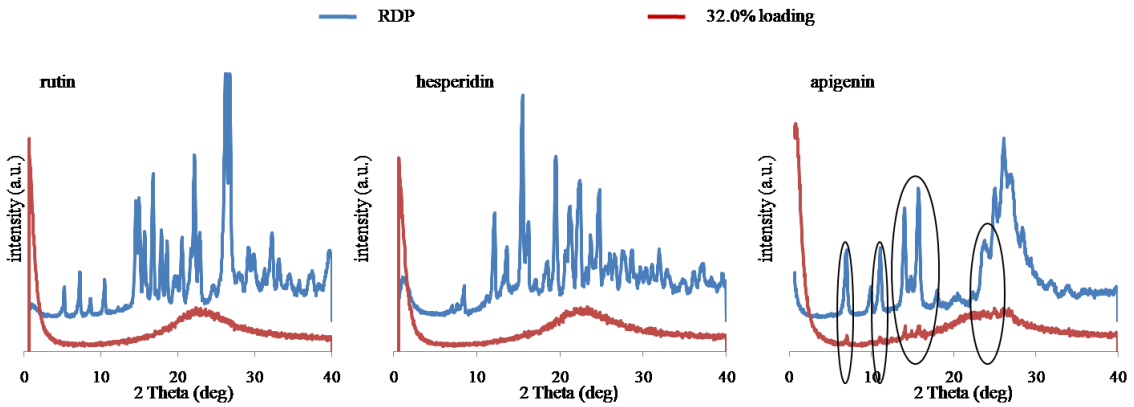

Fig. 1. X-ray spectra of silicas loaded with the anti-oxidants rutin (left), hesperidin (middle) and apigenin (right) as well as respective RDP as references.

Simply speaking, the theory of this loading method is as followed: the pores of the silica are filled with drug solution and the solvent is subsequently evaporated by temperature control. The drug precipitates and stays amorphous due to the space restriction by the pores as well as the interaction between the drug and the function group of the silica. To make sure the final product is in amorphous state, every step should be calculated to avoid overloading. According to this rule, the loading volume should be less than the unoccupied

pore volume after each loading step. The loading amount in each step in this study is originally designed for azithromycin (**chapter 3.2**), having a density of 1.18 g/cm^3. The density of apigenin, hesperidin and rutin is 1.55 g/cm^3, 1.65 g/cm^3 and 1.82 g/cm^3, respectively. The three flavonoids with densities larger than that of azithromycin were selected to be sure that there is enough space for every loading volume. The pore volume of the Syloid® SP53D-11920 is 0.9 ml/g, thus, the theoretical maximum loadings of the three flavonoids based on their densities are all above 50.0% (w/w): 58.2% for apigenin, 59.8% for hesperidin and 62.1% for rutin (**chapter 3.2**). 32.0% (w/w) loading should not be a challenge for the final product of amorphous state. Surprisingly, apigenin did not follow the rule. One explanation for those observation can be the difference in chemical structure. Both hesperidin and rutin have many hydroxyl groups interacting by hydrogen bonds with the oxygen (-Si-O-Si-) and silanol (-Si-OH) groups of the silica pore surface. On contrary, apigenin's hydroxyl groups are all linked to aromatic rings, hindering the interaction with the functional group of silica pore surface. Thus, it is more difficult to stabilize apigenin within the pores.

3.3.4.2. Particle size of nanocrystals

The mean particle size (z-ave) determined by photon correlaction spectroscopy (PCS) of 5% (w/w) apigenin nanosuspension with 1% (w/w) Plantacare® 2000 UP was 245 nm after production (Fig. 2). Its volume weighted equivalent sphere diameters of 50% [d(v)50%] and 90% [d(v)90%] of the measured size distribution by laser diffractometry (LD) was 150 nm and 400 nm, respectively. For 5% (w/w) hesperidin nanosuspension with 1% (w/w) Kolliphor® P 188 and 1% (w/w) euxyl® PE 9010, z-ave was 250 nm, d(v)50% was 220 nm, d(v)90% was 700 nm. Both or apigenin and hesperidin can be stabilized with only 1% surfactant. But for 5% (w/w) rutin nanosuspension preserved by 1% (w/w) euxyl® PE 9010, even stabilized with 2% (w/w) Tween® 80, its z-ave of 814 nm was still larger than that of the former two anti-oxidants.

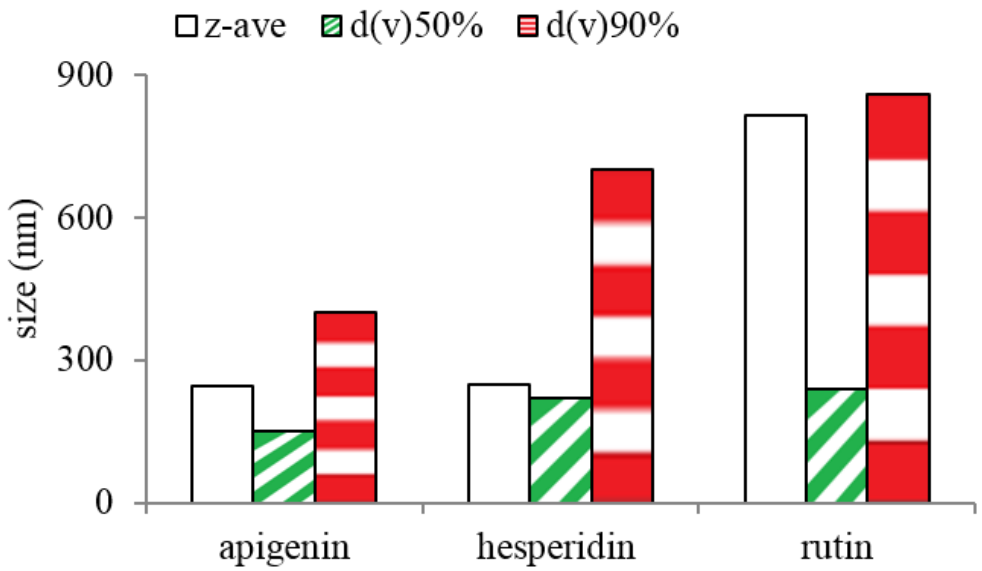

Fig. 2. Particle size (PCS diameter z-ave, LD diameter d(v)50%, d(v)90%) of obtained nanoparticles after production.

3.3.4.3. Distribution of anti-oxidants loaded smartPearls® in gel

Distribution of the gels were investigated by light microscope. It is a key factor to judge the potential of loaded silica particles after their incorporation into gels. In Fig. 3, no aggregation of the loaded silica particles could be observed after incorporation into gels and stored for 2 years at 4 °C until now. Even the silica with crystalline apigenin did not agglomerated. This can be attributed to the high viscosity of the HPC gel (Müller and Jacobs, 2002).

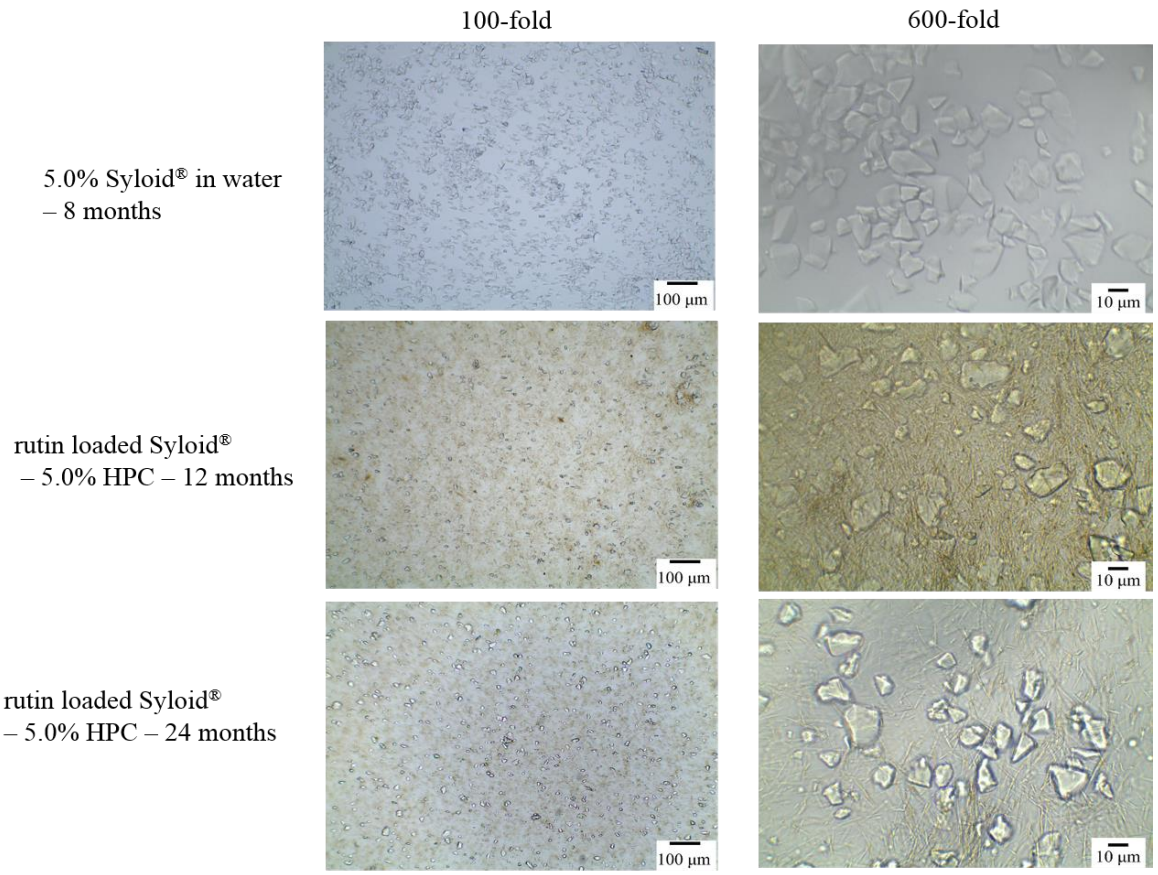

Fig. 3. (A) Light microscope pictures at 100-fold magnification (left) and at 600-fold magnification (right) of 5.0% (w/w) unloaded Syloid® dispersed in water after 8 months storage at 4 °C, and rutin loaded Syloid® in a 5.0% (w/w) HPC gel after 12 months and 24 months storage at 4 °C (scale bars from left to right: 100 µm and 10 µm).

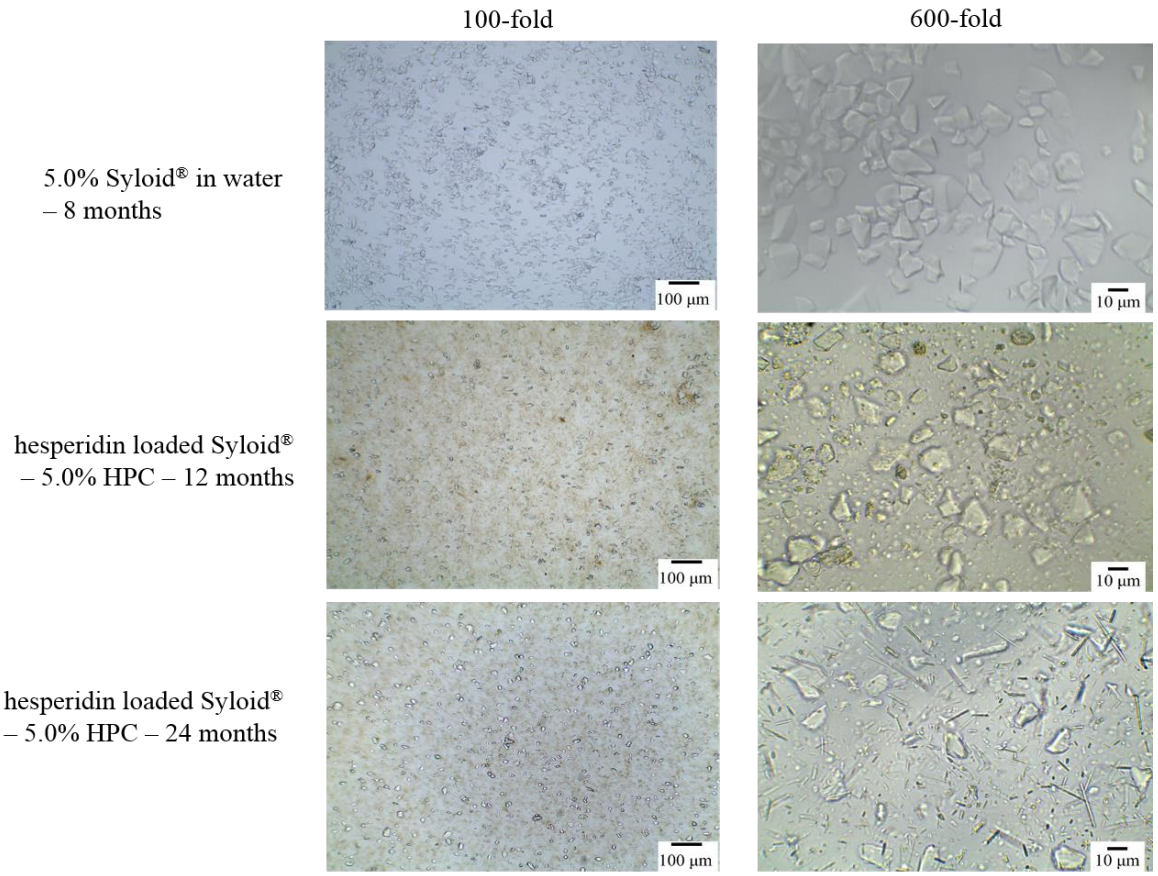

Fig. 3. (B) Light microscope pictures at 100-fold magnification (left) and at 600-fold magnification (right) of 5.0% (w/w) unloaded Syloid® dispersed in water after 8 months storage at 4 °C, and hesperidin loaded Syloid® in a 5.0% (w/w) HPC gel after 12 months and 24 months storage at 4 °C (scale bars from left to right: 100 µm and 10 µm).

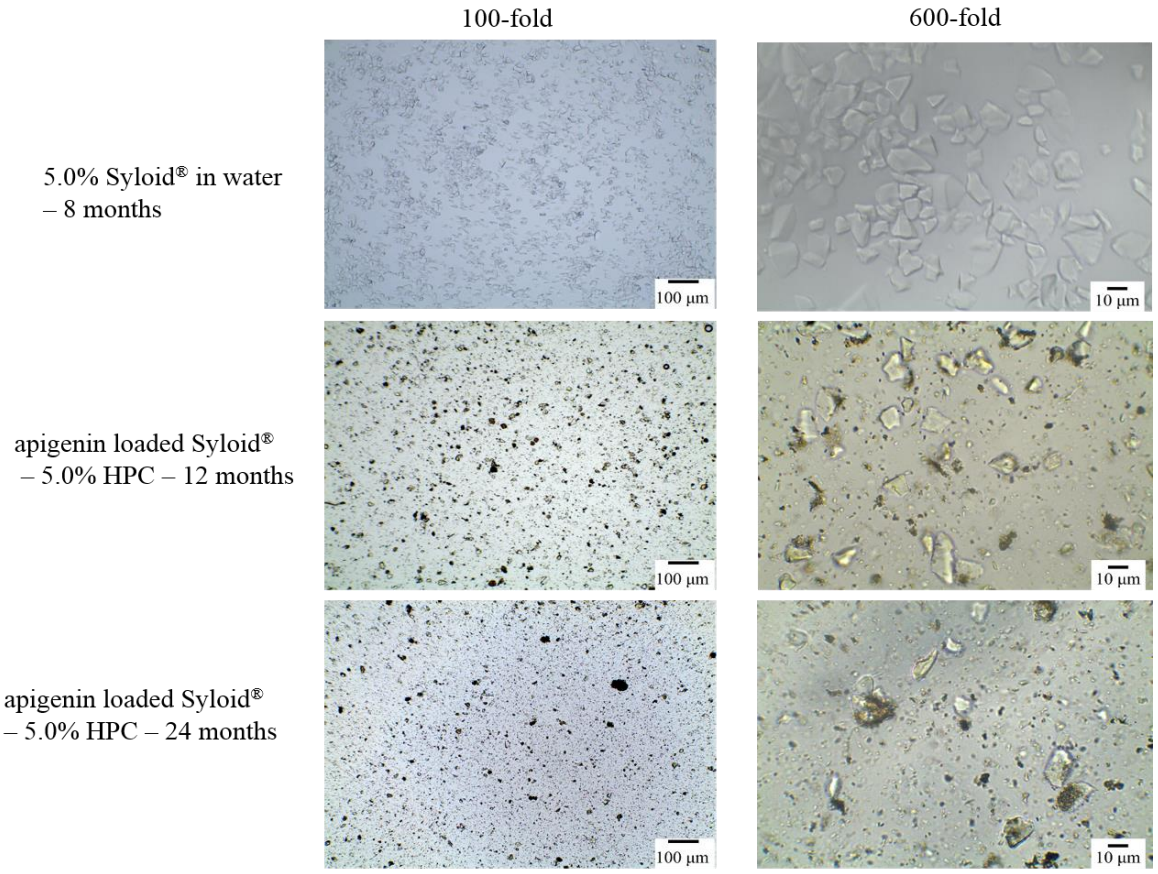

Fig. 3. (C) Light microscope pictures at 100-fold magnification (left) and at 600-fold magnification (right) of 5.0% (w/w) unloaded Syloid® dispersed in water after 8 months storage at 4 °C, and apigenin loaded Syloid® in a 5.0% (w/w) HPC gel after 12 months and 24 months storage at 4 °C (scale bars from left to right: 100 µm and 10 µm).

3.3.4.4. Stability of amorphous state of smartPearls® before and after incorporation into gels

Stability of amorphous state of the successful loaded smartPearls® (rutin and hesperidin) was detected by XRD. XRD patterns of raw drug powder (RDP), physical mixture of RDP and Syloid®, drugs-loaded Syloid® and unloaded Syloid® are shown in Fig. 4. Both of rutin and hesperidin loaded Syloid® kept the amorphous state until 1.5 years (data by now) at all measured storage temperatures (40 °C, RT and 4 °C) as no peaks of crystallinity were observed in the XRD spectra. Also, the common re-crystallization problem of normal amorphous products in liquid environments has been solved.

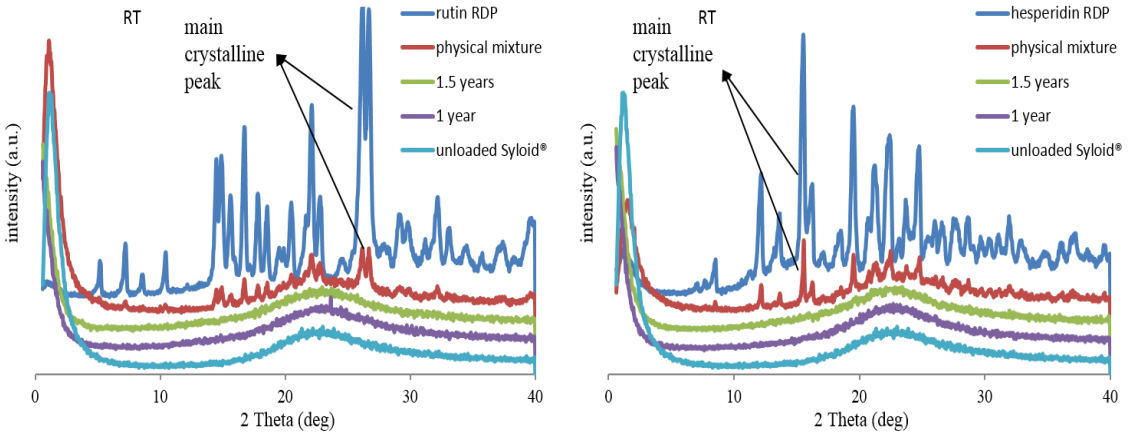

Fig. 4. (A) X-ray spectrum (vertical axis: intensity; horizontal axis: 2 Theta) of 32.0% rutin (left) or hesperidin (right) loaded Syloid® SP53D-11920 after 1 year (purple) and 1.5 years (green) at RT. RDP (dark blue), unloaded silica (light blue) and the physical mixture of RDP and silica (red) were shown additionally as references.

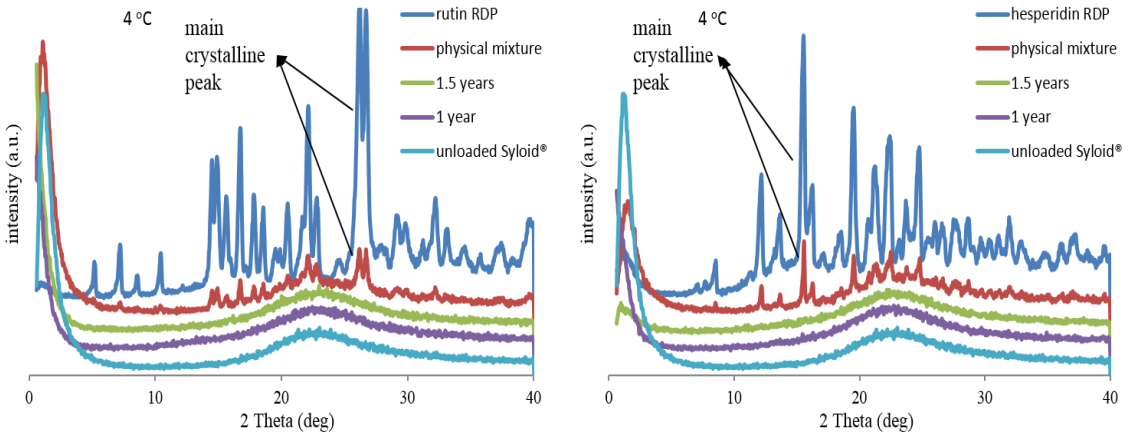

Fig. 4. (B) X-ray spectrum (vertical axis: intensity; horizontal axis: 2 Theta) of 32.0% rutin (left) or hesperidin (right) loaded Syloid® SP53D-11920 after 1 year (purple) and 1.5 years (green) at 4 °C. RDP (dark blue), unloaded silica (light blue) and the physical mixture of RDP and silica (red) were shown additionally as references.

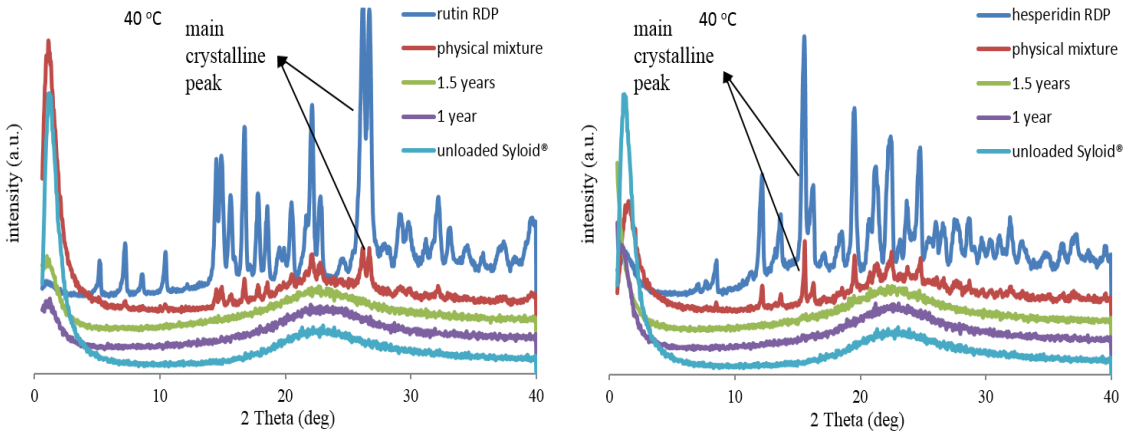

Fig. 4. (C) X-ray spectrum (vertical axis: intensity; horizontal axis: 2 Theta) of 32.0% rutin (left) or hesperidin (right) loaded Syloid® SP53D-11920 after 1 year (purple) and 1.5 years (green) at 40 °C. RDP (dark blue), unloaded silica (light blue) and the physical mixture of RDP and silica (red) were shown additionally as references.

In Fig. 5, smoothing curve of the background in the X-ray diffraction patterns was corresponding to the amorphous state of anti-oxidants loaded silicas in HPC gels, meaning that the HPC gels with loaded rutin or hesperidin smartPearls® could retain the amorphous state over a storage time of 18 months (until now). On contrary, presence of crystalline peaks in the X-ray spectrum of RDP and physical mixture (RDP and gel base) was observed. It is concluded that incorporation in HPC gels of smartPearls® with rutin and hesperidin did not lead to re-crystallization of the incorporated anti-oxidants for a long time even in liquid dispersion. This phenomenon may be contributed to the effective amorphization of smartPearls® technology, which is in consistent with the result in **chapter 3.2** and **chapter 3.4**.

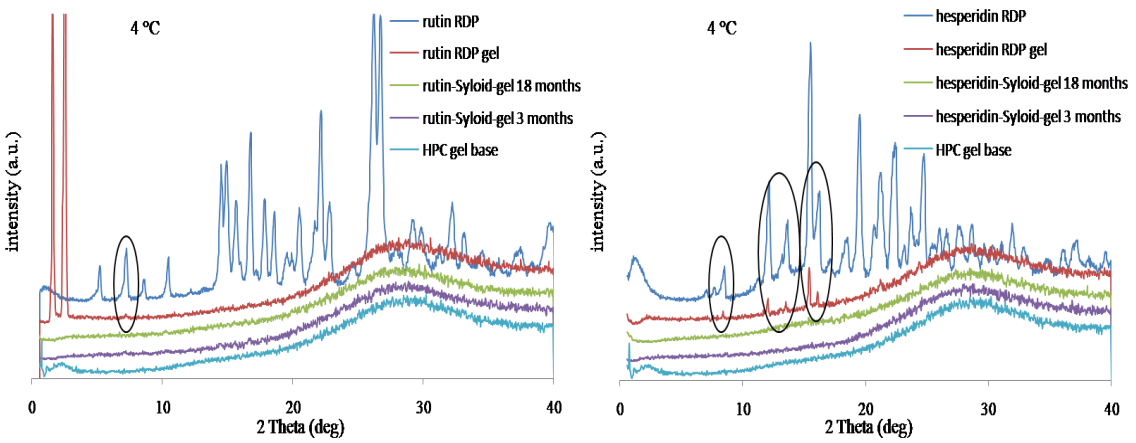

Fig. 5. X-ray spectrum (vertical axis: intensity; horizontal axis: 2 Theta) of rutin (left) and hesperidin (right) loaded Syloid® SP53D-11920 in gel after a storage time of 3 months (purple) and 18 months (green) at 4 °C. RDP (dark blue), HPC gel base (light blue) and the physical mixture of RDP and gel base (RDP gel, red) were shown additionally as references.

3.3.4.5. Ex vivo skin penetration

The stratum corneum is considered as the main barrier for most drugs (Kuswahyuning, et al. 2015). Thus, it was utilized to judge, which formulation possessing a higher percutaneous penetration. The penetrated amount of actives in the stratum corneum was studied by porcine ear tape stripping. The results of the porcine ear skin penetration study are shown in Fig. 6. The data were normalized by dividing the amount per tape (µg) by the drug concentration (%) in the respective formulation. Depth of skin penetration is correlated with the tape number where higher tape numbers stand for deeper penetration. The first tape can be excluded from the analysis, showing only non-penetrated drug. For both hesperidin (Fig. 6 A) and rutin (Fig. 6 B) loaded smartPearls®, improved skin penetration was achieved compared to either RDP or NC formulation. For example, the hesperidin smartPearls® penetration was up to 7 times higher compared to hesperidin NC (250 nm mean particle size) in the second tape. The rutin smartPearls® gel demonstrated up to 35 times higher penetration than rutin NC gel (814 nm mean particle size) in the 17th-19th tape. And both penetrated mainly up to around 20th tape (data above 5 µg/% per tape). The

silica formulations were clearly superior. Thus, rutin and hesperidin released from smartPearls® should possess higher dermal anti-oxidant activity.

On contrary, the apigenin loaded silica in crystalline state showed lower penetration than apigenin NC gel (245 nm mean particle size) almost in all the tapes (Fig. 6 C). Besides, it also showed shallower penetration than the other two anti-oxidants loaded silica in amorphous state because its most penetration (data above 5 µg/% per tape) only happened before 10th tape. When the anti-oxidant is in amorphous state (e.g., hesperidin, rutin), the solubility in the gel will be higher than that of crystalline anti-oxidant (e.g., apigenin). This is because the higher free energy in the amorphous system often serves as a driving potential for solubility. Thus, the higher solubility may explain why the penetration of hesperidin and rutin was higher and deeper as smartPearls® but not for apigenin.

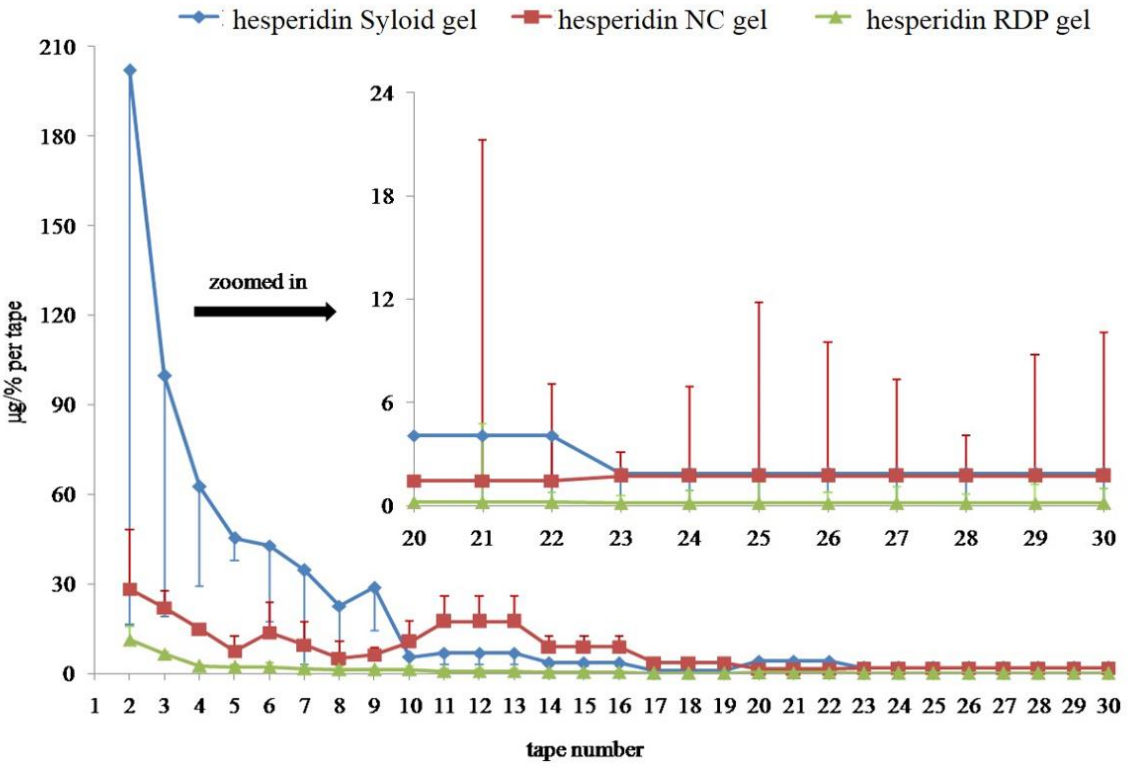

Fig. 6. (A) Normalized amount of hesperidin in each tape after 20 minutes porcine ear skin penetration, calculated by dividing the amount of drug (µg) per tape by the hesperidin concentration (%) in the applied formulation (n=3).

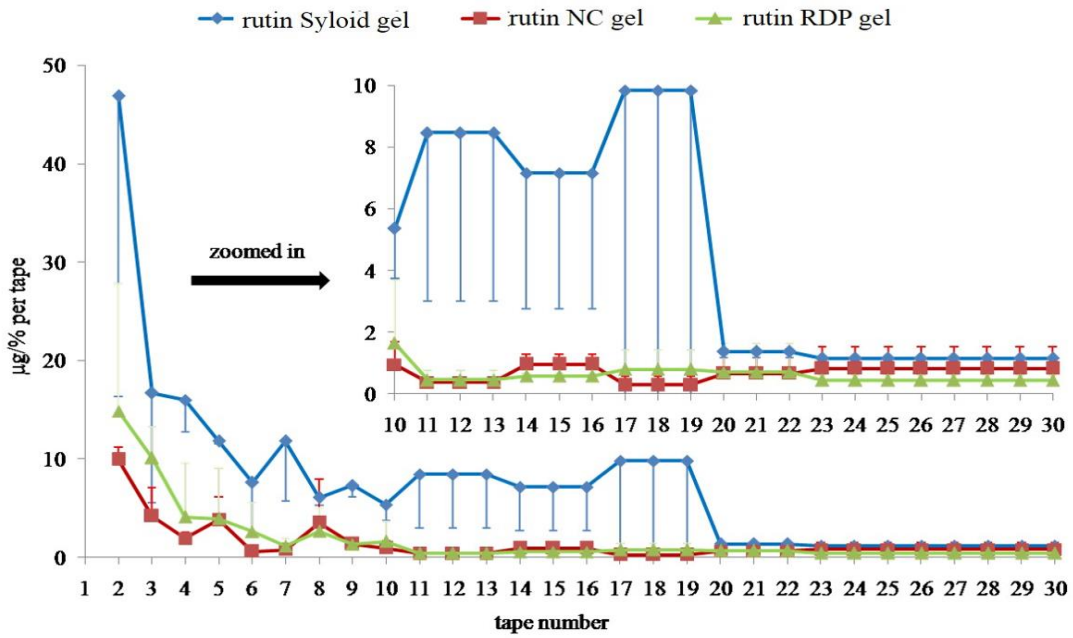

Fig. 6. (B) Normalized amount of rutin in each tape after 20 minutes porcine ear skin penetration, calculated by dividing the amount of drug (µg) per tape by the rutin concentration (%) in the applied formulation (n=3).

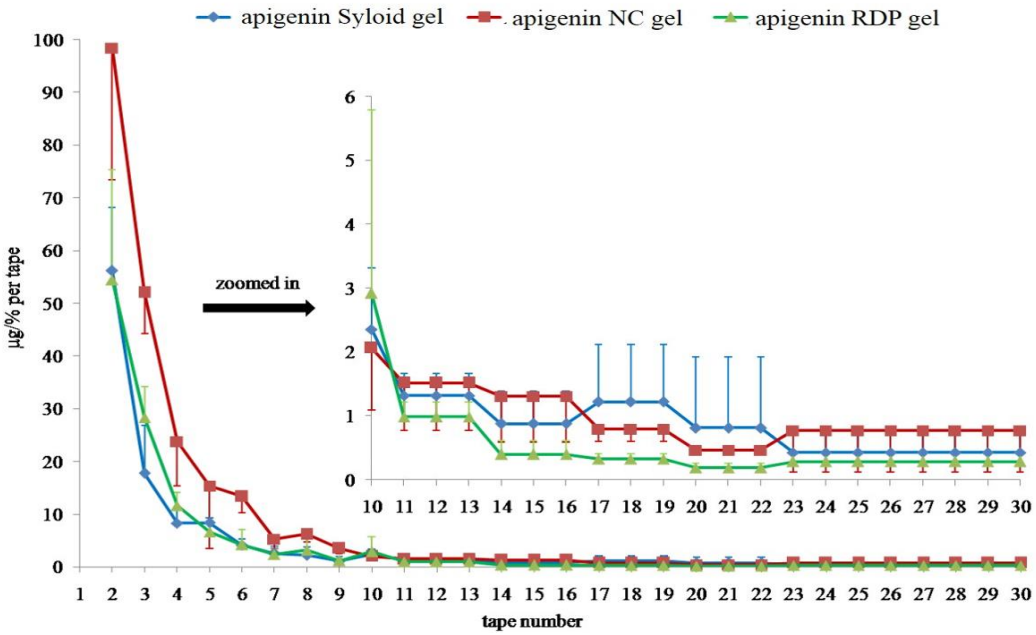

Fig. 6. (C) Normalized amount of apigenin in each tape after 20 minutes porcine ear skin penetration, calculated by dividing the amount of drug (µg) per tape by the apigenin concentration (%) in the applied formulation (n=3).

3.3.5. Conclusions

Three flavonoids with anti-aging effects were loaded onto Syloid® SP53D-11920 using the same loading procedure by smartPearls® technology. 32.0% (w/w) hesperidin smartPearls® and rutin smartPearls® were successfully achieved in amorphous state. However, apigenin was failed to get 32.0% (w/w) amorphous product, even this loading amount was far from the theoretical maximum loading (> 50%) calculated according to the density (**chapter 3.2**). The chemical structure of apigenin can be an explanation. It made guidance for further selection of substances for smartPearls®. The active with function groups can interact with the silica is assumed as an ideal candidate for smartPearls®.

The distribution of smartPearls® in the dermal vehicle was not affected by the state of loaded silicas (amorphous or crystalline). 5% (w/w) HPC gel hindered the agglomeration of all three loaded silicas. Homogeneous appearance kept at least for 2 years observed by light microscope. The phenomenon that hesperidin smartPearls® and rutin smartPearls® retained their amorphous state for at least 1.5 years at RT, 4 °C and 40 °C showed commercialized capacity of smartPearls® products. Their long-term stability in 5% (w/w) HPC gel, confirmed by XRD, strengthen this conclusion and make smartPearls® technology outweigh other amorphization methods. Liquid medium (e.g., gel) of dermal formulations can increase the hydration of the skin (Rougier, et al. 2011) and increse partition of drug to the more lipophilic skin (Monsuur, et al. 2014), resulting in higher dermal bioavailability (Rougier, et al. 2011). But seldom traditional amorphization approaches have been studied in liquid medium for dermal application. The penetration result of amorphous smartPearls® in this chapter was similar as the result in **chapter 3.2**. Both make a conclusion that the amorphous smartPearls® showed the higher skin penetration than their corresponding nanocrystals in the porcine ear penetration study.

3.3.6. References

Abla, M.J., Singh, N.D., Banga, A.K., 2016. Role of Nanotechnology in skin delivery of

drugs, in: Dragicevic, N., Maibach, H.I. (Eds.), Percutaneous penetration enhancers, chemical methods in penetration enhancement: Nanocarriers. Springer-Verlag GmbH, Berlin, pp. 1-2.

Byrn, S.R., Pfeiffer, R.R., et al., 1994. Solid-state pharmaceutical chemistry. Chem. Mater. 6, 1148-1158.

Casanova, F., Santos, L., 2016. Encapsulation of cosmetic active ingredients for topical application – a review. J. Microencapsul. 33, 1-17.

Chen, R. 2013. Tailor-made antioxidative nanocrystals: Production and *in vitro* efficacy. PhD thesis, Free University of Berlin, pp. 36.

Djekic, L., Primorac M., 2015. Percutaneous penetration enhancement poteltial of microemulsion-based organogels, in: Dragicevic, N., Maibach, H.I. (Eds.), Percutaneous penetration enhancers, chemical methods in penetration enhancement: Drug manipulation strategies and vehicle effects. Springer-Verlag GmbH, Berlin, pp. 263

Kuswahyuning, R., Grice, J.E., Moghimi, H.R., Roberts, M.S., 2015. Formulation effects in percutaneous absorption, in: Dragicevic, N., Maibach, H.I. (Eds.), Percutaneous penetration enhancers, chemical methods in penetration enhancement: Drug manipulation strategies and vehicle effects. Springer-Verlag GmbH, Berlin, pp. 112-115.

Lauer, A.C., 2001. Percutaneous drug delivery to the hair follicle, in: Bronaugh, R.L., Maibach, H.I. (Eds.), Topical absorption of dermatological products. Marcel Dekker Inc., New York, pp. 93.

Marsano, E., Bianchi, E., Sciutto, L., 2003. Microporous thermally sensitive hydrogels based on hydroxypropyl cellulose crosslinked with poly-ethyleneglicoldiglycidyl ether. Polymer 44, 6835-6841.

Mauludin, R., Müller, R.H., et al., 2009. Kientic solubility and dissolution velocity of rutin nanocrystals. Eur. J. Pharm. Sci. 36, 502-510.

Monsuur, F., Höfer, H., et al., 2016. Active-loaded particulate materials for topical administration.PCT/EP2015/071138. Germany. WO2016041992-A1.

Müller, R.H., MäderK., Gohla, S., 2000. Solid lipid particles (SLN) for controlled drug delivery – a review of the state of the art. Euro. J. Pharm. Biopharm. 50, 161-177.

Müller, R.H., Jacobs, C., 2002. Buparvaquone mucoadhesive nanosuspension: preparation, optimization and long-term stability. Int. J. Pharmceutics 237, 151-161.

Müller, R.H., Keck, C.M., 2012. Twenty years of drug nanocrystals: Where are we and where do we go? Euro. J. Pharm. Biopharm. 80, 1-3.

Müller, R. H., Monsuur, F., et al., 2014. smartPearls- novel amorphous delivery system based on porous materials to increase skin penetration of anti-oxidants, Workshop NutriOx, Metz. pp. 43.

Müller, R.H., Zhai, X., Romero, G.B., Keck, C.M., 2016. Nanocrystals for passive dermal penetration enhancement, in: Dragicevic, N., Maibach, H.I. (Eds.), Percutaneous penetration enhancers, chemical methods in penetration enhancement: Nanocarriers. Springer-Verlag GmbH, Berlin, pp. 284-285.

Nikolic, S., Keck, C.M., et al., 2011. Skin photoprotection improvement: synergistic interaction between lipid nanoparticles and organic UV filter. Int. J. Pharm. 414, 276-284.

Pardeike, J., Müller, R.H., 2010. Nanosuspensions: a promising formulation for the new phospholipase A2 inhibitor PX-18. Int. J. Pharm. 391, 322-329.

Peppas, N.A., Bures, P., et al., 2000. Hydrogels in pharmaceutical formulations. Euro. J. Pharm. Biopharm. 50, 27-46.

Romero, G.B., Chen, R., et al., 2015. Industrial concentrates of dermal hesperidin smartCrystals®– production, characterization & long-term stability. Int. J. Pharm. 482, 54-60.

Rougier, A., Lotte, C., Maibach, H.I., 2001. In vivo relationship between percutaneous absorption and transepidermal water loss, in: Bronaugh, R.L., Maibach, H.I. (Eds.), Topical absorption of dermatological products. Marcel Dekker Inc., New York, pp. 115.

Sekkat, N., Kalia, Y.N., et al., 2002. Biophysical study of porcine ear skin *in vitro* and its comparison to human skin *in vivo*. J. Pharm. Sci. 91, 2376-2381.

Shaal, L.A., Shegokar, R., Müller, R.H., 2011. Production and characterization of anti-oxidant apigenin nanocrystals as a novel UV skin protective formulation. Int. J. Pharm. 420, 133-140.

Shukal, S., Gupta, S., 2010. Apigenin: A promising molecule for cancer prevention. Pharm. Res. 27, 962-978.

Tavano, L., 2015. Liposomal gels in enhancing skin delivery of drugs, in: Dragicevic, N., Maibach, H.I. (Eds.), Percutaneous penetration enhancers, chemical methods in penetration enhancement: Drug manipulation strategies and vehicle effects. Springer-Verlag GmbH, Berlin, pp. 329-331.

Walters, K.A., Brain, K.R., 2009. Topical and transdermal delivery, in: Gibson, M. (Eds.), Pharmaceutical preformulation and formulation: A practical guide from candidate drug selection to commercial dosage form. Informa Healthcare USA Inc., New York, pp. 475-512.

Wei, Q., Keck, C.M., Müller, R.H., 2017a. Oral hesperidin – Amorphization and improved dissolution properties by controlled loading onto porous silica. Int. J. Pharm. 518, 253-263.

Wei, Q., Keck, C.M., Müller, R.H., 2017b. Preparation and tableting of long-term stable amorphous rutin using porous silica. Euro. J. Pharm. Biopharm. 112, 97-107.

Yourick, J.J., Brouaugh, R.L. 2001. Percutaneous penetration as it relates to the safety evaluation of cosmetic ingredients, in: Bronaugh, R.L., Maibach, H.I. (Eds.), Topical absorption of dermatological products. Marcel Dekker Inc., New York, pp. 378.

3.4. A stable amorphization technology based on smartPearls® for dermal delivery of poorly soluble cyclosporin A

3.4.1. Abstract

32.0% cyclosporin A was loaded surfactant-free onto Syloid® SP53D-11920 by smartPearls® technology. The loaded smartPearls® stabilized the amorphous state of cyclosporin A for at least 1 year at room temperature, confirmed by X-ray diffraction. Incorporating the loaded smartPearls® into a hydrogel (5.0% hydroxypropyl cellulose) the amorphous state of cyclosporin A remained for at least 1.5 years at 4 °C. Also the homogeneous distribution of the loaded smartPearls® within the hydrogel was observed over 2 years at 4 °C by light microscope. In comparison of the penetration efficiency on porcine ears between amorphous cyclosporin A loaded in smartPearls® and amorphous nanoparticles, smartPearls® showed 14 times higher efficiency, expressing superior penetration. Thus, all obtained data confirmed that smartPearls® can be a potential dermal delivery system for the poorly soluble cyclosporin A showing distinctly higher bioavailability, even superior than amorphous nanoparticles.

3.4.2. Introduction

Around 70-90% of newly developed potential actives for medicine and costimitics are hydrophobic actives (Müller and Keck, 2012). These substances are mostly classified as class II and IV according to the Biopharmaceutics Classification System (BCS) (Wei, et al. 2015) with low bioavailability (Engers, et al. 2010; Kawabata, et al. 2011). When applied in dermal delivery system, they often have the problem to penetrate into the skin due to the low concentration gradient resulting from the low saturation solubility (Tam, et al. 2008; Watkinson, et al. 2009; Zhai, et al. 2014). In certain cases the low concentration gradient can be overcome by dissolving the active into the oil phase of an oil-in-water cream (o/w cream) instead (Junyaprasert, et al. 2009). However, the concentration gradient is not the only determining factor influencing the penetration. The partitioning of the active, for

example, also plays a cruical rule. The high lipophilic active prefers to stay in the lipophilic environment of the oil droplets of the cream, instead of partitioning into the hydrophilic environment of the water phase or the mixed hydrophilic-lipophilic environment of the skin (Monsuur, et al. 2014). Thus, suspension formulations with particles dispersed in the aqueous medium are prefered in this study. The partially dissolved molecules with low concentration would prefer to leave the hydrophilic medium and therefore are partitioning into the more “comfortable environemnt” of more lipophilic skin.

The suspension formulations for dermal delivery entered successfully the market can be mainly classified as nanocrystals and lipid nanoparticles. JUVEDICAL Age-Decoder Face Fluid and Cream (main active: rutin) were the first dermal products with nanocrystals (Zhai, et al. 2014) on the cosmetic market in 2007 by the company Juvena (Switzerland), followed by EDELWEISS Wrinkle Fighter Eye Lift Fluid by the company Audorasan (Germany) (Pardeike, 2008). Lipid nanoparticles has the most comerical products for dermal delivery. First products emerged on the market were cosmetics by the company Dr. Rimpler GmbH (Germany) in 2005 (Müller, et al. 2007): Cutanova Cream NanoRepair Q10 and Intensive Serum NanoRepair Q10 (main active: coenzyme Q10). Some other examples (Pardeike, et al. 2009) include IOPE Super Vital Moist Cream (main active: coenzyme Q10) by the company AmorePacific (South Korea) in 2006, Swiss Cellular White Illuminating Eye Essence (main active: glycoprotiens) and Swiss Cellular White Illuminating Ampoules, whitening products from La Prairir (Switzerland) in 2007.

It has already been 30 years from the market introduction of first commerical nanotechnology dermal products including suspension formulation. New technology is in demand for the market of topical administration for both pharmaceutical drugs and cosmetical actives. smartPearls® technology, based on porous silicas, first appeared on the published patent at 2014 (Monsuur, et al. 2014). Altough it has similar theory with oral CapsMorph® (Wei, et al. 2015), this new technology focuses on topical administration. It combines nanosize and amorphization to increase the bioavailability. Unlike some other

traditional methods such as melting quenching (Miyazaki, et al. 2007), desolvation (Aucamp, et al. 2012) and hot melt extrusion (Sarode, et al. 2013) to amorphize drug, it has the advantage of long physical stabilization of the amorphous state without any surfactants. The mechanism is the confined space of the mesoporous carrier. Thanks to the tiny pores where the active molecules are located, the structure obstructs the alternation from irregular arrangement (amorphous state) to regular arrangement (crystalline state). Thus, the drug molecule prefer to retain in amorphous state within the tiny pores for a long time (Wei, et al. 2015). Due to the absence of the long-range molecular order, the amorphous form possesses weaker interactions between molecules than the crystalline state, resulting in higher affinity for a given solvent (Byrn, et al. 1994). Then the higher saturation solubility is achieved. In addition, the nano size of the pores can also increase saturation solubility due to Ostwald-Freundlich equation and Kelvin equation (Mauludin, et al. 2009; Pardeike and Müller, 2010). On one hand, the increased saturation solubility will bring increased dissolution velocity based on Noyes-Whitney equation. On the other hand, the nano size of the pores will enlarge surface area, resulting in further enhancement (Mauludin, et al. 2009). In the end, a raising concentration gradient between skin and the dermal formulation applied smartPearls® technology is obtained, leading to improved diffusive flux into the skin, and finally increased dermal bioavailability is achieved because of the increased penetration (Müller, et al. 2011).

Cyclosporin A is a highly liphophilic cyclic decapeptide drug with a log P value of 4.12 (Cholkar, et al. 2015; Goyal, et al. 2015; Yadav, et al. 2015). It can not only inhibite the activation of T-cell, avoiding the production of inflammatory cytokine, but also inhibite apoptosis by blocking the opening of mitochondrial permeability transition pores (Cholkar, et al. 2015). Thus, it is commonly used as an immnunosuppressive agent. However, its oral administration usually resulting in side effects such as vomiting, high blood pressure, liver dysfunction and so on (Roberts, et al. 2013). Therefore, the dermal applications of cyclosporin A were studied in recent years to treat dermatological disease such as psoriasis (Romero, et al. 2016) and immunological diseases during organs transplantation (Goyal, et

al. 2015). It was selected as the model drug to be loaded in the mesoporous silica by smartPearls® technology due to its special property possessing amorphous state of bulk powder and nanoparticles (Romero, et al. 2016).

smartPearls® technology enables the stabilization of actives in amorphous state, showing an increased saturation solubility and therfore also an improved skin penetration in comparison to crystalline raw drug powders (**chapter 3.2, 3.3**). If smartPearls® technology will perform also superior to raw drug powders being already in amorphous state, e.g., cyclosporin A will be examined in the following. The amourphous state of the loaded silica before and after incorporation into hdrogel were inverstigated. The firm distribution of the loaded silicia in hydrogel was observed as well. Porcine ear skin test was performed to analyze the penetration behavior of the loaded silica. Cyclosporin A nanoparticles in amorphous state were produced for comparison.

3.4.3. Experimental Section

3.4.3.1. Materials

Cyclosporin A was purchased from Selcia Limited (Ongar, United Kingdom). Syloid® SP53D-11920 was kindly provided from W. R. Grace & Co. KG (Worms, Germany) and D-α-tocopheryl polyethylenglycol 1000 succinate (Kolliphor® TPGS) from BASF SE (Ludwigshafen am Rhein, Germany). Hydroxypropyl cellulose (HPC, Klucel GF®) was brought from Caesar & Loretz GmbH (Hilden, Germany). Ethanol (96%) was used of analytical grade. Freshly produced ultrapurified water was obtained by reverse osmosis from a Millipak® Express 20 Filter unit (Milli-Q, Millipore GmbH, Merk, Germany). All materials were used as received.

3.4.3.2. Production of cyclosporin *A loaded smartPearls®*

Cyclosporin A was dissolved in ethanol (96%) in a ratio of 1:4 by weight. The so

obtained drug-ethanol-solution was filled in in a dark glass bottle equipped with a spraying nozzle. In the first loading step, 10.00 g drug-ethanol-solution was sprayed and admixed with 10.00 g Syloid® SP53D-11920 with a pestle in an ointment bowl (wetness impregnation method). Stirring was conducted during the whole loading process to get homogeneous distribution. Subsequently, the ethanol was evaporated in an oven at 40 °C before next loading step. The complete evaporation was monitored via weight loss determination. In the second loading step, 8.00 g drug-ethanol-solution was sprayed and admixed with 9.00 g of the obtained silica using the same method. After evaporating ethanol, 3.72 g drug-ethanol-solution was sprayed and admixed with 8.10 g of the obtained silica. 32.0% (w/w) cyclosporin A silicas was then achieved after the third loading. In total 4.70 g cyclosporin A was loaded onto 10.00 g Syloid® SP53D-11920.

3.4.3.3. Production of nanoparticles and gels

Nanoparticles were produced as reported (Romero, et al. 2016) to compare with the corresponding loaded smartPearls® in further studies. 5.0% (w/w) cyclosporin A was dispersed in 1.0% (w/w) TPGS solution using Ultra-Turrax T25 (Jahnke und Kunkel, Germany) for 1 minute at 8,000 rpm. The resulting coarse suspension was wet milled with 0.2 mm diameter yttrium-stabilized zirconia beads (Hosokawa Alpine, Germany) using a PML 2 bead mill (Bühler, Switzerland), with a small milling chamber at a rotation speed of 2,000 rpm for 30 minutes. The obtained nanoparticles were incorporated into HPC gel to get a final concentration of 5.0% (w/w) nanocrystals and 5.0% HPC (NC gel). The corresponding raw drug powder (RDP) gel of 5.0% active was produced as reference. The loaded smartPearls® were also incorporated into the 5.0% HPC gels to get 1.0% active (Syloid gel).

3.4.3.4. X-ray diffraction (XRD)

Amorphous state in smartPearls® and amorphous state of nanoparticles was determined by X-ray diffraction generator (XRD, Philips PW 1830, Amedo, Netherlands) using the

wide-angel X-ray scattering (2 Theta = 0.6-40°) with a scan rate of 0.04° per 2 seconds. A copper anode (Cu-Kα radiation) was used in the Goniometer PW18120 detector with a voltage of 40 kV and a current of 25 mA. Powder materials were dispersed finely and transformed into a sample holder. The tested nanosuspension was mixed with a guar gum (1.5% w/w) until creamy and put into a sample holder.

3.4.3.5. Light microscope (LM) and transmission electron microscope (TEM)

Light microscope (Motic Deutschland GmbH, Germany) was performed at 100-fold and 600-fold magnifications to observe any aggregation of the loaded smartPearls® in the hydrogel during storage. The morphological examination of the unloaded and loaded smartPearls® was performed by a high resolution transmission electron microscope (TEM, Tecnai™ G^2 20 S-TWIN, FEI Co., USA).

3.4.3.6. Ex vivo skin penetration study

Three porcine ears were freshly obtained from domestic pigs in a local slaughterhouse, and prepared by cutting the hairs with an electriccutter, washing with tap water and drying. For analyzing the penetration behavior, the cyclosporin A loaded Syloid® (Syloid gel, corresponding to 1.0% active), 5.0% nanoparticles gel (NC gel) and 5.0% RDP gel were applied homogenously onto one porcine ear skin with an area of 1.5 × 1.5 cm^2. An adhesive tape was pressed onto the skin using a roller and then removed rapidly after a penetration time of 20 minutes. Each area was taped for 30 times. The tape stripping study was repeated three times on three porcine ears with tested samples. Afterwards, the drug was quantitatively extracted from each tape strip by 3 hours shaking at 120 rpm and 25 °C in an Innova 4230 shaker (New Brunswick Scientific GmbH, Nürtingen, Germany), using 2 ml of acetonitrile/DMSO (1:1, v/v) as solvent. The resulting suspension was centrifuged (Heraeus Megafuge Centrifuge 3.0R, Kendro Laboratory Products GmbH, Hanau, Germany) at 15,493 × g for 15 minutes. Subsequently the obtained supernatant was analyzed by high performance liquid chromatography (HPLC) as described in section

3.4.3.7.

3.4.3.7. High performance liquid chromatography (HPLC) analysis

Cyclosporin A concentration was determined by HPLC with an auto sampler model 560, equipped with a solvent delivery pump system model 522 and a diode array detector model 430 (Kontron Instruments, Rossdorf, Germany). As column a Nucleosil-100 C18 reverse phase column (125 × 4 mm, 5 µm) was used. As mobile phase a mixture of acetonitrile/water/isopropanol at a ratio of 70:28:2 (v/v/v) was used with a flow rate of 1.2 ml/min. The column temperature was set to 60 °C. The UV detector measured cyclosporin A was at a wavelength of 210 nm.

3.4.4. Results and Discussions

3.4.4.1. Amorphous state of loaded smartPearls® and nanoparticles

XRD can differentiate whether the tested sample is still amorphous or crystalline (Souto, 2005): amorphous substance displays a regular baseline, while crystalline active presents many diffraction bands. These diffraction phenomena are compatible with the molecules either being arranged at random (amorphous) or in a regular network model (crystalline). XRD patterns of cyclosporin A as RDP, nanoparticles and smartPearls® are shown in Fig. 1. Normally the coarse active powders possess the thermodynamic more favorable crystalline state, but this was not the case for cyclosporin A. It is known that cyclosporin A raw drug powder is in the amorphous state instead of being crystalline because it is a peptide. This active remains in the amorphous state also after producing nanoparticles. For other actives, incorporation of crystalline RDP onto smartPearls® resulted in a transition of the solid state from crystalline to amorphous. However, cyclosporin A RDP was already amorphous and stayed amorphous after being loaded onto the silica up to 1 year at 4 °C (data until now).

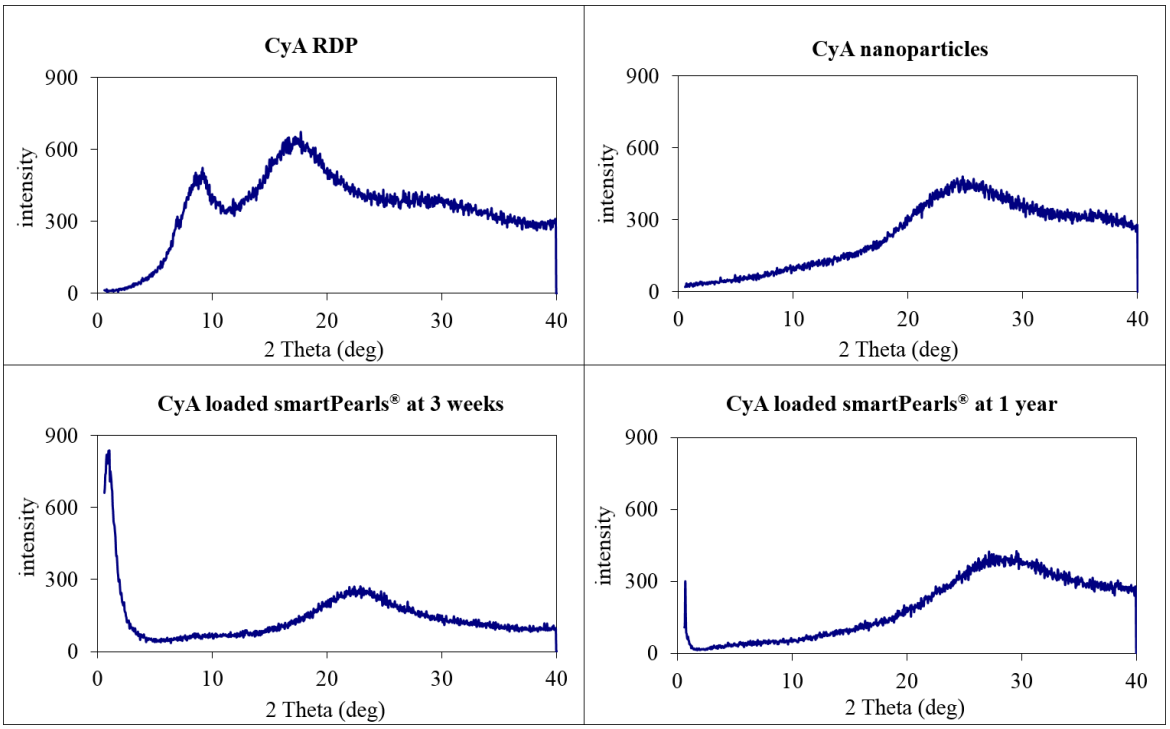

Fig. 1. X-ray diffractogram patterns of: cyclosporin A (CyA) RDP, CyA nanoparticles, CyA loaded smartPearls® after 3 weeks and 1 year at 4 °C.

3.4.4.2. Amorphous state of loaded smartPearls® in the gel

The aqueous environment of HPC gel did not change the amorphous state of loaded smartPearls® (Fig. 2). The amorphous state of cyclosporin A in the mesoporous silica and incorporated in the gel is stable up to 18 months at 4 °C (data until now). Thus, smartPearls® are a suitable dermal delivery system to overcome the common problem of amorphous drug about thermodynamical instability. The ability of the smartPearls® to retain the drug in amorphous state during storage may be attributed to the small pore size of 6 nm. The confined space hinders the alteration from high energy amorphous state to low energy crystal state (Wei, et al. 2015).

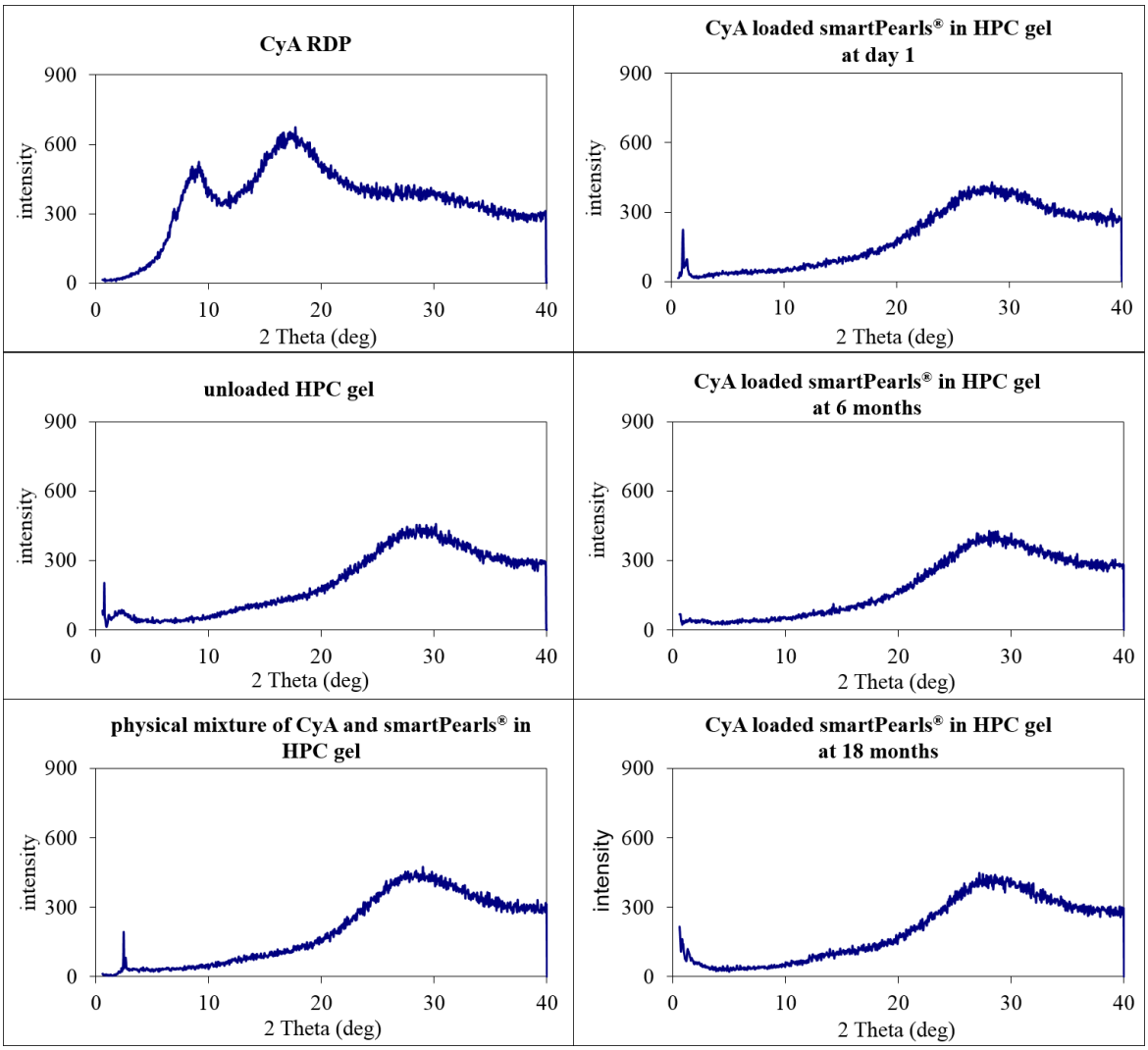

Fig. 2. X-ray diffractogram patterns of: cyclosporin A (CyA) RDP, HPC gel base (unloaded HPC gel), physical mixture (CyA RDP, HPC gel), CyA loaded smartPearls® in HPC gel at day 1 and after 6 months and 18 months at 4 °C.

3.4.4.3. Transmission electron microscope (TEM)

The morphological characterization of the 32.0% cyclosporin A loaded smartPearls® is shown in Fig. 3. Compared to the unloaded silica (Fig. 3, left), many dark shadows were observed in the loaded silicas (Fig. 3, right). These dark shadows could be the loaded drug inside the silica, showing the drug distribution in the silica carrier after loading.

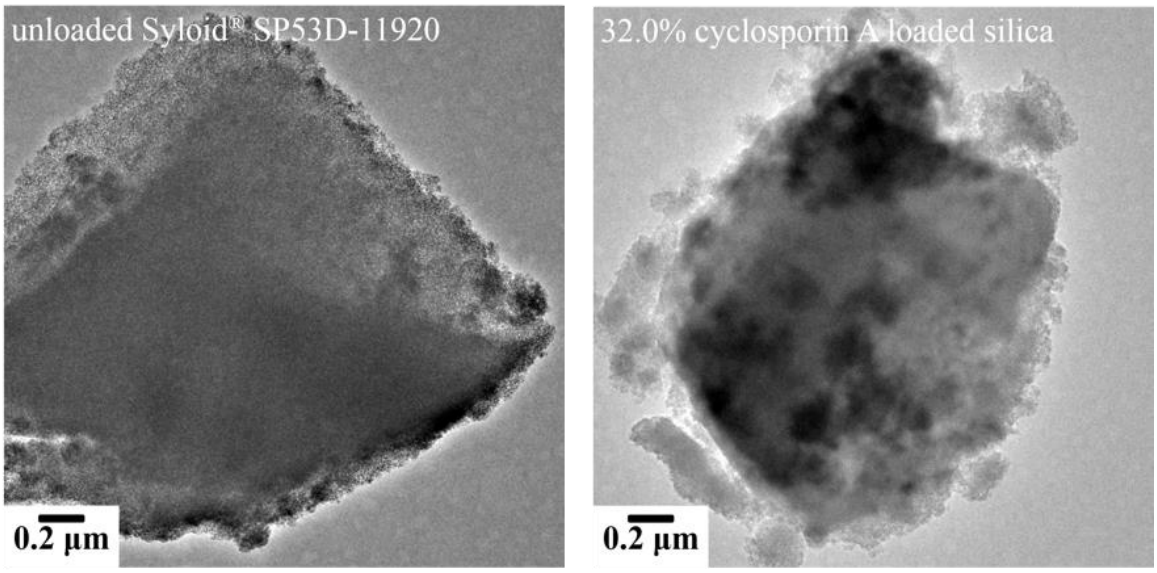

Fig. 3. TEM micrographs of the unloaded silica (left) and loaded silica (right).

3.4.4.4. Stability of Syloid® in gel formulations

Agglomeration tendency was observed for the 5.0% unloaded Syloid® in water after 8 months storage at 4 °C noticeable by the uneven distribution (Fig. 4). In contrast, no aggregation was observed for the loaded Syloid® in HPC gel for up to 2 years. The high viscosity of the gel base could be an explanation, since the adhesive properties of HPC in water (El-Kattan, et al. 2000; Fukui, et al. 2000) may avoid the random movements of the Syloid® particles.

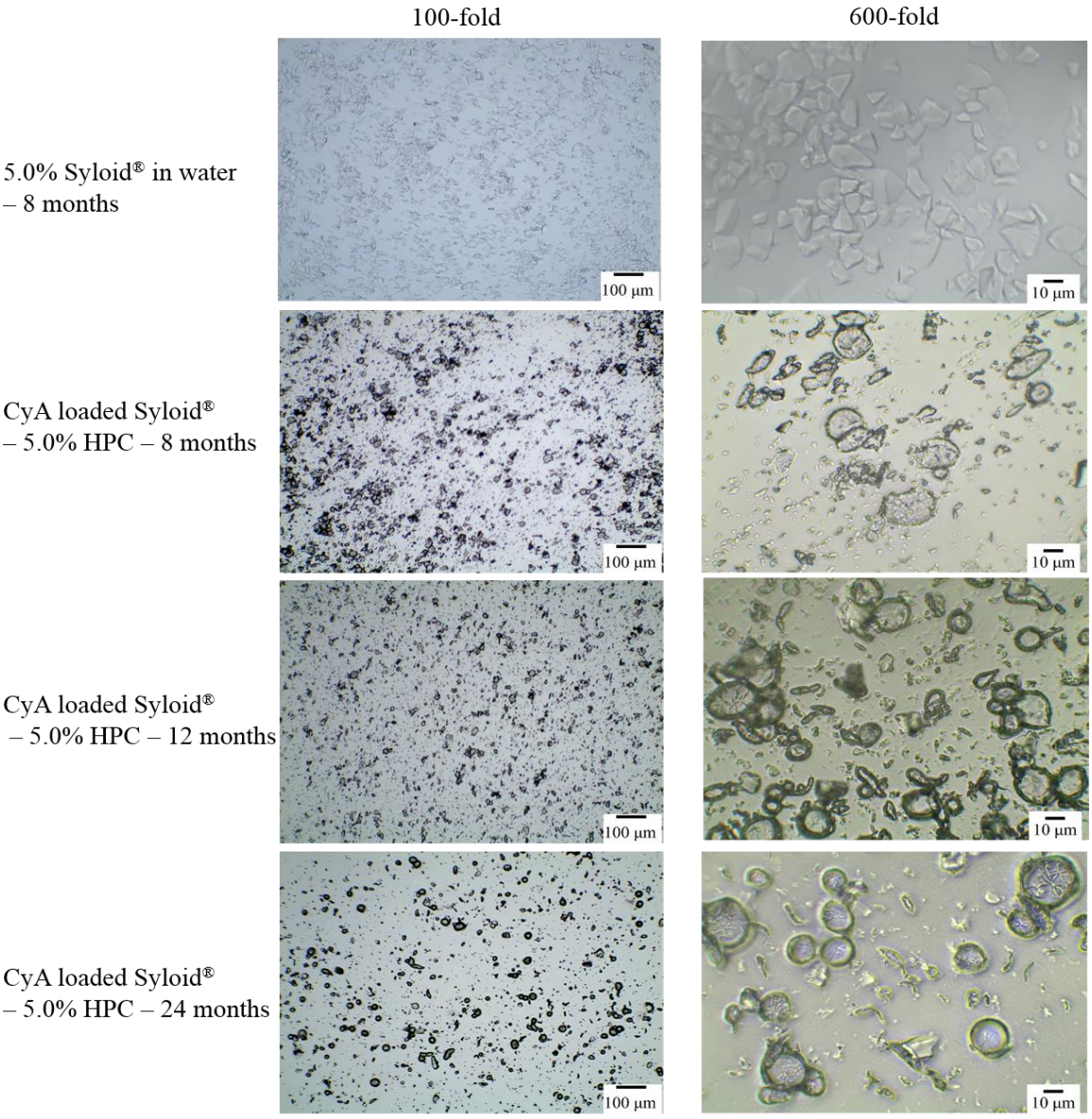

Fig. 4. Light microscope pictures at 100-fold (left) and 600-fold magnification (right) of 5.0% (w/w) unloaded Syloid® dispersed in water after 8 months storage at 4 °C, and cyclosporin A (CyA) loaded Syloid® in a 5.0% (w/w) HPC gel after 8 months, 12 months and 24 months storage at 4 °C (scale bars left: 100 µm and right: 10 µm).

3.4.4.5. Ex vivo skin penetration study

Porcine ear skin was used for the penetration study because it possesses many similarities to human skin such as epidermal thickness and lipid composition (Sekkat, et al. 2002). It is well-accepted and common used to evaluate the penetration profiles of topical

formulations. The results of the porcine ear skin penetration studies are shown in Fig. 5. Normalization was done by dividing the penetrated amount (µg) per tape by the percentage of active in the applied formulation. The data were plotted as µg/% versus the tape number. Depth of skin penetration was correlated with the tape number, whereas higher tape number represents a deeper penetration. The first tape was excluded from the analysis having only non-penetrated drug.

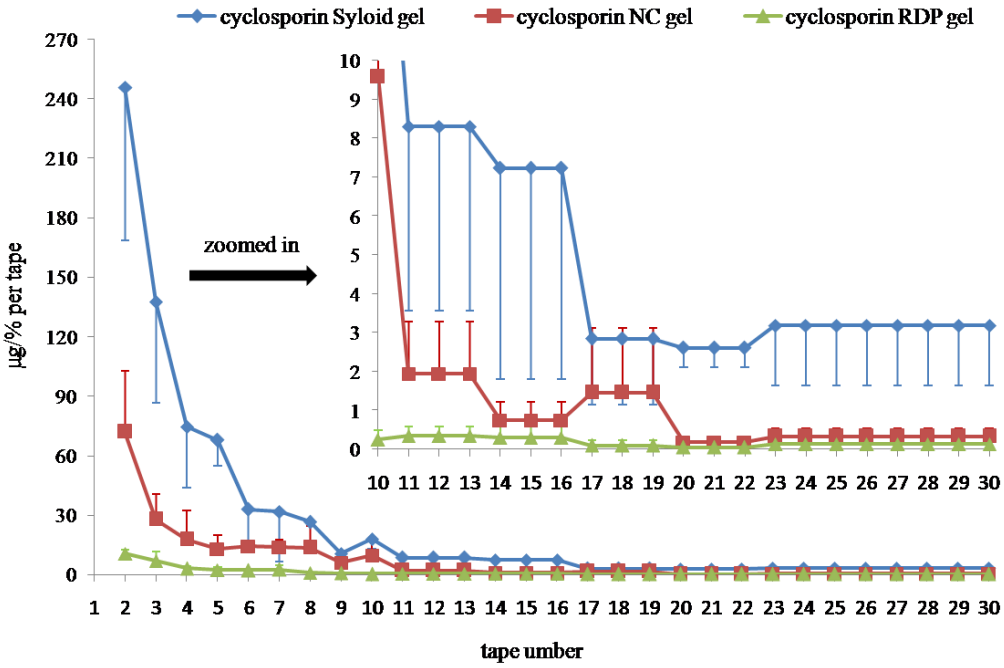

Fig. 5. Normalized amount of cyclosporin A in tapes after 20 minutes penetration, calculated by dividing the amount of drug (µg) per tape by the cyclosporin A concentration (%) in the applied formulation (n=3).

Cyclosporin Syloid gel showed both the deepest and highest amount of active penetrated the skin among all tested cyclosporin formulations (Fig. 5). Active amounts found in deeper skin layers (from tape 20 to 30) were up to 14 times higher for the Syloid gel compared to the nanoparticles (photon correclation spectrophory diameter of 290 nm; laser diffraction diameter d(v)50% of 240 nm and d(v)90% of 470 nm) (Romero, et al. 2016) in gel and up to 49 times higher for the RDP gel, despite that both the cyclosporin

nanoparticles and RDP were in the amorphous state. From the mechanistical point of view, the saturation solubility of all amorphous formulations, and thus penetration, should be the same. However, smartPearls® was superior, attributed to the superimposed Kelvin effect (increased dissolution pressure due to small mesopore size, in this case 6 nm). This high penetration proved that an increased skin penetration can not only be obtained from crystalline drugs such as azithromycin and rutin (**chapter 3.2, 3.3**) but also from amorphous RDP such as cyclosporin A loaded in smartPearls®.

3.4.5. Conclusions

smartPearls® technology can generate and control a high drug loading for amorphous poorly soluble raw drug powder (e.g., 32.0% cyclosporin A loaded Syloid® SP53D-11920). Additionally it allows to keep the drug in amorphous state and can easily be distributed homogeneously in water-containing gel bases for a long time (more than 1.5 years), avoiding potential re-crystallization problem of common amorphization method, paving the way for commercialization. Surprisingly, it was shown that for amorphous raw drug powders, like cyclosporin A, the skin penetration can be even further improved when loaded onto silica by smartPearls® technology. The dermal bioavailability of the cyclosporin A loaded silica was even higher compared to the amorphous nanoparticles. Moreover, it is applicable in new dermal commercial products since various porous particles can be purchased on the market. In sum, smartPearls® technology holds promise as a dermal delvery system for amorphous drug. However, scientific work and development are still necessary to render the processes industrially feasible. There is no doubt that such products will arrive on the market. Both scientific progress and the relevant toxicity experiments are required to be determined.

3.4.6. References

Aucamp, M., Liebenberg, W., et al., 2012. Physicochemical properties of amorphous roxithromycin prepared by quench cooling of the melt or desolvation of a chloroform

solvate. AAPS Pharm. Sci. Tech. 13, 467-476.

Byrn, S.R., Pfeiffer, R.R., et al., 1994. Solid-state pharmaceutical chemistry. Chem. Mater. 6, 1148-1158.

Cholkar, K., Gilger, B.C., et al., 2015. Topical, aqueous, clear cyclosporine formulation design for anterior and posterior ocular delivery. Trans. Vis. Sci. Tech. 4, 1-16.

EI-Kattan, A.F., Asbill, C.S., et al., 2000. Effect of formulation variables on the percutaneous permeation of ketoprofen from gel formulations. Drug Deliv. 7, 147-153.

Engers, D., Teng, J., et al., 2010. A solid-state approach to enable early development compounds: selection and animal bioavailability studies of an itraconazole amorphous solid dispersion. J. Pharm. Sci. 99, 3901-3922.

Fukui, E., Uemura. K., et al., 2000. Studies on applicability of press-coated tablets using hydroxypropylcellulose (HPC) in the outer shell for timed-release preparations. J. Control. Release 68, 215-223.

Goyal, R., Macri. L., et al., 2015. Formulation strategy for the delivery of cyclosporine A: Comparison of two polymeric nanospheres. Sci. Rep. 13, 1-12.

Junyaprasert, V.B., Teeranachaideekul, V., et al., 2009. Q10-loaded NLC versus nanoemulsions: stability, rheology and *in vitro* skin permeation. Int. J. Pharm. 377, 207-214.

Kawabata, Y., Wada, K., et al., 2011. Formulation design for poorly water-soluble drugs based on biopharmaceutics classification system: basic approaches andpractical applications. Int. J. Pharm. 420, 1-10.

Mauludin, R., Müller, R.H., et al., 2009. Kientic solubility and dissolution velocity of rutin nanocrystals. Eur. J. Pharm. Sci. 36, 502-510.

Miyazaki, T., Yoshioka, S., et al., 2007. Crystallization rate of amorphous nifedipine analogues unrelated to the glass transition temperature. Int. J. Pharm. 336, 191-195.

Monsuur, F., Höfer, H., et al., 2014. Active-loaded particulate materials for topical administration. US Patent 62050587. WO 2016041992A1.

Müller, R.H., Gohla, S., et al., 2011. State of the art of nanocrystals – Special features, production, nanotoxicology aspects and intracellular delivery. Eur. J. Pharm. Biopharm.

78, 1-9.

Müller, R.H., Keck, C.M., 2012. Twenty years of drug nanocrystals: Where are we and where do we go? Euro. J. Pharm. Biopharm. 80, 1-3.

Müller, R.H., Petersen, R.D., et al., 2007. Nanostructured lipid carriers (NLC) in cosmetic dermal products. Adv. Drug Deliv. Rev. 59, 522-530.

Pardeike, J., 2008. Nanosuspensions and nanostructured lipid carriers for dermal application. PhD thesis, Free University of Berlin, pp17.

Pardeike, J., Hommoss, A., et al., 2009. Lipid nanoparticles (SLN, NLC) in cosmetic and pharmaceutical dermal products. Int. J. Pharm. 366, 170-184.

Pardeike, J., Müller, R.H., 2010. Nanosuspensions: a promising formulation for the new phospholipase A2 inhibitor PX-18. Int. J. Pharm. 391, 322-329.

Roberts, E.S., Vanlare, K.A., et al., 2013. Safety, tolerability, and pharmacokinetics of 6-month daily dosing of an oral formulation of cyclosporine (ATOPICA for cats®) in cats. J. Vet. Pharmacol. Therap. 37, 161-168.

Romero, G.B., Arntjen, A., et al., 2016. Amorphous cyclosporin A nanoparticles for enhanced dermal bioavailability. Int. J. Pharm. 498, 217-224.

Sapino, S., Ugazio, E., et al., 2015. Mesoporous silica as topical nanocarriers for quercetin: characterization and in vitro studies. Euro. J. Pharm. Biopharm. 89, 116-125.

Sarode, A.L., Sandhu, H., et al., 2013. Hot melt extrusion for amorphous solid dispersions: temperature and moisture activated drug–polymer interactions for enhanced stability. Mol. Pharm. 10, 3665-3675.

Sekkat, N., Kalia, Y.N., et al., 2002. Biophysical study of porcine ear skin *in vitro* and its comparison to human skin *in vivo*. J. Pharm. Sci. 91, 2376-2381.

Souto, E. B., 2005. SLN and NLC for topical delivery of antifungals. PhD thesis, Free University of Berlin, pp70, 173.

Tam, J.M., McConville, J.T., et al., 2008. Amorphous cyclosporin nanodispersions for enhanced pulmonary deposition and dissolution. J. Pharm. Sci. 97, 4915-4933.

Watkinson, R.M., Herkenne, C. et al., 2009. Influence of ethanol on the solubility, ionization and permeation characteristics of ibuprofen in silicone and human skin. Skin

Pharmacol. Physiol. 22, 15-21.

Wei, Q., Keck, C.M., et al., 2015. CapsMorph® technology for oral delivery – theory, preparation and characterization. Int. J. Pharm. 482, 11-20.

Yadav, S., Gattacceca, F., et al. 2015. Comparative biodistribution and pharmacokinetic analysis of cyclosporine-A in the brain upon intranasal or intravenous administration in an oil-in-water nanoemulsion formulation. Mol. Pharm. 12, 1523-1533.

Zhai, X., Lademann, J., et al. 2014. Dermal nanocrystals from medium soluble actives – physical stability and stability affecting parameters. Eur. J. Pharm. Biopharm. 88, 85-91.

3.5. Screening silica-based carriers for amorphized hydrophobic drugs and the effect of loading concentration

3.5.1. Abstract

In this study, Syloid® SP53D-11920 was confirmed as a favorable mesoporous silica vehicle of poorly soluble drug in amorphization for dermal use in comparison with some other silicas/silicates. Absence of sandy feeling was observed by skin feeling test. The practical drug loading (29.3% w/w) of loaded Syloid® SP53D-11920 was quantified by HPLC versus other materials, i.e., AEROPERL® 300 Pharma (24.8% w/w) and Neusilin® US2 (26.4% w/w), with the same theoretical loading 33.2% w/w. According to the results detected by X-ray diffraction, the amorphous state of azithromycin in 33.2% drug loaded Syloid® SP53D-11920 remained unchanged at least for 24 months at 4 °C and 14 months at room temperature. The long-term physical stability was also assured in 10.0% drug loaded Syloid® SP53D-11920 during the storage of 24 months at room temperature. No structure change took place after loading drug based on the observation of scanning electron microscope. The high dissolution profile and saturation solubility of drug loaded Syloid® SP53D-11920 was also observed compared with crystalline raw drug powder (RDP) and physical mixture (silica and RDP). The drug concentration of the loading solution did not influence the loading capacity or the saturation solubility of loaded silicas. But it affected the physical stability and release profile.

3.5.2. Introduction

Converting crystalline active pharmaceutical ingredients (APIs) to their amorphous counterparts is one widely advocated strategy to enhance the bioavailability of hydrophobic APIs, which should be attributed to amorphous structure. The structure without long-range molecular order, resulting in high entropy, high enthalpy, high free energy and high molecular mobility (simply called “four high”), could significantly improve dissolution and saturation solubility (Löbmann, et al. 2012; Yani, et al. 2016).

However, the “four high” of the amorphous state could also result in re-crystallization during production, storage or administration, due to less favorable thermodynamic conditions. Once above alterations take place, the favorable advantages (increased dissolution and saturation solubility) of the amorphous state would consequently disappear (Elder, et al. 2013; Graeser, et al. 2009; Laitinen, et al. 2013). Common solutions to overcome this drawback are solid dispersions and the co-amorphous method. However, neither of them are prefect. For the solid dispersions method, the inconvenience in manufacturing and in processing to dosage forms needs to be improved. For the co-amorphous method, the difficulty to find two matched drugs limits the application (Laitinen, et al. 2013; Löbmann, et al. 2012).

Porous material has been considered as another alternative to yield the stable amorphization of poorly soluble APIs for several reasons (Kinnari, et al. 2011; Prestidge, et al. 2007; Qian and Bogner, 2012; Rancan, et al. 2012; Rigby, et al. 2008; Salonen and Lehto, 2008; Simovic, et al. 2011; Van Speybroeck, et al. 2009; Wei, et al. 2015; Williams, et al. 2013; Wu, et al. 2011). First, the low free energy state of the whole system keeps the amorphous state long lasting. In details, unloaded porous material holds high surface free energy because of the large surface area. After the absorption of drug molecules, the porous material will decrease the Gibbs free energy as a whole system. The lower free energy in turn will keep the amorphous drug, which is achieved by the tiny pore size, physical stable for a rather long time. Second, its unique properties lead to beneficial functions for loading drugs as listed following: 1) Small pore size [micropore < 2 nm; 2 nm < mesopore (the most common use) < 50 nm; macropore (seldom use) > 50 nm] can restrict re-crystallization and drug nucleation because of the spatial confinement. 2) High specific surface area (500-1,500 m^2/g) is promising for agents’ adsorption. 3) Large pore volume (1.0-1.7 cm^3/g) and surface chemistries such as siloxane groups with the oxygen (-Si-O-Si-) and silanol groups (-Si-OH) can be modified to control drug release. The interaction between drug and function groups of silicas can lead to amorphization as well.

Among various porous materials, silica-based vehicles are the most common investigated one (Williams, et al. 2013). Former researches about the pharmaceutical application of porous silicas mainly focused on oral drug delivery (Bimbo, et al. 2011; Guo, et al. 2013; Kinnari, et al. 2011; Rigby, et al. 2008; Van Speybroeck, et al. 2009) and somehow on implantable and injectable drug delivery (Salonen, et al. 2008; Sarkar, et al. 2016). However, little has been published regarding the porous silicas as vehicles to keep drug in amorphous state in dermal preparations. Even if some groups (Berlier, et al. 2013a; Berlier, et al. 2013b; Sapino, et al. 2015; Scalia, et al. 2013; Ugazio, et al. 2016) were interested in dermal delivery of silicas, none of them were focused on drug amorphization. Some of them only treated silica as stabilizer or thickener of the topical formulation (Frelichowska, et al. 2009; Rozman, et al. 2010). In addition, their nanometric silica particles may raise the risk of the toxicity (Michel, et al. 2013; Elle, et al. 2016). smartPearls® technology (Monsuur, et al. 2014) used in this study is the transfer of the CapsMorph® technology (Wei, et al. 2015) to dermal application, applying μm ranged silicas as the carrier for hydrophobic drugs, and also keeps the long physical stability of amorphous state of the drug.

Porous silicas with micropores cannot be favorable carriers on account of the slow diffusion (Riikonen, et al. 2009); porous silicas with macropores lost the benefit of the small pore size ascribed to the kind of flat surfaces (Qian and Bogner, 2012). Thus, in this work, a novel mesoporous silica (Syloid® SP53D-11920) was investigated as dermal APIs vehicle due to its very small pore size of 6 nm. Besides, the high specific surface area (550 m^2/g) of Syloid® SP53D-11920 could increase drug dissolution (Van Speybroeck, et al. 2009). What is more important, Syloid® is confirmed as a safe excipient by FDA and has been already used as a carrier for many drugs (Weerapol, et al. 2015; Yan, et al. 2015). Several other commercially available materials in μm size: microporous silicate Neusilin® SG2, mesoporous silica AEROPERL® 300 Pharma and mesoporous silicate Neusilin® US2 with different particle sizes, pore sizes, pore volumes and surface areas were also studied as reference. The aim of this study was to investigate how properties of the materials (e.g., pore size, particle size) or parameters of the loading procedure affect important

pharmaceutical properties (e.g., skin feeling, drug loading, physical stability, solubility properties and release).

3.5.3. Experimental Section

3.5.3.1. Materials

AEROPERL® 300 Pharma was kindly provided by Evonik Industries AG (Hanau, Germany) and Syloid® SP53D-11920 by W. R. Grace & Co. (Worms, Germany). Neusilin® SG2 and Neusilin® US2 were purchased from Fuji Chemical Industries Co., Ltd (Toyama, Japan) and azithromycin dihydrate (model drug, contains 95.4% azithromycin) from Haohua Industry (Jinan, China). Klucel GF® (hydroxypropyl cellulose) brought from Caesar & Loretz GmbH (Hilden, Germany) was used as gelling agent. Milli-Q water was obtained by reverse osmosis using a Millipak® Express 20 Filter unit (Merk, Germany). All materials were used as received.

3.5.3.2. Skin feeling test

Particles suspended in dermal formulations can create sandy feeling, in dependence of its particle size. A full range of different porous materials (Tab. 1) were incorporated at varying concentrations (1, 2 and 5%, w/w) in hydroxypropyl cellulose (HPC) gel base at 5% or mixed with Milli-Q water. Both sample types were transferred into glass vials, sealed and stored at 4 °C overnight before starting the skin examination. To assess the skin feeling, 20-40 mg/cm^2 of the silica gel was applied on the underside of volunteers' wrist (n=3) to investigate the skin feeling during application, and formulations were rubbed for a period of 1 min.

Table 1: Properties of silica materials used in skin feeling test.

	Syloid® SP53D-11920	AEROPERL® 300 Pharma (Evonik, 2011)	Neusilin® US2 (Fuji, 2009)	Neusilin® SG2 (Fuji, 2009)
particle size (μm)	12	30-40	44-177	125-500
specific surface area (m^2/g)	550	300	300	110
average pore size in diameter (nm)	6	2-50	5-6	1-2
pore volume (cm^3/g)	0.9	1.6	1.2	N/A
material	silicon dioxide	silicon dioxide	magnesium aluminometasilicate	magnesium aluminometasilicate

N/A: not available

3.5.3.3. Loading drug onto silicas

Azithromycin was selected as the model drug and loaded into Syloid® SP53D-11920, AEROPERL® 300 Pharma and Neusilin® US2. The maximum dissolvable amount of azithromycin in 10.0 g ethanol (96%) was around 5.0 g, representing a saturation solubility C_s in ethanol (96%) of 50% (w/w). Two drug-ethanol-solutions were prepared for drug loading: one with an azithromycin concentration half of C_s (C_s50% = 5.0 g azithromycin in 20.0 g ethanol (96%)) and another with a quarter of C_s (C_s25% = 5.0 g azithromycin in 40.0

g ethanol (96%)). The wetness impregnation method was used to load drug as described in **chapter 3.2**. Each kind of silica was spread on the bottom of a mortar to have a larger silica surface. They were loaded with drug by spraying one drug-ethanol-solution stepwise onto certain amounts of silica, using a glass bottle with nozzle. Meanwhile, this process was under stirring using a pestle. In each loading step, the amount of drug-ethanol-solution was calculated depending on the pore volume and drug density to minimize localization of drug on the silica surface. To exclude other factors, same amount of drug-ethanol-solution was used for the three different silicas. Subsequently, the ethanol was evaporated at 40 °C in an oven before next loading step. This process was repeated until the expected theoretical loading was reached. To obtain a theoretical loading of 10.0% (w/w) and 32.0% (w/w), C_s50% drug-ethanol-solution had to be applied 1 time and 3 times respectively; 7 repetitions were necessary to obtain a theoretical loading of 33.2% (w/w) applying the C_s25% drug-ethanol-solution. The details of the loading data in each step are expressed in Tab. 2.

To analyze the practical loading, approximately 100 mg loaded silicas were immersed in 10 ml methanol under sonication for 30 min and kept quiescence for 24 h. Then 1 ml the supernatant was centrifuged (Heraeus Megafuge Centrifuge 3.0R, Kendro Laboratory Products GmbH, Hanau, Germany) at RT for 10 min with 17,968 × g. Afterwards, the drug concentration of 75 µl supernatant was quantified by high performance liquid chromatography (HPLC) as described in **chapter 3.2**.

Table 2: Details of loading data of azithromycin onto silicas in each step.

	10.0% (w/w) final loading			32.0% (w/w) final loading			33.2% (w/w) final loading		
concentration of drug-ethanol-solution	C_s50%			C_s50%			C_s25%		
	obtained silica from the last step	drug-ethanol-solution	drug loading	obtained silica from the last step	drug-ethanol-solution	drug loading	obtained silica from the last step	drug-ethanol-solution	drug loading
loading step 1	10.00 g	5.56 g	10.0%	10.00 g	10.00 g	16.7%	10.00 g	9.00 g	9.1%
loading step 2	/			9.00 g	8.00 g	27.4%	8.00 g	5.40 g	14.9%
loading step 3	/			8.10 g	3.72 g	32.0%	6.00 g	4.32 g	20.3%
loading step 4	/			/			4.80 g	2.88 g	24.3%
loading step 5	/			/			3.60 g	2.16 g	28.0%
loading step 6	/			/			2.88 g	1.12 g	30.7%
loading step 7	/			/			2.30 g	1.08 g	33.2%

3.5.3.4. Physical stability of amorphous state

To evaluate the ability of different silicas for keeping the amorphous state of drug, 33.2% azithromycin loaded Syloid® SP53D-11920, AEROPERL® 300 Pharma and Neusilin® US2 were produced by C_s25% drug-ethanol-solution in 7 steps (section 3.5.3.3). The loaded silicas were stored at room temperature (RT) and 4 °C. The crystalline or amorphous state of loaded drug was monitored by X-ray diffraction (XRD) at different times for time points. The samples were analyzed with XRD by placing a thin layer of the loaded silica powder in a Philips X-ray Generator PW 1830. The diffraction angle range was between 0.6°-40° with a step size of 0.04° per 2 seconds. The diffraction pattern was measured at a voltage of 40 kV and a current of 25 mA. Unloaded silicas, physical mixture of corresponding silicas and raw drug powder were tested in the same manner as references. Physical mixture with 10.0% (w/w) azithromycin was manufactured by geometrical dilution using mortar and pestle. The mixture was gently grounded for 10 min to assure homogeneity. Besides, 32.0% (w/w) azithromycin loaded Syloid® SP53D-11920 and 10.0% (w/w) azithromycin loaded Syloid® SP53D-11920, AEROPERL® 300 Pharma and Neusilin® US2 were produced (section 3.5.3.3) to observe the influence of the drug loading on the physical stability of the amorphous state.

3.5.3.5. Surface morphology

Scanning electron microscope (SEM) can image the sample surface by scanning it with a high-energy beam of electrons in a raster scan pattern (Pardeike, 2008). A Zeiss DSM 982 GEMINI (Carl Zeiss, Oberkochen, Germany) was used in this study to monitor the surface morphologies of unloaded and loaded particles, physical mixtures of raw drug powder and each silica, and raw drug powder itself. The samples were sputter coated with gold and dried before imaging.

3.5.3.6. Drug dissolution experiment

For the drug dissolution test, 3 kinds of azithromycin loaded Syloid® SP53D-11920 were prepared: 1) Syloid® SP53D-11920 with a loading of 32.0% azithromycin, fabricated by C_s50% drug-ethanol-solution in 3 steps, freshly produced and in amorphous state; 2) Syloid® SP53D-11920 with a loading of 32.0% azithromycin, fabricated by C_s50% drug-ethanol-solution in 3 steps, long-stored (6 months) and in re-crystallized state; 3) Syloid® SP53D-11920 with a loading of 33.2% azithromycin, fabricated by C_s25% drug-ethanol-solution in 7 steps, freshly produced and in amorphous state. In details, every loaded Syloid® SP53D-11920 (2.4 g) was dispersed in 15.0 g Milli-Q water in one glass vial for each time point. The samples were stirred at 25 °C with a stirring speed of 100 rpm in an Innova 4230 incubator shaker (New Brunswick Scientific GmbH, Nürtingen, Germany) to assure adequate homogenization. 2 ml sample was taken using a syringe at certain interval (5 min, 10 min, 20 min, 40 min, 60 min, 2 h, 4 h, and 8 h). To avoid re-crystallization, the liquid was diluted 2 times by the dispersion medium and was immediately centrifuged (17,968 × g, Heraeus Megafuge Centrifuge 3.0R, Kendro Laboratory Products GmbH, Hanau, Germany) at RT for 10 min, and the supernatant was filtered over a 50 nm pore-sized nuclepore track-etched polycarbonate membrane (Whatman® 110603 filter). HPLC was performed to determine the concentration of dissolved drug after suitable dilution. The dissolution velocity was calculated by measuring the dissolved drug concentration as a function of time. Both the corresponding crystalline raw drug powder and the physical mixture were additionally tested as references. Physical mixture with 35.0% (w/w) azithromycin was produced by geometrical dilution using mortar and pestle. The mixture was gently grounded for 10 min to assure homogeneity.

3.5.4. Results and Discussions

3.5.4.1. Skin feeling test

As shown in Tab. 3, Neusilin® SG2 with a size above 125 µm caused sandy feeling on the

skin with and without HPC. Neusilin® US2 with a size range of 44 to 177 µm caused sandy feeling but only at higher concentrations (2% and 5%, w/w). The other materials having smaller particle sizes showed no sandy feeling during application, and thus they are suitable as dermal carriers. Especially the formulations with Syloid® SP53D-11920 had a pleasant feeling on the skin. Thus, silicas with small particle size distribution were more preferred in dermal application due to the pleasant skin feeling, e.g., 0.1 µm to 125 µm, and ideally less than 12 µm (Monsuur, et al. 2014).

Table 3: Type of silicas (left), maximum concentration (C_{max}) without sandy feeling on skin in gel (middle) and as suspension in water (right).

type of silica	C_{max} with 5% HPC (=gel)	C_{max} without HPC (=aqueous suspension)
Syloid® SP53D-11920	5%	5%
AEROPERL® 300 Pharma	5%	5%
Neusilin® US2	1%	1%
Neusilin® SG2	sandy feeling	sandy feeling

3.5.4.2. Loading drug into silicas

Syloid® SP53D-11920, AEROPERL® 300 Pharma and Neusilin® US2 were selected as drug carriers due to their performance in skin feeling test. The method commonly used to load drugs onto porous materials is based on wetness impregnation: concentrated drug solution is mixed with the material, followed by solvent evaporation at certain temperature (Kinnari, et al. 2011; Williams, et al. 2013). The loading theory contains two major parts (Prestidge, et al. 2007): 1) the large internal surface area of porous materials allows a high amount of drug loading; 2) the porous material can act as a sponge and thus most drugs depositing into the pores, instead of retaining on the pore surface. However, the location of the drug onto the surface is not avoidable but can be minimized. Here two different concentrated drug solutions (C_s50% drug-ethanol-solution and C_s25% drug-ethanol-solution) were used to load drug to test the influence of the drug

concentration of the loading solution. Moreover, even though various tools have been used to load drug by impregnation method, such as mixing the drug and materials in rotary evaporation and dried at vacuum (Yan, et al. 2015) or soaking the materials into drug solution under magnetic stirring (Guo, et al. 2013) or dropping the drug solution to the materials in an ointment bowl and mixing with a pestle (Wei, et al. 2015), a glass bottle with nozzle was firstly used as the main tool in this study. The spray loading method can not only maximize the distribution of the drug solution into the pores, but also avoid wet mass formulation, thus resulting in more homogenous distribution.

According to the HPLC results (Fig. 1), Syloid® SP53D-11920 possessed highest actual drug loading among the three materials for all theoretical loadings (10.0%, 32.0% and 33.2%, w/w), either with the C_s50% drug-ethanol-solution or with the C_s25% drug-ethanol-solution. It indicated that Syloid® SP53D-11920 was the most suitable dermal carrier among the tested materials independent on loading step and drug-ethanol-solution concentration. This is possibly contributed to its larger specific surface area (550 m^2/g) compared to the others (Tab. 1), even though it has the smallest pore volume among the three. By the same weight, Syloid® SP53D-11920 with larger specific surface area provides more area to absorb the drug. The obtained results were consistent with the mechanisms of loading drug onto porous silicas (Prestidge, et al. 2007). Beside the reason discussed above, it could also be attributed to the plenty of silanol groups, interacting with azithromycin by hydrogen bonds (Kinnari, et al. 2011).

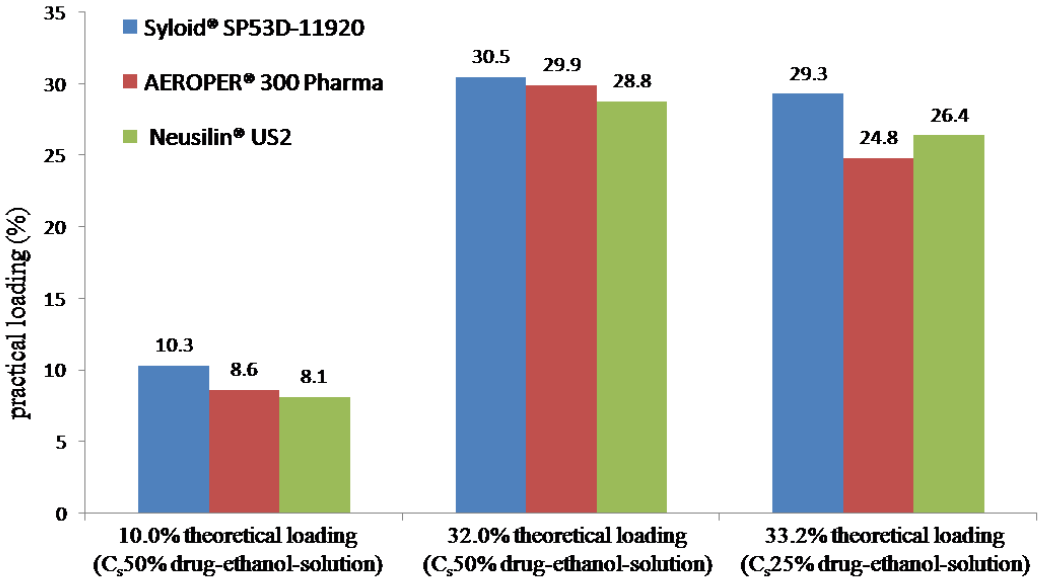

Fig. 1. Comparison of practical and theoretical loadings among three different types of silica.

3.5.4.3. Physical stability of amorphous state

The amorphous state of the drug is a key parameter for evaluating practically the most-suited drug-carrier (Riikonen, et al. 2009). Three loaded materials were evaluated by XRD at different temperatures and different points in time, to monitor their amorphous state. If crystalline peaks within the X-ray spectrum were detected, the drug was no longer completely in the amorphous state. The main crystalline peak (the highest intensity) of the three physical mixtures were all around 10 degree (Fig. 2), attributed to the distinctive peak of azithromycin (Zhang, et al. 2010). When stored at 4 °C, all three 33.2% azithromycin loaded silicas, which were produced by C_s25% drug-ethanol-solution, retained in amorphous state up to 24 months (by now) deduced from the absence of crystalline peak at 10 degree. But when stored at RT, only Neusilin® US2 maintained in amorphous state for 18 months. The other two silicas (Syloid® SP53D-11920 and AEROPERL® 300 Pharma) kept the amorphous state for 14 months, while a crystalline peak was noticed after 15 months' storage at RT. It can be concluded, that lower temperature can decrease the risk of re-crystallization, since low temperature leads to less molecular mobility of azithromycin

in certain silicas by decreasing the Gibbs free energy of the system (Laitinen, et al. 2013; Yani, et al. 2016).

The reason, why Neusilin® US2 kept the amorphous state of azithromycin the longest among the three carriers, is that the molecular mobility of the active in silicas depends on both pore size and the interactions between the active and the materials (Laitinen, et al. 2013). It seemed that Neusilin® US2 possesses stronger interactions (hydrogen bonding, electrostatic and hydrophobic interactions) (Xu, et al. 2013) with azithromycin than the other silicas (empirical formula of Neusilin®: $Al_2O_3 \cdot MgO \cdot 1.7SiO_2 \cdot xH_2O$ (Qian and Bogner, 2012) and the other two: SiO_2). If this hypothesis was correct, then it is clearly azithromycin in Neusilin® US2 has less molecular mobility, resulting in longer amorphous state. But further work is necessary to verify the inference. However, the complex chemical composition of Neusilin® US2 can lead to unexpected interaction with loading actives and thus not suited as a universal carrier. The materials with simple composition Syloid® SP53D-11920 and AEROPERL® 300 Pharma are more suitable.

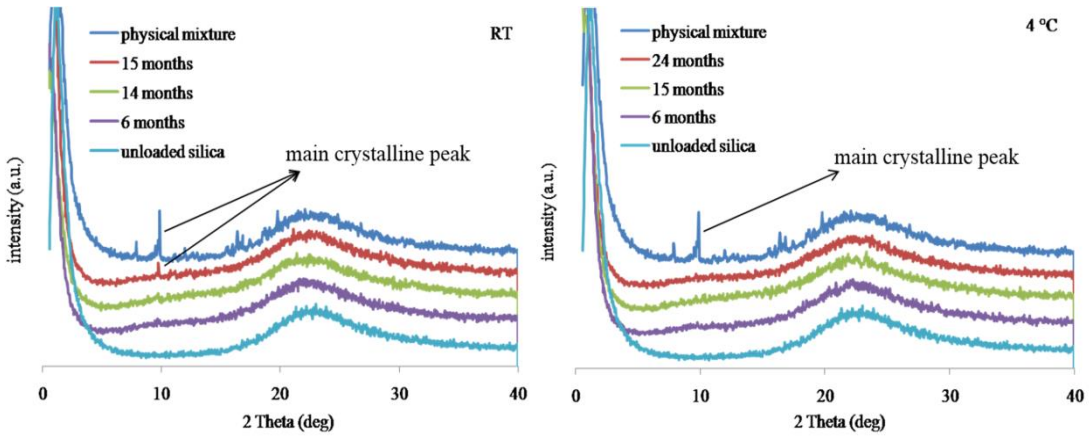

Fig. 2. (A) X-ray spectrum (vertical axis: intensity; horizontal axis: 2 Theta) of 33.2% azithromycin loaded Syloid® SP53D-11920 at RT (left) and 4 °C (right).

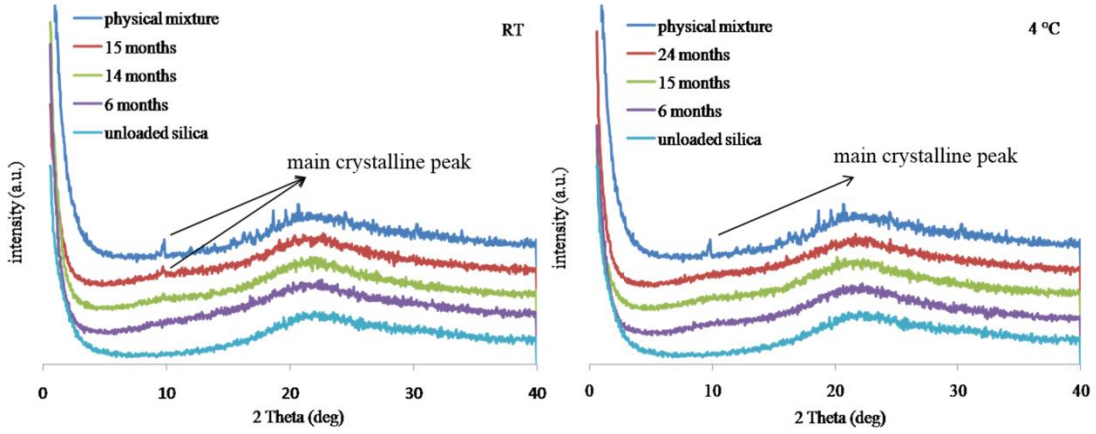

Fig. 2. (B) X-ray spectrum (vertical axis: intensity; horizontal axis: 2 Theta) of 33.2% azithromycin loaded AEROPERL® 300 Pharma at RT (left) and 4 °C (right).

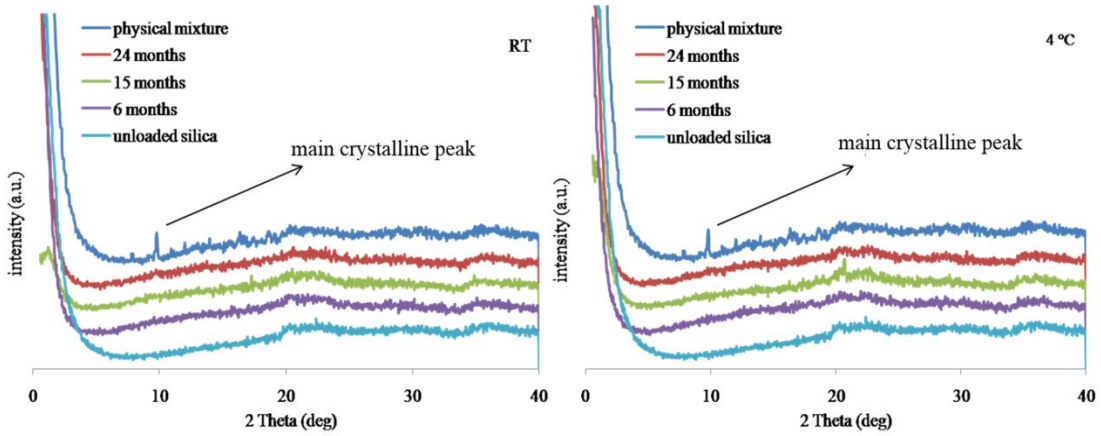

Fig. 2. (C) X-ray spectrum (vertical axis: intensity; horizontal axis: 2 Theta) of 33.2% azithromycin loaded Neusilin® US2 at RT (left) and 4 °C (right).

Concluded from Fig. 3, the 32.0% (w/w) loaded Syloid® with C_s50% showed much shorter physical stability compared to the 33.2% (w/w) loaded Syloid® with C_s25%, even though they had identical practical loading (section 3.5.4.2). For 32.0% (w/w) loaded Syloid®, there already existed a crystalline peak in day 7 at the X-ray spectrum. The crystalline peaks were also observed at 32.0% (w/w) loaded AEROPERL® 300 Pharma and Neusilin® US2 at day 7 (Fig. 3). The higher concentrated loading soluiton seems to be the reason. It may lead to more distribution of drug on surface than the lower conecentrated loading solution at each loading step. Surface-localized drug is more prone to form crystals, than the one in the space-restricted pores.

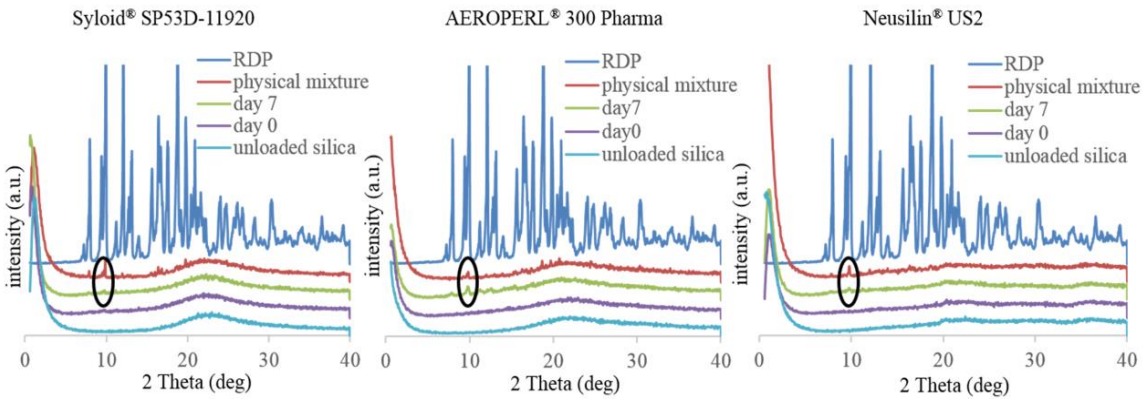

Fig. 3. X-ray spectrum (vertical axis: intensity; horizontal axis: 2 Theta) of 32.0% azithromycin loaded Syloid® SP53D-11920, AEROPERL® 300 Pharma and Neusilin® US2 at RT. Black circles pointed out the crystalline peaks.

It can be also induced from Fig. 4 that all the three 10.0% loaded silicas (Syloid® SP53D-11920, AEROPERL® 300 Pharma and Neusilin® US2), which were produced by C_s50% drug-ethanol-solution in one loading step, retained their amorphous state for at least 24 months (data until now) at room temperature. Comparing this result with that of 32.0% loaded silicas by C_s50% (Fig. 3), it is easy to make a conclusion that decreasing the drug amount loaded by the silicas may extend the period of the amorphou state. When the loading solution has the equivalent concentration, lower drug amount meaning reduces the number of loading cycles, thus decreasing the risk of the distribution of the drug on surface. In the end, re-crystallization is less.

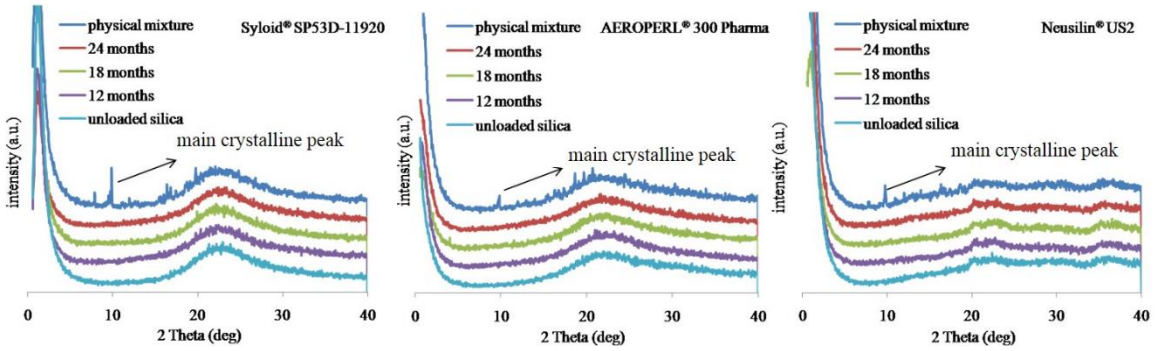

Fig. 4. X-ray spectrum (vertical axis: intensity; horizontal axis: 2 Theta) of 10.0% azithromycin loaded Syloid® SP53D-11920, AEROPERL® 300 Pharma and Neusilin® US2 at RT.

3.5.4.4. Surface morphology

According to the observation by SEM (Fig. 5), azithromycin raw drug powder showed irregular structure and seemed looser than the carriers due to the cracks visible in the Fig. 5 (A) (magnification 2000 fold). And the apparent raw drug powder disappeared after loading, whereas existed (the one pointed by the red arrow) when only physical mixed (Fig. 5 (B)), consistent with the XRD result (Fig. 2). In addition, Fig. 5 (B) displays that the structure of Syloid® SP53D-11920 and Neusilin® US2 after the loading was unchanged. On contrary, AEROPERL® 300 Pharma got more and more destroyed with each loading step. This result indicated that the AEROPERL® 300 Pharma is not as strong as the former two against certain mechanical force.

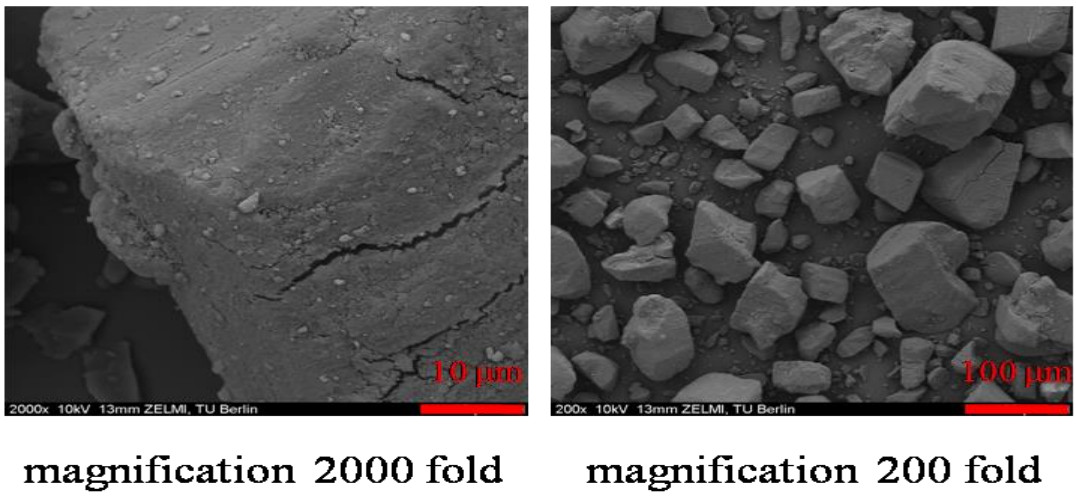

Fig. 5. (A) SEM pictures of raw drug powder with magnification of 2000 fold (left) and 200 fold (right) (scale bars from left to right: 10 µm and 100 µm).

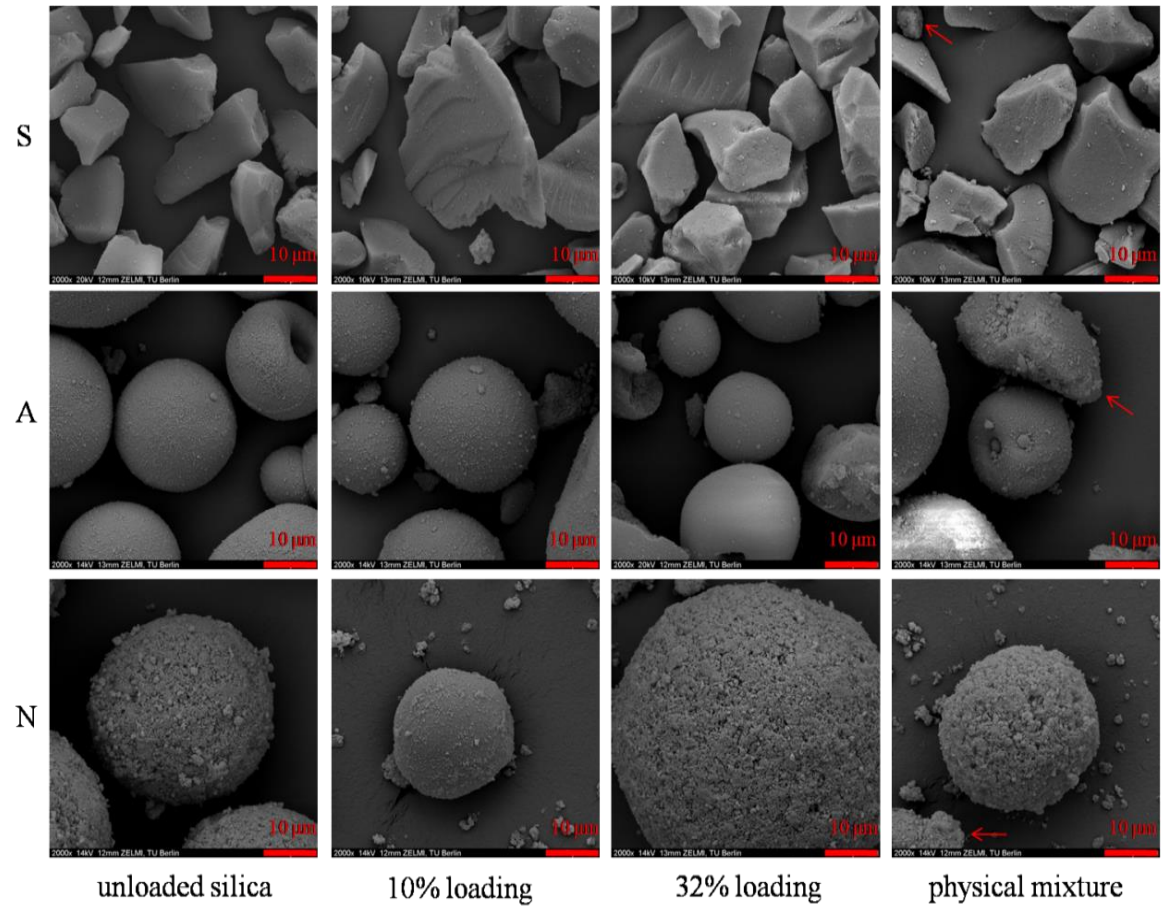

Fig. 5. (B) SEM pictures of unloaded silicas, loaded silicas and physical mixture with magnification of 2000 fold. S represents Syloid® SP53D-11920, A AEROPERL® 300 Pharma and N Neusilin® US2. The arrow pointed to raw drug powder (scale bar: 10 µm).

3.5.4.5. Drug dissolution experiment

In considering the result of section 3.5.4.2, 3.5.4.3 and 3.5.4.4, only Syloid® SP53D-11920 was selected for drug dissolution test. Two amorphous Syloid® formulations – one loaded with higher concentrated (C_s50%) drug-ethanol-solution named "Syloid® loaded by high concentration (amorphous)", the other one loaded with lower concentrated (C_s25%) drug-ethanol-solution named "Syloid® loaded by low concentration (amorphous)" – exhibited very quick release in the first 5 min (Fig. 6). A faster drug release was obtained for "Syloid® loaded by high concentration (amorphous)" compared to "Syloid® loaded by low concentration (amorphous)", particularly in the first 40 min. In details, for the former formulation, the release profile depicted a burst release at first 40 min. And

re-crystallization happened after oversaturation, judging from the sudden decreased release between 40 min and 60 min. Subsequently, the release rate slowly increased as that of "Syloid® loaded by low concentration (amorphous)". In the end, the two formulations nearly reached the same release amount in 8 h, meaning they have equivalent saturation solubility in 8 h, which should be contributed to their nearly similar practical loading (mentioned in Fig. 1).

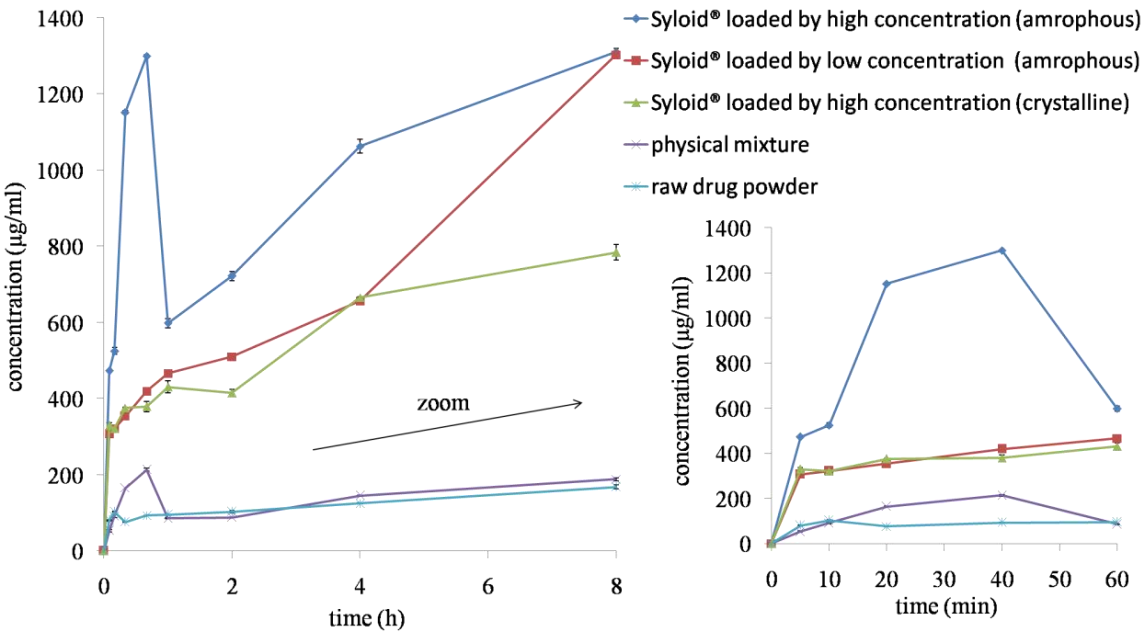

Fig. 6. Dissolution profiles of azithromycin from practically equivalent amount of drug loaded Syloid® SP53D-11920, produced by high concentrated drug-ethanol-solution (C_s50% drug-ethanol-solution; 32.0% theoretical loading; total amorphous drug or part of crystal drug) and low concentrated drug-ethanol-solution (C_s25% drug-ethanol-solution; 33.2% theoretical loading; total amorphous drug) in Milli-Q water at 25 °C. The dissolution curves of physical mixture (35.0% drug) and raw drug powder are presented as reference.

It was assumed that the higher drug-ethanol-solution concentration might lead to a remaining of more amorphous drug molecular dispersed around the surface (chemically combined or physically entrapped) of the silica carrier instead in the pores. When dispersed

in water, the physically entrapped amorphous drug molecular around the surface dissolved in the beginning, causing a burst release. Bigger surface-dispersion portion of "Syloid® loaded by high concentration (amorphous)" lead to longer quick release (0-40 min); smaller surface-dispersion portion of "Syloid® loaded by low concentration (amorphous)" lead to only 5 min quick release. Then the release trend between 1 h to 4 h could be explained by the chemically combined drug molecular on the surface. While the release profile between 4 h to 8 h of the two formulations should be attributed to in-pores-drug releasing from the pores. Because less concentrated drug solution is easier to be packed into pores due to capillary forces, more in-pores-drug of "Syloid® loaded by low concentration (amorphous)" lead to faster release rate in that period of time. This finding was in agreement with other scientists' (Kinnari, et al. 2011; Van Speybroeck, et al. 2009). Those researchers concluded that 1) the physically entrapped drug could bring about the first faster release; 2) the chemical interaction between drug and silica carriers as well as the drug packed deeper inside the pores could cause the later slower release.

It was also known from Fig. 6 that the release trend of the physical mixture resembling that of "Syloid® loaded by high concentration (amorphous)": both displayed quick release until 40 min, and then decreased to 60 min, followed by slow increase to the end. This may be due to high degree interaction existing between physically mixing drugs and silica carriers as well (Van Speybroeck, et al. 2009). However, the saturation solubility of the physical mixture is much lower (188 μg/ml in 8 h, versus 1,310 μg/ml in 8 h for "Syloid® loaded by high concentration (amorphous)"). To explain this phenomenon, the release profile of "Syloid® loaded by high concentration (crystalline)" should be studied. It was easy to make a conclusion from Fig. 6 that drug amorphization resulted in an improved dissolution rate and saturation solubility compared to the crystalline azithromycin (1,310 μg/ml in 8 h for "Syloid® loaded by high concentration (amorphous)", versus 784 μg/ml in 8 h for "Syloid® loaded by high concentration (crystalline)"), even though both were loaded on the silica by the same method. Thus, the physical mixture did have interaction between the drug and the silica, but this force could not make drug amorphization as much as the loading method

could. Last, the final similar release amount of the physical mixture as that of the crystal raw drug powder indicated physical mix was not an ideal method to produce amorphous drug as good as smartPearls® technology.

3.5.5. Conclusions

Much effort has been put into obtaining a better comparison between the novel mesoporous silica material Syloid® SP53D-11920 and other three μm sized common used silica/silicate carriers: AEROPERL® 300 Pharma, Neusilin® SG2 and Neusilin® US2. Regarding its skin feeling, loading capacity, physical stability and surface morphology, Syloid® SP53D-11920 can be recommended as a dermal active carrier. Besides, according to the long lasting amorphous state, high dissolution rate and high saturation solubility of azithromycin in the loaded Syloid® SP53D-11920, this silica material is an alternative for dermal vehicle of azithromycin analogous hydrophobic APIs.

In the smartPearls® technology, the drug concentration of the loading solution did neither influence the loading capacity nor the saturation solubility (C_s) of loaded silicas. However, it affected distinctly the physical stability and release profile. Based on these results, optimized stability of the amorphous state for commercial smartPearls® products can be achieved using lower concentrated loading solutions. Besides, compared to the silica loaded with high drug amount, the silica loaded with low drug amount is more physical stable in amorphous state. In addition, smartPearls® technology has stronger ability to stabilize amorphous state than simply physical mix of the silica and raw drug powder. The results showed also the opportunity to modulate release via different loading parameters, and highlight the need for more intensive systematic investigations for better understanding of basic mechanisms of this novel delivery system.

3.5.6. References

Berlier, G., Gastaldi, L., et al., 2013a. MCM-41 as a useful vector for rutin topical

formulations: synthesis, characterization and testing. Int. J. Pharm. 457, 177-188.

Berlier, G., Gastaldi, L., et al., 2013b. Stabilization of quercetin flavonoid in MCM-41 mesoporous silica: positive effect of surface functionalization. J. Colloid Interface Sci. 393, 109-118.

Bimbo, L.M., Mäkilä, E., et al., 2011. Functional hydrophobin-coating of thermally hydrocarbonized porous silicon microparticles. Biomaterials 32, 9089-9099.

Elder, D.P., Holm, R., et al., 2013. Use of pharmaceutical salts and cocrystals to address the issue of poor solubility. Int. J. Pharm. 453, 88-100.

Elle, R.E., Rahmani, S., et al., 2016. Functionalized Mesoporous silica nanoparticle with antioxidants as a new carrier that generates lower oxidative stress impact on cell. Mol. Pharmaceutics 13, 2647-2660.

Evonik, 2011. Industry Brochure: AEROSIL® Colloidal Silicon Dioxide for Pharmaceuticals. https://www.aerosil.com/sites/lists/IM/Documents/IB-AEROSIL-for-Pharmaceuticals-EN.pdf (accessed 10.10.2015).

Frelichowska, J., Bolzinger, M.A., et al., 2009. Topical delivery of lipophilic drugs frow o/w Pickering emulsions. Int. J. Pharm. 371, 56-63.

Fuji, 2009. Neusilin Brochure: The specialty excipient Neusilin®. http://www.harke.com/fileadmin/images/pharma/Broschueren/Fuji_Neusilin.pdf (accessed 24.10.2015).

Graeser, K.A., Patterson J.E., et al., 2009. Correlating thermodynamic and kinetic parameters with amorphous stability. Eur. J. Pharm. Sci. 37, 492-498.

Guo, Z., Liu, X.M., et al., 2013. Effects of particle morphology, pore size and surface coating of mesoporous silica on Naproxen dissolution rate enhancement. Colloid. Surface. B 101, 228-235.

Kinnari, P., Mäkilä, E., et al., 2011. Comparison of mesoporous silicon and non-ordered mesoporous silica materials as drug carriers for itraconazole. Int. J. Pharm. 414, 148-156.

Laitinen, R., Löbmann, K., et al., 2013. Emerging trends in the stabilization of amorphous drugs. Int. J. Pharm. 453, 65-79.

Löbmann, K., Strachan, C., et al., 2012. Co-amorphous simvastatin and glipizide combinations shown improved physical stability without evidence of intermolecular interactions. Eur. J. Pharm. Biopharm.81, 159-169.

Michel, K., Scheel, J., et al., 2013. Risk assessment of amorphous silicon dioxide nanoparticles in a glass cleaner formulation. Nanotoxicology 7, 974-988.

Monsuur, F., Höfer, H., et al., 2014. Active-loaded particulate materials for topical administration. US Patent 62050587. WO 2016041992A1.

Pardeike, J., 2008. Nanosuspensions and nanostructured lipid carriers for dermal application. PhD thesis, Free University of Berlin. P68.

Prestidge, C.A., Barnes, T.J., et al., 2007. Mesoporous silicon: a platform for the delivery of therapeutics. Expert Opin. Drug Deliv. 4, 101-110.

Qian, K., Bogner, R.H., 2012. Application of mesoporous silicon dioxide and silicate in oral amorphous drug delivery systems. J. Pharm. Sci. 101, 444-463.

Rancan, F., Gao, Q., et al., 2012. Skin penetration and cellular uptake of amorphous silica nanoparticles with variable size, surface functionalization, and colloidal stability. ACS Nano. 6, 6829-6842.

Rigby, S., Fairhead, M., et al., 2008. Engineering silica particles as oral drug delivery vehicles. Curr. Pharm. Des. 14, 1821-1831.

Riikonen, J., Mäkilä, E., et al., 2009. Determination of the physical state of drug molecules in mesoporous silicon with different surface chemistries. Langmuir 25, 6137-6142.

Rozman, B., Gosenca, M., et al., 2010. Dual influence of colloidal silica on skin deposition of vitamins C and E simultaneously incorporated in topical microemulsions. Drug Dev. Ind. Pharm. 36, 852-860.

Salonen, J., Kaukonen, A.M., et al., 2008. Mesoporous silicon in drug delivery applications. J. Pharm. Sci. 97, 632-653.

Salonen, J., Lehto, V., 2008. Fabrication and chemical surface modification of mesoporous silicon for biomedical applications. Chem. Eng. J. 137, 162-172.

Sapino, S., Ugazio, E., et al. 2015. Mesoporous silica as topical nanocarriers for quercetin: characterization and *in vitro* studies. Eur. J. Pharm. Biopharm. 89, 116-125.

Sarkar, A., Ghosh, S., et al., 2016. Targeted delivery of quercetin loaded mesoporous silica nanoparticles to the breast cancer cell. Biochim. Biophys. Acta 1860, 2065-2075.

Scalia, S., Franceschinis, E., et al., 2013. Comparative evaluation of the effect of permeation enhancers, lipid nanoparticles and colloidal silica on in vivo human skin penetration of quercetin. Skin Pharmacol. Physiol. 26, 57-67.

Simovic, S., Ghouchi-Eskandar, N., et al., 2011. Silica materials in drug delivery applications. Curr. Drug Discov. Technol. 8, 250-268.

Ugazio, E., Gastaldi, L., et al., 2016. Thermoresponsive mesoporous silica nanoparticles as a carrier for skin delivery of quercetin. Int. J. Pharm. 511, 446-454.

Van Speybroeck, M., Barillaro, V., et al., 2009. Ordered mesoporous silica material SBA-15: A broad-spectrum formulation platform for poorly soluble drugs. J. Pharm. Sci. 98, 2648-2658.

Weerapol, Y., Limmatvapirat, S., et al., 2015. Enhanced dissolution and oral bioavailability of nifedipine by spontaneous emulsifying powders: Effect of solid carriers and dietary state. Eur. J. Pharm. Biopharm. 91, 25-34.

Wei, Q., Keck, C.M., et al., 2015. CapsMorph® technology for oral delivery – theory, preparation and characterization. Int. J. Pharm. 482, 11-20.

Williams, H.D., Trevaskis, N.L., et al. 2013. Strategies to address low drug solubility in discovery and development. Pharmacol. Rev. 65, 315-499.

Wu, C., Wang, Z., et al., 2011. Development of biodegradable porous starch foam for improving oral delivery of poorly water soluble drugs. Int. J. Pharm. 403, 162-169.

Xu, W., Riikonen, J., et al., 2013. Mesoporous systems for poorly soluble drugs. Int. J. Pharm. 453, 181-197.

Yan, H., Sun, E., et al., 2015. Improvement in oral bioavailability and dissolution of tanshinone II A by preparation of solid dispersions with porous silica. J. Pharm. Pharmacol. 67, 1207-1214.

Yani, Y., Chow, P.S., et al., 2016. Pore size effect on the stabilization of amorphous drug in a mesoporous material: Insights from molecular simulation. Micropor. Mesopor. Mat. 221, 117-122.

Zhang, Z., Zhu, Y., et al., 2010. Preparation of azithromycin microcapsules by a layer-by-layer self-assembly approach and release behaviors of azithromycin. Colloid. Surface. A. 362, 135-139.

4. SUMMARY

Azithromycin nanosuspension was achieved in **chapter 3.1** with higher drug content (10%, w/w) and smaller particle size (189 nm) compared to the already published one (1% w/w drug, 400 nm diameter) by only 1% (w/w) TPGS. The producing method (bead milling) was even more time-efficient (10 min). Physical stability of the nanocrystals was observed after 1 year storage at 4 °C via PCS, LD and light microscope.

Topical HPC gels with incorporated actives of different forms were applied on porcine ears for penetration study via tape stripping method. These forms include raw drug powder in crystalline state (**chapter 3.1 to chapter 3.4**), raw drug powder in amorphous state (**chapter 3.4**), raw drug powder with a penetration enhancer (propylene glycol, **chapter 3.1**), nanocrystals in crystalline state (**chapter 3.1 to chapter 3.3**), nanocrystals in crystalline state with the penetration enhancer (**chapter 3.1**), nanoparticles in amorphous state (**chapter 3.4**), smartPearls® with amorphous drug (**chapter 3.2 to chapter 3.4**) and smartPearls® with crystalline drug (**chapter 3.3**). It can be concluded from all the data that smartPearls® with the amorphous drug showed the most superiority on penetration efficacy compared to all the other tested drug forms. It even showed higher penetration efficacy than clinical effective gel with ethanol inside (**chapter 3.2**).

The second best form was the azithromycin nanocrystals in crystalline state (**chapter 3.1**). They expressed higher penetration efficacy not only than 1) raw drug powder in crystalline state, but also than 2) raw drug powder with penetration enhancer as well as 3) nanocrystals in crystalline state with penetration enhancer and 4) clinical effective gel with drug-ethanol-solution. Thus, the penetration enhancer (propylene glycol) increases further the saturation solubility and dissolution velocity, but not the penetration efficacy. Except the case of penetration enhancer, the penetration efficacy depended on the saturation solubility and dissolution velocity: the higher the saturation solubility or dissolution velocity, the higher penetration efficacy was achieved (**chapter 3.1 to chapter 3.4**).

The stability of amorphous state of active in smartPearls® was long enough (e.g., 2 years)

(**chapter 3.2 to chapter 3.4**) for industrial application, even in hydrogels (**chapter 3.2 to chapter 3.4**). Various factors affected the stability (**chapter 3.5**), including the concentration of the loading solution and the final loading amount. The lower the loading solution was concentrated or the less loading steps (lower final loading amount) were used, the better was the long-term stability. Moreover, the loading concentration did not only have influence on physical stability, but also on dissolution velocity (**chapter 3.5**). Low loading concentrations lead to no burst but sustained release. In contrast, it did not affect the saturation solubility or practical maximum loading.

In the end, Syloid® SP53D-11920 was a promising candidate on dermal application using smartPearls® technology (**chapter 3.5**). Regarding the feeling on the skin (Syloid® SP53D-11920 did not scratch when applied), morphological observation, loading capacity and stability test, it behaved as well as or even better than other classical carriers like AEROPERL® 300 Pharma, Neusilin® US2 and Neusilin® SG2.

5. ZUSAMMENFASSUNG

In **Kapitel 3.1** wurde die Herstellung einer Azithromycin-Nanosuspension beschrieben, deren Wirkstoffkonzentration (10%) und Partikelgröße (189 nm) den bislang publizierten Standard (1% und 400 nm) deutlich übertrifft. Für die Stabilisierung wurde 1% (m/m) TPGS verwendet. Die Herstellungsmethode mit der Perlenmühle war darüber hinaus zeiteffizienter (10 min). Bei einer Lagertemperatur von 4 °C wurde die Stabilität der Nanopartikel über 1 Jahr mittels PCS, LD und Lichtmikroskop nachgewiesen.

Verschiedene Modifikationen von Wirkstoffen wurden in HPC-Gelen eingearbeitet und mittels Tape-Stripping am Schweineohr deren verglichen. Zu diesen Modifikationen zählten kristallines Wirkstoffpulver (**Kapitel 3.1-3.4**), Wirkstoffpulver im amorphen Zustand (**Kapitel 3.4**), Wirkstoffpulver mit einem Penetrationsverstärker (**Kapitel 3.1**), Nanokristalle im amorphen Zustand (**Kapitel 3.4**), smartPearls® beladen mit amorphem Wirkstoff (**Kapitel 3.2-3.4**) sowie smartPearls® mit kristallinem Wirkstoff (**Kapitel 3.3**). Aus diesen Daten kann geschlussfolgert werden, dass smartPearls® mit amorphem Wirkstoff die stärkste Penetration hat. Sogar die Penetration einer als klinisch wirksam getesteten Gel mit Ethanol konnte übertroffen werden (**Kapitel 3.2**).

Das zweitbeste Ergebnis in der Penetrationsstudie lieferten die Azithromycin Nanokristalle (**Kapitel 3.1**). Die Ergebnisse zeigen, dass der Zusatz von Penetrationsverstärker zwar die Sättigungslöslichkeit und Lösungsgeschwindigkeit von Nanokristallen erhöhen, jedoch nicht deren dermale Bioverfügbarkeit. Zusammenfassend lässt sich sagen, dass – mit Ausnahme der Penetrationsverstärker – die Penetration mit der Sättigungslöslichkeit sowie der Lösungsgeschwindigkeit steigt. Je höher die Sättigungslöslichkeit und Lösungsgeschwindigkeit, desto höhere dermale Bioverfügbarkeiten werden erreicht (**Kapitel 3.1-3.4**).

Die Stabilisierung des amorphen Zustandes erfolgreich beladener smartPearls® war ausreichend lang (z.B. 2 Jahre) (**Kapitel 3.2-3.4**) für eine industrielle Anwendung, sogar

nach Einarbeiten in einer wässrigen Gelgrundlage (**Kapitel 3.2-3.4**). Diverse Faktoren beeinflussen die Stabilität (**Kapitel 3.5**), wie zum Beispiel die Wirkstoffkonzentration der Beladungslösung, sowie die finale Beladung selbst. Je geringer die Konzentration der Beladungslösung bzw. je weniger Beladungsschritte vorgenommen wurden, desto langzeitstabiler war die Formulierung. Darüber hinaus hat die Beladungskonzentration nicht nur einen Einfluss auf die physikalische Stabilität, sondern auch auf die Lösungsgeschwindigkeit. Je geringer die Wirkstoffkonzentration der Lösung, desto geringer die Lösungsgeschwindigkeit. Im Gegensatz dazu hat sie keinen Einfluss auf die Sättigungskonzentration oder die praktische Höchstbeladung.

Letztendlich zeigte sich Syloid® SP53D-11920 als eine vielversprechende Möglichkeit der dermalen Applikation mithilfe der smartPearls® -Technologie (**Kapitel 3.5**) bezüglich des Tragegefühls auf der Haut (kratzfreies Auftragen), der morphologischen Beobachtung, der Beladungskapazität sowie dem Stabilitätstest erwiesen sie sich gleichwertig oder besser als die klassischen Träger wie AEROPERL® 300 Pharma, Neusilin® US2und Neusilin® SG2.

ABBREVIATIONS

APIs	active pharmaceutical ingredients
AZ	azithromycin
BCS	biopharmaceutics classification system
BM	bead milling
C_{max}	maximum concentration
C_s	saturation solubility
CyA	cyclosporine A
DLS	dynamic light scattering
DMSO	dimethyl sulfoxide
DSC	differential scanning calorimetry
ECD	European Cosmetic Directive
FDA	US Food and Drug Administration
HPC	hydroxypropyl cellulose
HPLC	high performance liquid chromatography
HPMC	hydroxypropyl mehtylcellulose
HPH	high pressure homogenization
LD	laser diffractrometry
LM	light microscope
log P	logarithm of partition coefficient
NC	nanocrystals
NLC	nanostructured lipid carriers
PCS	photo correlation spectroscopy
PDI	polydispersity index
PEG	polyethylene glycol
PG	propylene glycol
PVG	povidone
RDP	raw drug powder
RT	room temperature

SEM	scanning electron microscope
SLN	solid lipid nanoparticles
TEM	transmission electron microscope
TPGS	D-α-tocopheryl polyethylenglycol 1000 succinate
XRD	X-ray diffraction
ZP	zeta potential

PUBLICATIONS

Full papers

1. **Jin, N.,** Zhao, Y. X., Deng, S. H., Sun, Q., Preparation and in vitro anticancer activity of oxymatrine mixed micellar nanoparticles. Die Pharmazie. 2011, 66(7): 506-510 (doi: https://doi.org/10.1691/ph.2011.0356)

2. Zhang, H., Chen, C., Hou, L., **Jin, N.**, Shi, J., Wang, Z., Liu, Y., Feng, Q., Zhang, Z., Targeting and hyperthermia of doxorubicin by the delivery of single-walled carbon nanotubes to EC-109 cells. J. Drug Target. 2013, 21(3): 312-319 (doi: http://dx.doi.org/10.3109/1061186X.2012.749880)

Proceedings

1. **Jin, N.,** Staufenbiel, S., Helf, T., Müller, R. H., Azithromycin nanocrystals for dermal use against Borreliosis infection, S27, CRS Local Chapter Germany, Kiel, 27-28 February 2014

2. **Jin, N.,** Staufenbiel, S., Keck, C. M., Müller, R. H., Production of dermal azithromycin nanocrystals for prevention of Lyme Borreliosis infection. #30, P. 60, 9th World Meeting on Pharmaceutics, Biopharmaceutics and Pharmaceutical Technology, Lisbon, 31 March -03 April 2014

3. Staufenbiel, S., **Jin, N.,** Müller, R. H., Protein adsorption patterns from different coated azithromycin nanocrystals. #515, Int. Symp. Control. Rel. Bioact. Mater. 41, Chicago/llingois, 13-16 July 2014

4. Staufenbiel, S., Romero, G. B., **Jin, N.,** Keck, C. M., Müller, R. H., Cyclosporin smartPearls® for improved topical delivery. #42, P. 26, 1st European Conference on Pharmaceutics, Reims, 13-14 April 2015

5. **Jin, N.,** Staufenbiel, S., Keck, C. M., Müller, R. H., Azithromycin smartCrystals® for prevention of infections by tick bites. #125, P. 18, 1st European Conference on Pharmaceutics, Reims, 13-14 April 2015

6. **Jin, N.,** Staufenbiel, S., Keck, C. M., Müller, R. H., smartPearls® – stability and

performance in topical gels. #126, P. 31, 1st European Conference on Pharmaceutics, Reims, 13-14 April 2015

7. Müller, R. H., **Jin, N.,** Monsuur, F., Höfer, H. H., Keck, C. M., Staufenbiel, S., smartPearls™ for the dermal delivery of azithromycin against borreliosis infection. Int. Symp. Control. Rel. Bioact. Mater. 42, Edingburgh/Scotland, 26-29 July 2015

8. Keck, C. M., **Jin, N.,** Monsuur, F., Höfer, H. H., Müller, R. H., Staufenbiel, S., smartPearls™ for the dermal delivery of physically stable amorphous cyclosporine, Int. Symp. Control. Rel. Bioact. Mater. 42, Edingburgh/Scotland, 26-29 July 2015

9. Müller, R. H., **Jin, N.,** Romero, G., Pyo, S. M., Keck, C. M., smartPearls® – special features & basic mechanisms of this micro-sized dermal delivery system for poorly soluble. CRS Local Chapter Germany, Saarbrücken, 7 March 2016

10. **Jin, N.,** Müller, R. H., Pyo, S. M., Monsuur, F., Keck, C. M., Effect of loading procedure on dissolution profiles of loaded smartPearls®. 10th World Meeting on Pharmaceutics, Biopharmaceutics and Pharmaceutical Technology, Glasgow, 4-7 April 2016

11. Müller, R. H., **Jin, N.,** Pyo, S. M., Monsuur, F., Keck, C. M., smartPearls® concept – novel dermal delivery system for poorly soluble amorphous actives. 10th World Meeting on Pharmaceutics, Biopharmaceutics and Pharmaceutical Technology, Glasgow, 4-7 April 2016

Abstracts

1. **Jin, N.,** Staufenbiel, S. Helf, T., Müller, R. H., Comparison of methods to produce dermal azithromycin nanosuspensions to prevent lyme borreliosis infection. P. 38, 9th European Workshop on Particulate Systems (EWPS), Utrecht, 13-14 March 2014

2. **Jin, N.,** Staufenbiel, S., Keck, C. M., Müller, R. H., Improved solubility properties of topical azithromycin nanocrystals for prophylaxis of borreliosis infection. P.7, 18th Jahrestagung der Gesellschaft für Dermopharmazie (GD), Berlin, 07-09 April 2014

3. Staufenbiel, S., **Jin, N.,** Keck, C. M., Müller, R. H.**,** Surfactant optimization for dermal

azithromycin nanocrystals. P. 18, 18th Jahrestagung der Gesellschaft für Dermopharmazie (GD), Berlin, 07-09 April 2014

4. **Jin, N.,** Staufenbiel, S., Müller, R. H., Penetration behavior of dermal azithromycin nanocrystals for Lyme Borreliosis infection. P. 3, Tag der Pharmazie, DPhG Landesgruppe Berlin-Brandenburg, Berlin, 04 July 2014

5. Staufenbiel, S., **Jin, N.,** Müller, R. H., Protein coronas from sterically stabilized i.v. azithromycin nanocrystals – effect of number of PEG chains. P. 45, Tag der Pharmazie, DPhG Landesgruppe Berlin-Brandenburg, Berlin, 04 July 2014

6. **Jin, N.,** Staufenbiel, S., Arntjen, A., Schäfer, K.-H., Keck, C. M., Müller, R. H., Evaluation of dermal azithromycin nanocrystals for Lyme Borreliosis infection. P. 18, Third International Conference in Advanced Manufacturing for Multifunctional Miniaturised Devices (ICAM3D), Tsukuba/Ibaraki, 27-28 August 2014

7. **Jin, N.,** Staufenbiel, S., Keck, C. M., Müller, R. H., Pig ear skin penetration of azithromycin nanocrystals for Lyme Borreliosis infection. P. 9, DPhG-Jahrestagung, Frankfurt, 24-26 September 2014

8. Staufenbiel, S., **Jin, N.,** Müller, R. H., Influence of different i.v. azithromycin nanocrystal stabilizers to surface hydrophobicity and protein corona in regard to drug targeting properties. DPhG-Jahrestagung, Frankfurt, 24-26 September 2014

9. **Jin, N.,** Staufenbiel, S., Arntjen, A., Keck, C. M., Müller, R. H., Azithromycin nanocrystals for topical prevention of systemic Lyme Borreliosis infection. P. 38, Workshop NutriOx 2014, Metz, 1-3 October 2014

10. Müller, R. H., Monsuur, F., Höfer, H. H., **Jin, N.,** Staufenbiel, S., Keck, C. M., smartPearls™ – novel amorphous delivery system based on porous materials to increase skin penetration of anti-oxidants. Workshop NutriOx 2014, Metz, 1-3 October 2014

11. **Jin, N.,** Staufenbiel, S., Keck, C. M., Müller, R. H., Development of dermal azithromycin nanocrystals for prevention of Lyme Borreliosis. M1102, AAPS Annual Meeting, San Diego, 2-6 November 2014

12. Staufenbiel, S., **Jin, N.,** Keck, C. M., Müller, R. H.**,** Determination of surface

hydrophobicity and protein adsorption onto differently coated azithromycin nanocrystals. R6080, AAPS Annual Meeting, San Diego, 2-6 November 2014

13. **Jin, N.,** Staufenbiel, S., Keck, C. M., Müller, R. H., smartCrystals® – enhancement of drug penetration without penetration enhancer. P. 13, Menopause, Andropause, Anti-aging, Vienna, 11-13 December 2014

14. Keck, C. M., Pyo, S. M., **Jin, N.,** Müller, R. H., Knauer, J., Rutin smartCrystals - most effective anti-oxidant activity & skin penetration. P. 14, Menopause, Andropause, Anti-aging, Vienna, 11-13 December 2014

15. Keck, C. M., Monsuur, F., Höfer, H. H., **Jin, N.,** Staufenbiel, S., Müller, R. H., smartPearls - new dermal injection-like delivery system without use of a needle. Menopause, Andropause, Anti-aging, Vienna, 11-13 December 2014

16. **Jin, N.,** Keck, C. M., Staufenbiel, S., Monsuur, F., Höfer, H. H., Müller, R. H., smartPearls™ – novel dermal delivery system for amorphous cosmetic and pharma actives. P. 4, 19th Jahrestagung der Gesellschaft für Dermopharmazie (GD), Berlin, 17 March 2015

17. **Jin, N.,** Staufenbiel, S., Keck, C. M., Monsuur, F., Höfer, H. H., Müller, R. H., Lyme-borreliosis-preventing azithromycin dermal formulations – smartCrystals® versus smartPearls®. P. 1, 8th Polish-German Symposium on Pharmaceutical Sciences: Retrospects, Insights and Prospects, Kiel, 29-30 May 2015

18. Keck, C. M., **Jin, N.,** Du, W., Staufenbiel, S., Monsuur, F., Höfer, H. H., Müller, R. H., smartPearls™: novel dermal amorphous delivery system based on porous particles. P. 44, DPhG-Jahrestagung, Düsseldorf, 23-25 September 2015

19. **Jin, N.,** Staufenbiel, S., Monsuur, F., Höfer, H. H., Keck, C. M., Müller, R. H., Novel Azithromycin dermal formulation: SmartPearls™ for prophylaxis of lyme borreliosis. M1286, AAPS Annual Meeting and Exposition, Orlando, 26-29 October 2015

20. **Jin, N.,** Romero, G. B., Staufenbiel, S., Monsuur, F., Höfer, H. H., Keck, C. M., Müller, R. H., Dermal delivery of cyclosporine A — smartPearls™ versus amorphous drug nanoparticles. T2099, AAPS Annual Meeting and Exposition, Orlando, 26-29 October 2015

21. **Jin, N.,** Staufenbiel, S., Monsuur, F., Höfer, H. H., Keck, C. M., Müller, R. H., Novel dermal smartPearls™ for more effective delivery of poorly soluble anti-oxidants. T2100, AAPS Annual Meeting and Exposition, Orlando, 26-29 October 2015

22. Keck, C. M., Pyo, S. M., **Jin, N.,** Monsuur, F., Müller, R. H., smartPearls® – exploiting the penetration enhancing effect of amorphous actives. Menopause, Andropause, Anti-aging, Vienna, 10-12 December 2015

23. Keck, C. M., **Jin, N.,** Romero, G., Monsuur, F., Müller, R. H., smartPearls® – a new dermal microdelivery system for poorly soluble drugs by amorphization. 20th Jahrestagung der Gesellschaft für Dermopharmazie (GD), Berlin, 16 March 2016

24. **Jin, N.,** Pyo, S. M., Keck, C. M., Müller, R. H., smartPearls® for dermal delivery of amorphous actives – effect of loading concentration on stability & release. DPhG-Jahrestagung, Munich, 04-07 October 2016

25. **Jin, N.,** Pyo, S. M., Monsuur, F., Höfer, H. H., Keck, C. M., Müller, R. H., Influence of drug loading concentration on smartPearls® technology. AAPS Annual Meeting and Exposition, Denver, 13-17 November 2016

26. Pyo, S. M., **Jin, N.,** Keck, C. M., Müller, R. H., smartPearls® for optimized topical delivery of soluble amorphous actives. 10th European Workshop on Particulate Systems (EWPS), Copenhagen, 19-20 January 2017

27. **Jin, N.,** Pyo, S. M., Keck, C. M., Müller, R. H., Nicotine-loaded solid lipid nanoparticles for chewing gum. 9th Polish-German Symposium on Pharmaceutical Sciences, Kraków, 26-27 May 2017

28. **Jin, N.,** Pyo, S. M., Keck, C. M., Müller, R. H., Dermal smartPearls – Effect of amorphous state on dissolution profiles and penetration efficacy. 44th Controlled Release Society Annual Meeting & Exposition, Boston, 16-19 July 2017

CURRICULUM VITAE

For reasons of data protection, the curriculum vitae is not published in the electronic version.

For reasons of data protection, the curriculum vitae is not published in the electronic version.

ACKNOWLEDGEMENTS

First of all, I would like to appreciate Prof. Rainer H. Müller for his guidance, supervision, suggestion and encouragement in my professional area such as research plan, poster making and paper writing. I learned a lot from his speech, methodology for experiment and paper writing. And I will never forget how friendly and nice he was to foreign students like me. He emailed me the map of the office before I came to Germany, made me feel relax in the strange environment. He emailed me the details how to go to the train station to join a conference in another city. He even drove the foreign students to a conference in another city and talked about the culture and common sense of Germany.

Secondly, many thanks to Prof. Cornelia M. Keck. Without her, I would not perform the penetration study in time. In addition, I learned various professional skills and technology theories from her lectures.

Thanks also to Ms. Corinna Schmidt, Ms. Inge Volz and Ms. Gabriela Karsubke. Ms. Corinna Schmidt showed me how to produce nanocrystals by HPH, how to measure samples by PCS and LD. Mr. Inge Volz showed me how to manage the tapes after porcine ear penetration study, how to prepare samples for standard curves for HPLC. They also supported my work by their professional technical skills. Ms. Gabriela Karsubke supported me with administrative help and advice in practical issues.

Special thanks to Dr. Sven Staufenbiel and Dr. Sung Min Pyo. Dr. Staufenbiel not only helped me a lot in the beginning of my research, but also was patient to answer my questions about basic scientific theories and daily life of Germany. Dr. Pyo paid a lot patience to double check of my thesis. And she helped me finding the way back to the hotel at midnight after conference dinner in another city, which I will never forget.

I would also like to thank all my colleagues and friends in Berlin for their help. For example, Birthe Herziger and Daniel Koepke helped me in the German version summary.

Dr. Qionghua Wei showed me how to generate amorphous productions on mesoporous silicas. Dr. Xiangyu Li helped me to release pressure by talking and showed me how to measure viscosity of gels. Dr. Xiaoying Hu showed me how to produce SLN by HPH. Dr. Gregori B. Romero and Dr. Xuezhen Zhai showed me how to produce nanocrystals by BM and how to measure samples by light microscope. Dr. Robert and David Hespeler solved my computer problem with wifi connection and printer connection. Yuan Ding helped me to handle my samples test and encouraged me a lot. Besides, I would like to thank my friends such as Qi Su, Nan Zhang and so on for personal help.

In the end, I would like to thank the financial support from the China Scholarship Council (CSC) and the care from my family as well. I would like to appreciate my mother Ms. Jian especially. Her generous contribution and love helps me to finish my thesis writing.